FREQUENCY- AND PRESSURE- DEPENDENT DYNAMIC SOIL PROPERTIES FOR SEISMIC ANALYSIS OF DEEP SITES

by

Dominic Assimaki

Diploma of Civil Engineering (1998)
National Technical University of Athens.

Submitted to the Department of Civil and Environmental Engineering
in partial fulfillment of the requirements
for the degree of

MASTER OF SCIENCE IN CIVIL AND ENVIRONMENTAL ENGINEERING

at the

MASSACHUSETTS INSTITUTE OF TECHNOLOGY

February 2000

Signature of Author.....
Department of Civil and Environmental Engineering
November 3, 1999

Certified by.....
Eduardo Kausel, Professor of Civil and Environmetal Engineering
Thesis Supervisor

Accepted by.....
Daniele Veneziano, Professor of Civil and Environmetal Engineering
Chairman, Departmental Committee on Graduate Students

FREQUENCY– AND PRESSURE–DEPENDENT DYNAMIC SOIL PROPERTIES FOR SEISMIC ANALYSIS OF DEEP SITES

by

Dominic Assimaki

Submitted to the Department of Civil and Environmental Engineering
on November 3, 1999 in partial fulfillment of the requirements for the degree of
Master of Science in Civil and Environmental Engineering.

ABSTRACT

Most of the analytical techniques for evaluating the response of soil deposits to strong earthquake motions employ numerical methods, initially developed for the solution of linear elastic, small – strain problems. Various attempts have been made to modify these methods to handle nonlinear stress – strain behavior induced by moderate to strong earthquakes.

However, questions arise regarding the applicability of commonly used standardized shear modulus degradation and damping curves versus shear strain amplitude. The most widely employed degradation and damping curves, are those originally proposed by Seed & Idriss, 1969. Laboratory experimental data (Laird & Stokoe, 1993) performed on sand samples, subjected to high confining pressures, show that for highly confined materials, both the shear modulus reduction factor [G/G_0] and the damping [ξ] versus shear strain amplitude fall significantly outside the range used in standard practice, overestimating the capacity of soil to dissipate energy.

The equivalent linear iterative algorithm also diverges when soil amplification is performed in deep soft soil profiles, due to the assumption of a linear hysteretic damping being independent of frequency. High frequencies associated with small amplitude cycles of vibration have substantially less damping than the predominant frequencies of the layer, but are artificially suppressed when all frequency components of the excitation are assigned the same value of hysteretic damping.

This thesis presents a simple four – parameter constitutive soil model, derived from Pestana's (1994) generalized effective stress formulation, which is referred to as MIT-S1. When representing the shear modulus reduction factors and damping coefficients for a granular soil subjected to horizontal shear stresses imposed by vertically propagating shear [SH] waves, the results are found to be in very good agreement with available laboratory experimental data.

Simulations for a series of " true" non-linear numerical analyses with inelastic (Masing-type) soils and layered profiles subjected to broadband earthquake motions, taking into account the effect of the confining pressure, are thereafter presented. The actual inelastic behavior is closely simulated by means of equivalent linear analyses, in which the soil moduli and damping are frequency dependent. Using a modified linear iterative analysis with frequency- and depth-dependent moduli and attenuation, a 1-km deep model for the Mississippi embayment near Memphis, Tennessee, is successfully analyzed. The seismograms computed at the surface not only satisfy causality (which cannot be taken for granted when using frequency-dependent parameters), but their spectra contain the full band of frequencies expected.

Thesis Supervisor : Eduardo Kausel
Title : Professor of Civil and Environmental Engineering

ACKNOWLEDGEMENTS

This work would not have been accomplished, without the collaboration of many individuals. I am first indebted to my thesis supervisor, Prof. Eduardo Kausel, who supported my work and provided superior intellectual challenges. I have learned enormously from him and gained insight to numerous problems that I have encountered throughout this challenging experience. This work would not have been accomplished without his continuous support and enthousiasm, without the energy that he dedicated, both as a mentor and as a friend.

I would also like to thank:
Prof. Andrew Whittle, for his contribution to the soil behavior and modelling aspects of this thesis, for providing new ideas and insightful comments towards my work.
Prof. Kenneth Stokoe, for providing experimental data, essential for the completion of this research project.
I would also like to acknowledge the partial economic support provided by Grant GT-2 from the Mid-America Earthquake Center, under the sponsorship of the National Science Foundation.

Acknowledgements also go out to:
Prof. George Gazetas, who encouraged me to pursue graduate studies in Civil Engineering. His spirit and enthousiasm will always nourish my interest for research.
The faculty of the Mechanics and Materials group at MIT.

I am specially grateful to my fellow *soil* and *dynamic* friends from MIT: Federico Pinto, Jorge Gonzales, Martin Nussbaumer, Yun Kim, Alexis Liakos, Christoph Haas, Attasit "Pong" Korchaiyapruk, Dimitris Konstandakos, Karen Veroy, Joon Sang Park, Daniel Dreyer and Monica Starnes, for the unforgettable experiences we have lived together, and for making my life at MIT enjoyable and my effort less tiring.

To my family I owe the most. This work would not have been possible without their continuous support and love. This thesis is dedicated to them, who have been the main source of my strength throughout this challenging period of my life.
Finally, I would like to thank George Kokossalakis, who has been continuously there for me, supporting my efforts, and helping me overpass obstacles that I wouldn't have managed to, if I were on my own. This thesis is literary completed thanks to him.

To my family and George

TABLE OF CONTENTS

LIST OF TABLES

LIST OF FIGURES

LIST OF SYMBOLS

CHAPTER 2

G	Shear Modulus
G_0, G_{max}	Small Strain Shear Modulus
ξ	Material Damping Ratio
ξ_{min}	Small Strain Material Damping Ratio
γ	Shear Strain Amplitude
ΔE	Area enclosed in the hysteresis loop
σ'_m	Effective mean principle stress
e	Void Ratio
N	Number of loading cycles
S[%]	Degree of Saturation for cohesive soils
OCR	Overconsolidation Ratio
c, φ	Effective Strength Stress Parameters
τ	Shear Stress
τ_{max}	Maximum Shear Stress - Shear Strength
γ_r	Reference Strain (= τ_{max} / G_{max})
u	In-situ pore water pressure
PI	Plasticity Index
K_0	Effective Coefficient of Lateral Earth Pressure at Rest
G_s	Specific Gravity
ρ	Soil Density
D_{60}	Soil Particle Diameter at which 60% of the soil is finer
D_{30}	Soil Particle Diameter at which 30% of the soil is finer
D_{10}	Soil Particle Diameter at which 10% of the soil is finer

CHAPTER 3

σ'_v	Effective Overburden Pressure
p_a	Atmospheric Pressure
K	Tangent Bulk Modulus
K_{max}	Small strain bulk modulus

C_b Small Strain Stiffness at load reversal

μ_0' Poisson's Ratio at load reversal

ω Non-linear Poisson's Ratio

τ_{rev} Stress Reversal Point

ξ_s Non-dimensional distance in stress-space describing changes in the mean effective stress and stress ratio relative to conditions at the stress reversal point

K_{0NC} Lateral Stiffness Coefficient of the Normally Consolidated Deposit

OCR_1 Overconsolidation Ratio at $K_0 = 1$

ρ_r Tangential Slope of the Hydrostatic Swelling Curve in a $\log e$ - $\log \sigma'$ space

ω_s Small strain nonlinearity in shear

φ'_{cs} Friction angle at large strain (critical state) conditions

C, C_1, C_2 Parameters depending on mean effective stress level

ρ_c Soil Matrix Compressibility - Slope of the Limiting Compression Curve (LCC) in a $\log e$ - $\log \sigma'$ space

$d\varepsilon$ Incremental Volume change

$d\varepsilon^e$ Elastic Incremental Volume change component

$d\varepsilon^p$ Plastic Incremental Volume change component

σ'_r Reference Stress at a unit void ratio

e_0 Formation Void Ratio (Void Ratio at σ'_m=0)

σ'_{lim} Upper limit of effective stress, where compressibility of soil particles is significant

e_{min} Lower limit of void ratio, where the void space becomes discontinuous and assumptions of free drainage are no longer valid

V_s Shear Wave Velocity

C_c Compression Index (= $de / d\log\sigma'$)

w_L Liquid Limit

CHAPTER 4

ω Angular Frequency or Circular Frequency

δ Angle of phase difference

γ_a Shear Strain Amplitude

τ_a Shear Stress Amplitude

$\overline{\gamma}$ Shear Strain in complex variables

$\bar{\tau}$	Shear Stress in complex variables
μ	Elastic Modulus
μ'	Loss Modulus
μ^*	Complex Modulus
n	Loss Coefficient
W	Energy Stored
ΔW	Energy Dissipated
τ_f	Failure Stress - Shear Strength
ξ_0	Large Strain Material Damping Ratio
γ_y	Yield Strain
τ_y	Yield Stress
a, r	Parameters of the Ramberg - Osgood Model, defining the stress-strain relationship
k_i	Spring Stiffness of the i^{th} element, in the parallel series model
τ_{yi}	Critical Slipping Stress of the i^{th} element, in the parallel series model
$\tan(a_i)$	Tangent Stiffness at (γ_i, τ_i)
N	Number of elastoplastic springs
n	Number of elements that remain elastic

CHAPTER 5

f_1	Fundamental Frequency of the soil column
E_d^i	Energy dissipated by the i^{th} element, in the parallel series model
$u(x,t)$	Solution of the one-dimensional wave equation
c	Wave propagation velocity
$P(t)$	Instantaneous Power
$\bar{P}$	Average Power Dissipated
γ_{RMS}	RMS value of the Shear Strain

APPENDIX I

N	Number of loading cycles
γ_c^e	Elastic Strain Threshold
γ_c^v	Volumetric Strain Threshold
G_N	Shear Modulus after N cycles of loading
G_1	Shear Modulus in the first cycle of loading

δ	Degradation index
t_g	Geological Age of the soil deposit
G_{lab}	Shear Modulus measured in the laboratory
G_{field}	Estimated value of Shear Modulus in the field

APPENDIX II

I_s	Mass Moment of Inertia of soil specimen
I_m	Mass Moment of Inertia of membrane
I_0	Mass Moment of Inertia of rigid end mass at the top of the specimen
l	Length of the specimen
V_s	Shear Wave Velocity of the specimen
ω_n	Undamped Natural Circular Frequency of the system.
r_{eq}	Equivalent radius of the soil specimen
θ_{max}	Angle of twist at the top of the specimen
Z_1, Z_2	Two successive strain amplitudes of motion
δ	Logarithmic Decrement
A	Shear Strain Amplitude, defined as 0.707 A_{max} for the half-power bandwidth method
f_1	Frequency below the resonance where the strain amplitude is A
f_2	Frequency above the resonance where the strain amplitude is A
f_r	Resonant Frequency of the specimen
$\dot{x}$	Particle velocity
T	Period of motion
c	Viscous Damping Coefficient
W_s	Energy Stored
W_d	Energy Dissipated
C_c	Critical Damping Coefficient
m	Mass of the system

CHAPTER 1

INTRODUCTION

1.1 OVERVIEW OF THE PROBLEM

Analytical techniques for evaluating the response of soil deposits to strong earthquake motions have received considerable attention in recent years. Most of these procedures employ numerical methods, which were initially developed for the solution of linear elastic, small – strain problems. As the stress – strain relationships for soils at the level of strains that might be induced by moderate to strong earthquakes are nonlinear, various attempts have been made to modify these methods to handle nonlinear stress – strain behavior.

The majority of practical methods of analysis for soil amplification require the soil to be modeled as linearly visco – elastic material. The approximate method most frequently used at present is the equivalent linear method (Seed & Idriss, 1969), an iterative method, which is performed as follows:

a) From laboratory tests (usually cyclic loading), the secant moduli and damping ratios of the soil as a function of strain are obtained.

b) The linear visco – elastic analyses are then carried out iteratively, values of modulus and damping ratio being changed in successive cycles until they correspond to the levels of strain computed. Analyses are done with lumped masses, springs and dashpots or with finite elements, in the time domain or in the frequency domain using Fast Fourier Transform.

Whilst the linear iterative solution may not provide an exact solution to the non-linear soil dynamic analysis under consideration, it does often produces acceptable results for engineering purposes (Constantopoulos, Roesset & Christian, 1973). SHAKE (Schnabel, Lysmer & Seed, 1972) is perhaps the best known and most widely used computer program using this type of iterative linear algorithm.

The shear modulus degradation and damping curves versus shear strain amplitude most widely used in practice, are the ones originally proposed by Seed & Idriss, 1969, for sands and saturated clays. However, questions arise, regarding the range of applicability of standardized

curves, irrespective of state soil variables, such as the void ratio (density) and the confining pressure (mean effective stress).

Laboratory experimental data (Laird & Stokoe, 1993) performed on sand samples, subjected to confining pressures up to 5 Mpa, show that for the highly confined material, both the shear modulus reduction factor [G/G_0] and damping [ξ] versus shear strain amplitude plot significantly outside the range used in standard practice. Therefore, the use of the Seed – Idriss curves in dynamic response analyses involving cohesionless soils at very high confining pressures would generally be unconservative by overestimating the capacity of soil to dissipate energy.

The equivalent linear iterative algorithm also diverges when soil amplification or deconvolution is performed in deep soft soil profiles, due to the assumption of a linear hysteretic damping, independent of frequency. Since material damping is a function of amplitude, high frequencies associated with small amplitude cycles of vibration have substantially less damping than the predominant frequencies of the layer, but are artificially suppressed as in standard practice, all frequency components of the excitation are assigned the same value of hysteretic damping.

This thesis presents a simple four – parameter model, derived from a generalized effective stress soil model referred to as MIT-S1 (Pestana, 1994), that can represent the shear modulus reduction factors and damping coefficients for a granular soil subjected to horizontal shear stresses imposed by vertically propagating shear [SH] waves. Results are found to be in very good agreement with available laboratory experimental data.

Successively, a linear – hysteretic frequency – dependent damping model is developed, and results are compared to a non-linear Masing soil model, consisting of elastoplastic springs in parallel. For consistency, the yield strain and stiffnesses of the springs are also derived using the stress – strain characteristics of MIT-S1.

Finally, the proposed model is implemented in a frequency – domain, soil amplification computer code, and simulations are performed for earthquake excitations prescribed at rigid bedrock underlying the soil deposit. Results are compared with *exact* nonlinear analyses, where the soil deposit is modeled as a lumped – mass, multi – degree of freedom system, with the nonlinear elements represented by a set of elastoplastic springs in parallel.

1.2 ORGANIZATION OF THE STUDY

Chapter 2 describes briefly the nonlinear characteristics of soil, when subjected to large strain amplitudes, as well as the environmental and loading factors affecting the shear modulus degradation and damping curves. The effect of confining pressure in successively described in detail, for dry, wet cohesionless and cohesive soils. Finally, laboratory experimental data from resonant column and torsional shear tests, performed on dry sand specimens under high confining pressures, are presented, alerting the need of formulating a theoretical soil model, capable of representing the effects of confining pressure on the nonlinear stress – strain soil characteristics. Appendices to this chapter include:

i. detailed description of the parameters affecting the stiffness and damping characteristics of soils (Appendix I), and
ii. description of the resonant column and torsional shear equipment and measurement techniques for the evaluation of secant modulus and damping ratio of the soil, as a function of the shear strain amplitude (Appendix II).

Chapter 3 presents a simple four – parameter soil model, based on a generalized effective stress model, referred to as MIT-S1 (Pestana, 1994). The model parameters depend both on the soil type as well as on soil state variables and characteristics, such as current void ratio (density), confining pressure (mean effective stress) and small strain nonlinearity. Analytical expressions for the shear modulus degradation and damping curves are derived, results are compared with available experimental data and simulations are performed for soil amplification of a deep soil deposit, successively compared to the results derived using Seed – Idriss standard practice curves.

Chapter 4 describes in detail available linear viscoelastic and nonlinear stress – strain soil models. For each model, general stress – strain equations are presented, as well as analytical expressions for the equivalent hysteretic damping ratio.

Chapter 5 alerts initially one of the shortcomings of the equivalent - linear analysis, namely the assumption of linear hysteretic damping, independent of frequency. The problem is stated by simulations performed using a nonlinear model of elastoplastic springs in parallel, subjected to the superposition of two sinusoidal motions. Successively, a linear - hysteretic frequency - dependent model is presented, with stress - strain characteristics derived from MIT-S1. The performance of the model under arbitrary loading conditions, namely an earthquake excitation, is compared to a non-linear model, consisting of elastoplastic springs in parallel, the stiffness and yield deformation

of which, are also derived from the MIT-S1 formulation. Appendices to this chapter include the FORTRAN computer code used for the simulations (Appendix III.1).

Chapter 6 presents soil amplification simulations, performed with the equivalent linear iterative algorithm using frequency - and pressure - dependent dynamic soil properties. Results are compared with these obtained by exact incremental nonlinear analyses, where the soil deposit is simulated as a lumped mass multi – degree of freedom system, with the nonlinear elements being represented by a parallel series model. For consistency of the comparison, the stress – strain characteristics of the nonlinear springs are derived from the one-dimensional formulation of MIT-S1, described in Chapter 3. Appendices to this chapter include the FORTRAN computer code used for the nonlinear soil amplification analysis (Appendix III.2).

CHAPTER 2

SHEAR MODULUS AND DAMPING FOR DYNAMIC RESPONSE ANALYSIS

2.1 INTRODUCTION

It is now standard practice in seismic engineering to take into consideration the non-linear behavior of soils undergoing time-varying deformations caused by earthquakes. While it is in principle possible to perform true incremental analyses in which the soil properties are adjusted according to the load path and instantaneous levels of strain, this is seldom done in practice. Instead, in the most widely used approach, approximate linear solutions are obtained using an iterative scheme originally proposed by Seed and Idriss (1969). In this method, the soil properties are chosen in each iteration in accordance with some characteristic measure of strain computed in the previous iteration. While the linear iterative solution may not provide an exact solution to the non-linear soil dynamics problem at hand, it does often produces acceptable results for engineering purposes (Constantopoulos, Roesset & Christian, 1973). SHAKE (Schnabel, Lysmer & Seed, 1972) is perhaps the best known and most widely used computer program using this type of iterative linear algorithm.

Much progress has also been made recently in laboratory experiments attempting to simulate the in-situ conditions that might exist in deep soil deposits (Laird & Stokoe, 1993). Soil samples subjected in these tests to confining pressures as high as 5 Mpa have revealed patterns of non-linear behavior that, while qualitatively similar to the response under lower confining pressures, exhibited less degradation of shear modulus with strain (i.e. remained nearly elastic). The damping due to hysteresis was correspondingly smaller. Testing at higher confining pressures has proved a difficult task. Thus, it is desirable to develop an analytical model that can supplement the experimental data, and can be used in computer models of wave propagation in soils, such as SHAKE.

2.2 NON-LINEAR SOIL BEHAVIOR

Once shearing strains exceed about 10^{-5} (referred to as the linear threshold), the stress-strain behavior of soils becomes increasingly nonlinear, and there is no unique way of defining shear modulus or damping. Therefore, any approach to characterize the soil for analyses of cyclic loading of larger intensity must account for the level of cyclic strain excursions.

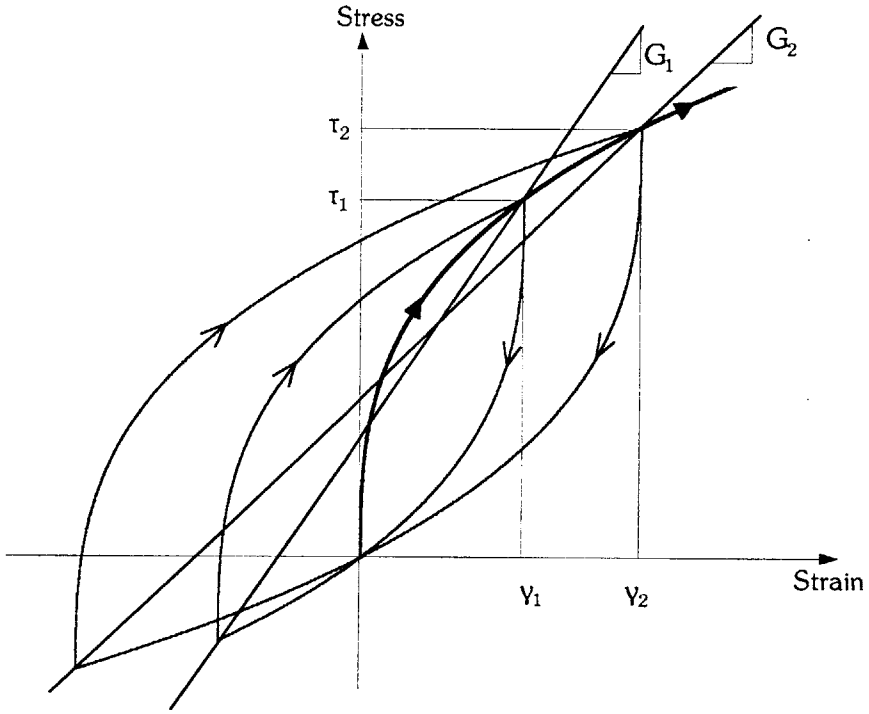

Figure 2.1 Loading-unloading at different strain amplitudes

When ground motions consist of vertically propagating shear waves and the residual soil displacements are small, the response can often be characterized in sufficient detail by the shear modulus and the damping characteristics of the soil under cyclic loading conditions. It is usual practice to express the non-linear stress-strain behavior of the soil in terms of the secant shear modulus and the damping associated with the energy dissipated in one cycle of deformation. With reference to the hysteresis loop shown in Figure 2.1, the secant modulus is usually defined as the ratio between maximum stress and maximum strain, while the damping factor is proportional to the area (ΔE) enclosed by the hysteresis loop, and corresponds to the energy dissipated in one cycle of motion. It is readily apparent that each of the aforementioned properties depends on the magnitude of the strain for which the hysteresis loop is determined, so they are functions of the maximum cyclic strain.

The simplified response illustrated in Figure 2.1 can be described through a *backbone curve*, corresponding to first loading, together with a set of rules for unloading and reloading, as proposed by Masing. Rheological models of this type can be represented by a set of elasto-plastic springs in parallel, with input parameters obtained by curve fitting the measured data.

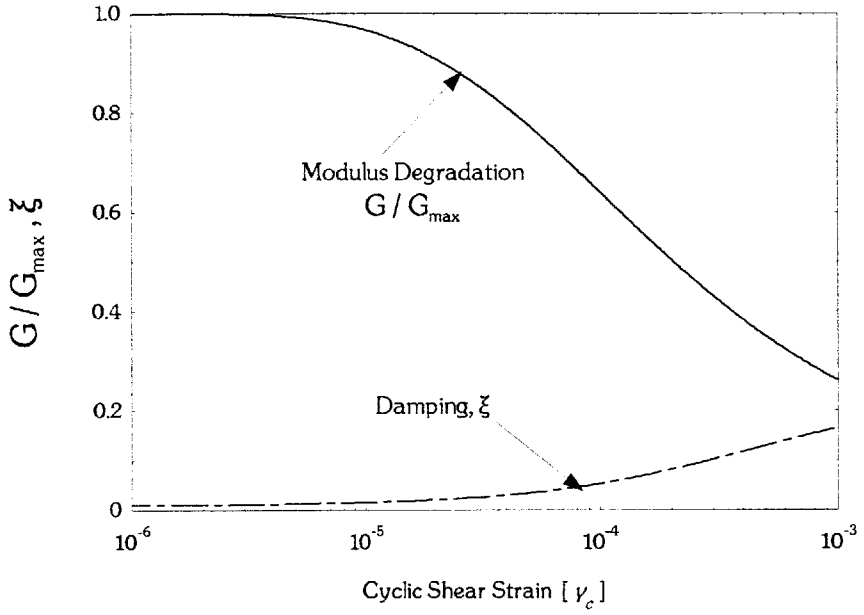

Figure 2.2 Secant modulus and damping ratio as function of maximum strain

When opting for an equivalent linear analysis, the characterization of the soil consists of three parts (Figure 2.2):

i. The maximum shear modulus (G_{max}), defined in the very small strain (linear) region.

ii. The reduction curve for G/G_{max} versus maximum cyclic strain γ_c (referred to as modulus degradation curve), with G being the secant modulus, and

iii. The fraction of hysteretic (or material) damping ξ versus the maximum cyclic strain γ_c. This parameter is proportional to the area ΔE enclosed by the hysteresis loop, and normalized it by the" elastic" strain energy, according to the following expression:

$$\xi = \frac{1}{2\pi} \frac{\Delta E}{G \gamma_c^2} \qquad \{1\}$$

Typically G/G_{max} decreases and ξ increases as γ_c becomes larger, and in fact it has been noticed that a fast decrease in G/G_{max} with γ_c, corresponding to a strongly nonlinear soil, is associated with a strong increase of ξ with γ_c in the same soil, and vice versa.

In the case of dry cohesionless soils, the physical origin of the variation in modulus and damping with cyclic strain, as reflected in the shapes of the curves in Figure 2.2, is now well understood. Both parameters are related to the frictional behavior at the interparticle contacts and the rearrangement of the grains during cyclic loading (Dobry et al., 1982; Ng and Dobry, 1992; Ng and Dobry, 1994). Therefore, even crude analytical models of particles can be used to mimic the shear modulus reduction factor, G / G_{max}, and material damping, ξ, versus γ_c curves, provided that they include friction and allow for particle rearrangements.

It should be noted however that reversible behavior is associated with minimal rearrangement of particle contacts and irrecoverable, plastic, strains become significant only at strain levels $\gamma_c \geq 10^{-3}$. For smaller cyclic strain amplitudes therefore, dissipation of energy must be related to frictional behavior at contacts, yet the physical mechanisms related to nonlinear stress – strain phenomena below the volumetric threshold ($\gamma^v_c \approx 10^{-3}$) are not clearly defined.

A comprehensive survey of the factors affecting the shear moduli and damping factors of soils and expressions for determining these properties have been presented by Hardin & Drnevich (1972a & b). In this study it was suggested that the primary factors affecting moduli and damping factors are:

- Strain amplitude, γ
- Effective mean principle stress, σ'_m
- Void ratio, e
- Number of cycles of loading, N
- Degree of saturation for cohesive soils, S[%]

and that less important factors include:

- Octahedral shear stress
- Overconsolidation ratio, OCR
- Effective strength stress parameters, c and φ'
- Time effects

Table 2.1 summarizes the effect of these parameters on the shear modulus degradation curves and damping. Further details can be found in Appendix I of the present study.

Increasing Factor	G / Gmax	ξ
Cyclic Strain, γ_c	Decreases with γ_c	Increases with γ_c
Confining Pressure, σ'_m	Increases with σ'_m (effect decreases with increasing PI)	Decreases with σ'_m (effect decreases with increasing PI)
Void Ratio, e	Increases with e	Decreases with e
Geologic Age, t_g	May increase with t_g	May decrease with t_g
Cementation, c	May increase with c	May decrease with c
Overconsolidation Ratio, OCR	Not affected	Not affected
Plasticity Index, PI	Increases with PI	Decreases with PI
Strain Rate, $d\gamma/dt$	G / Gmax probably not affected if G and Gmax measured at the same strain rate $d\gamma/dt$	Stays constant or may increase with $d\gamma/dt$
Number of Loading Cycles, N	Decreases after N cycles of large γc for clays; for sands can increase (drained conditions) or decrease (undrained conditions)	Not significant for moderate γ_c and number of cycles, N

Table 2.1 Effect of Environmental and Loading conditions on modulus ratio and damping ratio of Normally Consolidated and Moderately Consolidated Soils (Hardin & Drnevich, 1972, modified by Dobry & Vucetic, 1987)

Amongst the aforementioned parameters affecting the dynamic response of soils, apart from the well known strain amplitude (γ), the effective mean principle stress (σ'_m) is more pronounced in the dynamic analysis of deep soil deposits studied herein, and it will be therefore analyzed separately in the proceeding section.

2.3 Effect of Confining Pressure on Modulus and Damping

2.3.1 Cohesionless Soils

The modulus degradation and damping curves most often used for dry cohesionless soils, such as sands, gravels and cohesionless silts, are those proposed by Seed and Idriss (1970). Based on experimental data by Hardin & Drnevich (1970) and others, these standard curves are extensively used in equivalent linear analysis of earthquake excitations and machine vibrations. The Seed & Idriss approach assumes that the G / G_{max} and ξ curves are essentially the same for sands, gravels and cohesionless silts. Their generic response curves, assume that

the degradation curves are independent of the cycle number considered, as well as the void ratio (or relative density), sand type and confining pressure, factors which, according to the same study, do affect significantly the maximum shear modulus G_{max}, defined below the elastic threshold, $\gamma^e_c \approx 10^{-5}$.

Laboratory measurements provide evidence in support of some of these simplifying assumptions. They show that void ratio, overconsolidation, sand type and cycle number (Dobry et al., 1982, Iwasaki et al., 1978) do indeed have relatively small influence on the measured backbone curves. They also show that the method of sand deposition, existence of static shear stress, grain size (sands vs. gravels) are also of secondary importance (Hardin, 1965, Hardin & Drnevich, 1972a, Tatsuoka et al., 1979, Seed et al., 1986). However, the influence of the confining pressure is significant and cannot possibly be ignored, especially when performing dynamic analyses for deep soil sites.

A number of laboratory studies (see Section 2.4) on hydrostatically[1] consolidated sands have shown that their stress-strain response becomes more linear as the confining pressure increases (i.e. for a given shear strain amplitude, γ, as σ'_0 increases, G / G_{max} increases and ξ decreases). In addition, large confining pressures lead to substantial reductions in material damping at small strain, i.e. ξ_{min}. The reason for these effects with increasing σ'_0 is related to the different rates at which the small strain modulus and the shear strength of the soil increase when the pressure increases (Hardin & Drnevich, 1972a, Seed et al., 1986, Laird & Stokoe, 1993).

To illustrate this assertion, consider the hyperbolic model frequently used to represent the stress strain behavior of soils. In this model, the backbone curve is defined in terms of two parameters, namely the small stain shear modulus G_{max} and the shear strength τ_{max}. The hyperbolic equation for the backbone curve is:

$$\tau = \frac{\gamma}{\left(1 / G_{max} + \gamma / \tau_{max}\right)} \qquad \{2\}$$

Alternatively, $\tau = [\ \gamma / (\ \gamma_r\ +\ \gamma)]\ \tau_{max}$, in which $\gamma_r = \tau_{max} / G_{max}$ is a reference strain (Hardin & Drnevich, 1972b). Therefore, the corresponding modulus degradation curve is only a function of the reference strain, namely:

[1] Laboratory data show minor influence of K_0 on the shear modulus degradation and damping curves (Hardin & Drnevich, 1972a)

$$\frac{G}{G_{max}} = \frac{1}{1+(\gamma/\gamma_r)} \qquad \{3\}$$

For an isotropically consolidated sand subjected to a pure shear loading, Coulomb's strength law indicates that $\tau_{max} = \sigma_0 \tan\varphi$, in which φ is the angle of internal friction of the soil. On the other hand, the low strain shear modulus is usually approximated as $G_{max} = A\ \sigma_0^m$, where $m = 0.5 \pm 0.1$ and A is a constant. Consequently, γ_r is proportional to $\sigma_0^{0.5}$ and as σ_0 increases, both γ_r and G/G_{max} increase, as verified by the experimental data (Shibata & Soelarno, 1975).

In particular, the analytical expression given by Shibata & Soelarno, 1975 to incorporate in the shear modulus degradation curves the effect of the confining pressure is:

$$\frac{G}{G_{max}} = \frac{1}{1+1.000\left(\frac{\gamma}{\sigma_0^{0.5}}\right)} \qquad \{4\}$$

in which γ = shearing strain (in. / in.); and σ_0 = confining pressure (kg /cm^2). Once a confining pressure is assumed, values of G/G_{max} are computed for various strain levels. This is the earliest attempt that has been made to take into account the modification of the shear modulus degradation curves due to the confinement of the soil deposit, yet, along with the widely used Seed & Idriss curves, this same curve is used independent from the characteristics of the soil under consideration.

A later section presents experimental results obtained by Laird & Stokoe (1993) who determined the degradation curves of isotropically consolidated sand specimens subjected to confining pressures as high as σ_0 = 3.5 MPa. It will be seen that high values of σ_0, lead to degradation curves that lie beyond the bands given by Seed-Idriss (1970). Hence, use of the standard curves for dynamic response analyses involving cohesionless soils at very high confining pressures could be unconservative, since those curves might severely overestimate non-linear effects in the soil as well as its tendency to dissipate energy.

2.3.2 WET COHESIONLESS SOILS

The degree of saturation in cohesionless soils certainly affects the reduction curves for shear moduli and damping at large shear strain amplitudes (i.e. larger than the volumetric

threshold $\gamma_c \geq 10^{-3}$). For smaller strain amplitudes, the soil behavior can be approximated as *uncoupled*, i.e. minimum volume change and pore pressure generation, are introduced by shearing. Therefore, it is presumed that the curves for dry materials may also be applicable to saturated granular soils for shear strain amplitudes $\gamma_c \leq 10^{-3}$, with the response controlled by the in-situ effective confining pressure:

$$\sigma' = \sigma - u \qquad \{5\}$$

where: u the in-situ pore water pressure.

Clearly, if water is not trapped between the soil particles during shear, it does not participate in the stress-strain response or in the energy dissipation in the material. In such case, damping is completely caused by friction due to interactions between the particles, as if the soil was dry. It should be noted, however, that this might not apply to small strain, high frequency cyclic loads in a resonant column test. In such case, damping values will be higher for a saturated material because of viscous effects caused by the relative movement between the solid phase and the pore water. This difference in damping between dry and saturated soil is generally not significant for low-frequency dynamic phenomena such as earthquakes, but may be relevant to high-frequency vibrations such as generated by explosions and machine vibrations.

2.3.3 COHESIVE SOILS

Based on experimental data on normally consolidated undisturbed specimens of clay and silt obtained from several depths at a site in Japan, tested under confining pressures ranging from 0.2 to 0.7 kg/cm^2, two general features can be clearly observed:

i. For the only specimen of non-plastic silt (PI = 0), the shear modulus degradation curve plots together with the sand curve, and
ii. The shear modulus degradation curves of the rest of the cohesive soil samples plot above the sand curve, with their location being higher when the PI is higher, more or less irrespective of confining pressure.

These results are typical of many others published in the literature, indicating that the shear modulus degradation (G / G_{max}) and damping (ξ) curves of saturated cohesive soils in sedimentary deposits are essentially independent of effective confining pressure, void ratio,

and overconsolidation and are largely a function of the Plasticity Index (PI) of the clay (Zen, et al., 1978; Kokusho, et al., 1982; Ishihara, 1986; Romo & Jaime, 1986; Dobry & Vucetic, 1987; Sun, et al.,1988; Dobry & Vucetic, 1991).

While comparisons between G/G_{max} and ξ curves of natural clays do show an influence of void ratio, e, it is primarily due to the fact that high plasticity clays tend to have greater values of e than low plasticity soils, with the effect of e largely disappearing when the Plasticity Index of the clay is considered (Lodde & Stokoe, 1982; Vucetic & Dobry, 1991).

2.4 EXPERIMENTAL DATA ON COHESIONLESS SOILS

To determine the dynamic properties of granular soils at significant depths, laboratory tests were performed by Laird & Stokoe (1993), at UT Austin. The objective of the experiments was to determine the dynamic properties of soils at significant depths, both for dry and saturated specimens at confining pressures up to σ_0 = 3.5 MPa. The results of these tests demonstrate the effects of confining pressure on shear modulus and damping described previously.

Washed mortar sand was used to build remolded sand specimens. The sand is poorly-graded, with a medium to fine grain size, and classifies as (SP) in the Unified Classification System. For the construction of the remolded sand specimens, the undercompaction method (Ladd, 1978) was used.

Resonant column and torsional shear (RCTS) equipment was used to investigate the dynamic characteristics of the samples tested at high confining pressures, developed by the group at UT Austin (Isenhower, 1979, Lodde, 1982, Ni, 1987, and Kim, 1991). The equipment is of the fixed-free type, with the bottom of the specimen fixed and the torsional excitation applied at the top. Both resonant column (RC) and torsional shear (TS) tests were performed in a sequential series on the same specimen over a range of shearing strains from about 10^{-6} to slightly more than 10^{-3}, by changing the frequency of the forcing function.

The primary difference between the two types of tests is the excitation frequency. In the RC test, frequencies above 20 Hz are required and inertia of the specimen and drive system are needed to analyze these measurements. On the other hand, slow cyclic loading with frequencies generally below 5 Hz is prescribed in the TS tests and inertia does not enter the data analysis. Further information about the test equipment and measurement techniques

used for the aforementioned laboratory program, can be found in Appendix II of the present study.

In addition to the remolded specimens, four undisturbed specimens, two from Treasure Island and two from Lotung were tested at high confining pressures. The samples from Treasure Island were obtained from depths of 33 ft (10.1 m) and 110 ft (33.6 m) and were classified as a sand with silt (described as SP-SM in the Unified Classification System). The Lotung samples include a silty sand (SM) from a depth of 59 ft (18.0 m) and a silt (ML) from a depth of 146ft (44.5 m). For the undistirbed specimens, the confining pressures tested were based on the estimated in situ mean efffective stress, assuming the effective coefficient of earth pressure at rest $K_0 = 0.5$. The behavior of the undisturbed samples, tested over a range of confining pressures varying from 0.25 $\bar{\sigma}_m \div 4.00\ \bar{\sigma}_m$, was very similar to that of the remolded specimens.

Figures 2.3 and 2.4 show the shear modulus degradation and material damping curves of a remolded sand specimen for different values of confining pressure respectively. The results show that the elastic threshold (i.e. the cyclic strain at the linear limit), increases with the confining pressure.

Figures 2.5 and 2.6, on the other hand, show the dependence with the level of confinement of the small-strain shear modulus, G_{max} and material damping, ξ_{min}. Clearly, materials with higher confinement are stiffer at small values of strains.

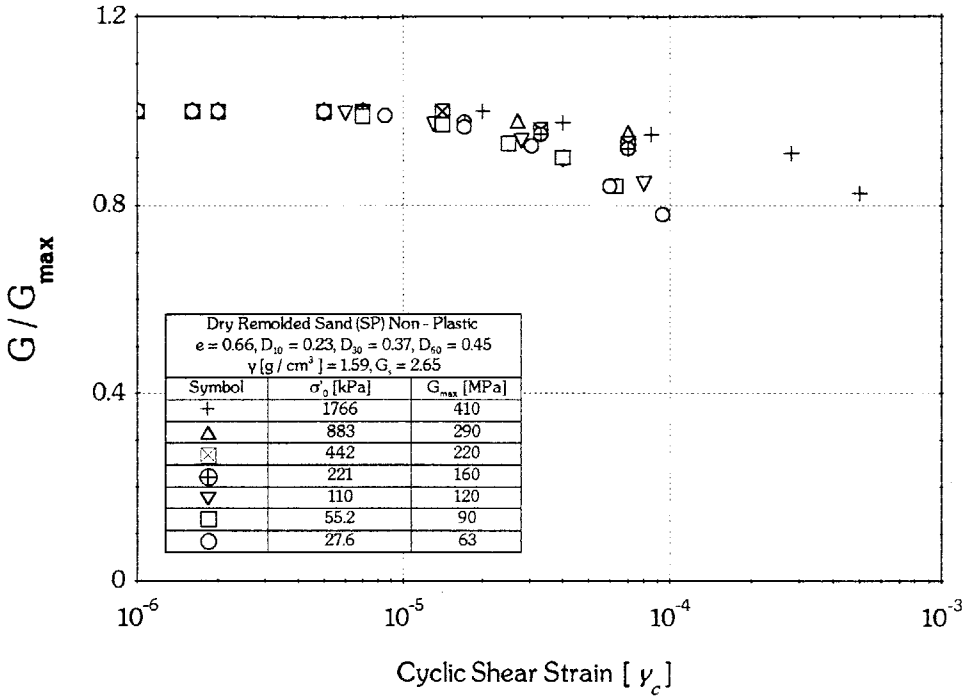

Figure 2.3 Effect of Confining Pressure on Shear Modulus Degradation Curves measured for Dry Remolded Sand (Laird & Stokoe, 1993)

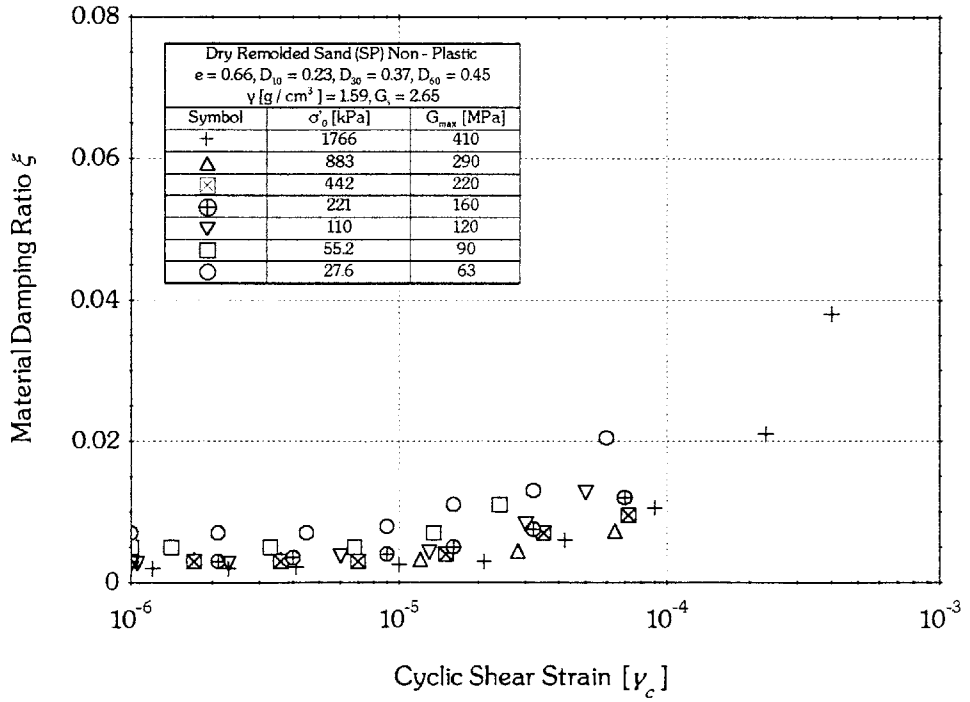

Figure 2.4 Effect of Confining Pressure on Material Damping Ratio measured for Dry Remolded Sand (Laird & Stokoe, 1993)

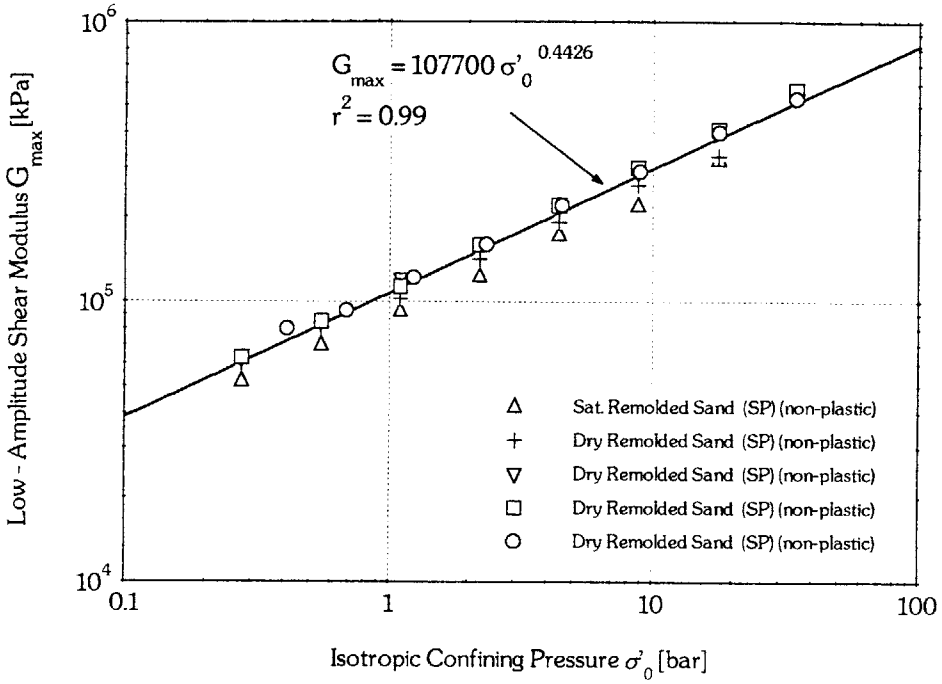

Figure 2.5 Variation in Maximum (Low Amplitude) Shear Modulus with Confining Pressure for Remolded Sand Samples (Laird & Stokoe, 1993)

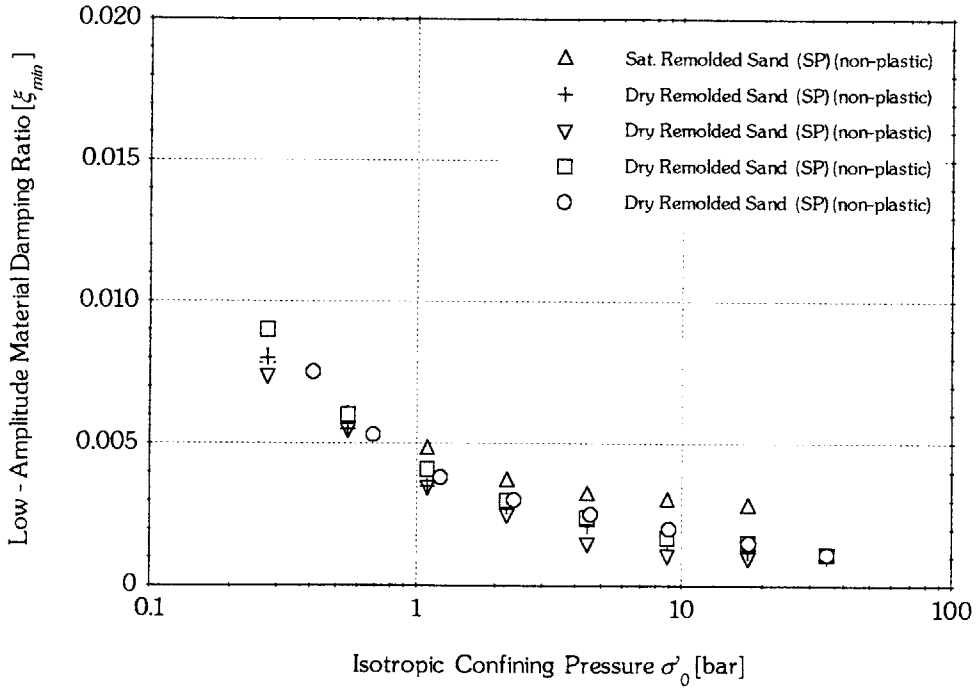

Figure 2.6 Variation in Low-Amplitude Material Damping Ratio with Confining Pressure for Remolded Sand Samples (Laird & Stokoe, 1993)

2.5 CONCLUSIONS

The most important environmental and loading conditions on the shear modulus degradation and damping curves have been briefly introduced, and special emphasis has been given to the effect of confining pressure on the dynamic soil behavior.

Experimental results performed over a wide range of mean effective stresses have been presented, alerting the need of taking into account the confining pressure effects, especially when deep soil deposits are studied.

The need to implement concisely the experimental results presented previously into a computer code for seismic amplification provided the motivation for formulating a theoretical model representing the effect of confining pressure on the soil behavior under cyclic loading (see Chapter 3).

2.6 REFERENCES

Chen, A. T. F., Stokoe, K. H., II (1979). "Interpretation of Strain Dependent Modulus and Damping from Torsional Soil Tests", Report No. USGS - GD - 79 - 002, NTIS NO. PB - 298479, U.S. Geological Survey, 46 P.

Dobry, R., Ladd, R.S., Yokel, F.Y., Chung, R.M. & Powell, D. (1982). "Prediction of pore water pressure buildup and liquefaction of sands during earthquakes using the cyclic strain method", *NBS Building Science Series 138*, National Bureau of Standards, Gaithersburg, Maryland

Hardin, B. O. (1965). "The nature of damping in sands", *Journal of Soil Mechanics and Foundation Engineering Division*, ASCE, Vol. 91, No. SM1, February, pp. 33-65.

Hardin, B. O. & Drnevich, V. P. (1970)." Shear modulus and damping in soils: I. Measurement and parameter effects, II. Design equations and curves" , *Technical Reports UKY 27-70-CE 2 and 3*, College of Engineering, University of Kentucky, Lexington, Kentucky.

Hardin, B. O. & Drnevich, V. P. (1972a)." Shear modulus and damping in soils: Measurement and parameter effects" , *Journal of Soil Mechanics and Foundation Engineering Division*, ASCE, Vol. 98, No. SM6, June, pp. 603-624.

Hardin, B. O. & Drnevich, V. P. (1972b)." Shear modulus and damping in soils: Design equations and curves" , *Journal of Soil Mechanics and Foundation Engineering Division*, ASCE, Vol. 98, No. SM7, pp. 667-692.

Isenhower, W. M. (1979). "Torsional Simple Shear/Resonant Column Properties of San Francisco Bay Mud", *M.S. Thesis*, GT 80-1, University of Texas at Austin, December, pp. 307.

Iwasaki, T., Tatsuoka, F. & Takagi, Y. (1978). "Shear Moduli of Sands under Cyclic Torsional Shear Loading", *Soils and Foundations*, Vol. 18, No. 1, pp. 39-56.

Kim, D.S. (1991). "Deformational Characteristics of Soils at Small to Intermediate Strains from Cyclic Tests", *Ph.D. Dissertation*, Geotechnical Engineering, Department of Civil Engineering, University of Texas at Austin, August.

Ladd, R.S. (1978). "Preparing Test Specimens using Undercompaction", *Geotechnical Testing Journal*, ASTM, Vol. 1, No. 1, March, pp. 16-23.

Laird, J. P. & Stokoe, K. H. (1993). " Dynamic properties of remolded and undisturbed soil samples tested at high confining pressures" , *Geotechnical Engineering Report GR93-6*, Electrical Power Research Institute.

Ni, S. H. (1987). "Dynamic Properties of Sand under True Triaxial Stress States from Resonant Column/Torsional Shear Tests", *Ph.D. Dissertation*, Geotechnical Engineering, Department of Civil Engineering, University of Texas at Austin, August.

Ray, R. P. & Woods, R. D. (1988)," Modulus and Damping due to uniform and variable cyclic loading" , *Journal of Geotechnical Engineering*, ASCE, **114** (8), pp. 861-876

Schnabel, P. G., Lysmer, J. & Seed, H. B. (1972). " SHAKE. A computer program for earthquake response analysis of horizontally layered sites" , *Report EERC 72-12*, University of California, Berkeley.

Seed, H. B. & Idriss, I. M. (1970)," Soil moduli and damping factors for dynamic response analyses" , *Report EERC 70-10*, Earthquake Research Center, University of California, Berkeley.

Seed, H. B., Wong R. T., Idriss, I. M. & Tokimatsu T. (1984)," Moduli and damping factors for dynamic analyses of cohesionless soils" , *Report EERC 84-14*, Earthquake Research Center, University of California, Berkeley.

Seed, H. B., Wong R. T., Idriss, I. M. & Tokimatsu T. (1986)," Moduli and damping factors for dynamic analyses of cohesionless soils" , *Journal of Soil Mechanics and Foundation Division*, ASCE, Vol. 112, No. SM11, pp. 1016-1032.

Shibata, T. & Soelarno, D. S. (1975), " Stress strain characteristics of sands under cyclic loading" , *Proc.. Japanese Society of Civil Engineering*, **239**, pp. 57-65.

Stokoe, K. H., Hwang, S. K., Lee, J. N. & Andrus, R. D. (1994)." Effects of various parameters on the stiffness and damping of soils at small to medium strains" , *Proc. Int. Symposium on Prefailure Deformation Characteristics of Geomaterials*, Japan.

Tatsuoka, F., Iwasaki, T., Fukushima, S. & Sudo, H. (1979). '' Stress Conditions and Stress Histories affecting Shear Modulus and Damping of Sand under Cyclic Loading'' , *Soils and Foundations*, Vol. 19, No. 2, pp. 29-43.

Whitman, R. V., Dobry, R. & Vucetic, M. (1997). *Soil Dynamics* (book manuscript in preparation).

CHAPTER 3

MIT-S1 MODEL FOR CLAYS AND SANDS

3.1 INTRODUCTION

The formulation and evaluation of constitutive models which can simulate reliably the complex stress - strain - strength behavior of soils is an iterative process which attempts to extend predictive capabilities, while controlling complexity such that input parameters are clearly defined.

There has been a substantial literature describing constitutive models for soils, yet suffering from one or more shortcomings which include:

i. Perhaps the most important limitation of (most) existing elasto-plastic models for sands is that their input parameters depend on density and confining pressure. This situation arises in formulations, which assume that the yield surface, peak friction angle and dilatancy rates are functions of the initial density (i.e. void ratio or relative density). As a result, the stress - strain - strength properties of a given sand at two different initial states (void ratio or relative density) are characterized as two separate materials with different sets of input parameters.

ii. In general, sand models do not describe critical state (i.e. large strain) conditions, in contrast to most existing models for cohesive soils.

iii. Most constitutive models for sands are isotropic (e.g. Lade, 1977; Nishi & Esashi, 1982; Jefferies, 1993; Crouch, 1994) although there is significant evidence that these soils exhibit not only inherent anisotropy (i.e. due to depositional conditions) but also induced anisotropy due to consolidation strain history and shear strain history. Existing models describing anisotropic stress - strain - strength properties do not describe evolving anisotropy and only describe peak conditions (e.g. Tatsuoka, 1980; Hirai, 1987; Yasufuku et al., 1991b).

iv. Finally, most models are formulated for freshly deposited (i.e. normally consolidated) sand and do not describe overconsolidated behavior. Amongst others, the bounding surface formulation (e.g. Dafalias & Hermann, 1982) has been intoduced to describe more realistically overconsolidated behavior, but they have been consistently introduced in otherwise isotropic models.

Pestana (1994) developed a generalized, effective stress soil model, referred to as MIT-S1, which describes the rate independent behavior of freshly deposited and overconsolidated soils.

The MIT-S1 model formulation is based on the incrementally linearized theory of rate-independent elastoplasticity. It retains the basic three-component structure of the MIT-E3 model (Whittle, 1987), namely:

i. An elastoplastic model for normally consolidated soils with a single yield function, and non-associated flow and hardening rules to describe the evolution of anisotropic stress-strain properties.
ii. Equations for the small strain non-linearity and hysteretic stress-strain response in unload-reload cycles.
iii. Bounding surface plasticity for irrecoverable, anisotropic and path dependent behavior of overconsolidated soils.

In addition, the MIT-S1 model addresses two well-known features of soil behavior:

i. The yield behavior is a function of previous stress history and depends on the current mean effective stress and density;
ii. Dense sands and heavily overconsolidated clays exhibit dilative behavior during shearing, while normally consolidated clays experience primarily contractive behavior.

Provided that modulus degradation and damping for 1-D wave propagation problems involve relatively small strain amplitudes (i.e. plastic components of deformation can be ignored), a reduced form of the MIT-S1 model can be used to model the behavior of granular materials under cyclic shear and constant effective stress. The goal is to develop, on a theoretical basis, the effect of confining pressure on both the shear degradation curves and the material damping. The model is then used in the simulation of one-dimensional amplification effects in a deep soil deposit. A brief description of the MIT-S1 input parameters required for one-dimensional analysis is first presented, followed by a derivation of analytical expressions for the shear modulus degradation and damping ratio curves. The following paragraphs use the notation introduced by Pestana (1994).

3.2 Model Formulation

3.2.1 Elastic Components

Most generalized soil models assume that the elastic bulk modulus is given by a power law function of the mean effective stress while the shear modulus is obtained by assuming a constant Poisson's ratio μ'. The resulting elastic formulation is found to be non-conservative (i.e., generates

or dissipates energy during a closed stress path; e.g. Houlsby, 1985). Conservative elastic formulations both for granular soils as well as clays have been recently proposed (Loret & Luong, 1982, Lade & Nelson, 1987, Houlsby, 1985). In these cases, the resulting elastic bulk and shear moduli are complex functions of the shear stress (or stress ratio), and of the mean effective stress.

In the MIT-S1 model, there is no region of true linear elastic behavior. However, the response immediately after a load reversal is controlled by the small elastic moduli (K_{max},G_{max}) defined as follows:

$$\frac{K_{max}}{p_a}=C_b\left(\frac{1+e}{e}\right)\left[1+\left(\frac{K_{max}}{2\,G_{max}}\right)\frac{\tau}{\sigma'}\right]^{1/6}\left(\frac{\sigma'}{p_a}\right)^{1/3} \qquad \{1\}$$

$$\frac{2\,G_{max}}{K_{max}}=3\left(\frac{1-2\,\mu_0'}{1+\mu_0'}\right) \qquad \{2\}$$

where $\sigma'=\sigma'_v\,(1+2\,K_0)/3$ is the mean effective stress, K_0 ($=\sigma'_{h0}/\sigma'_{v0}$) is the lateral stress coefficient, σ'_v the effective overburden pressure, p_a is the atmospheric pressure, C_b is a material constant and μ'_0 is the small strain Poisson's ratio (observed immediately after a load reversal). In principal, this ratio can be determined from the effective stress path measured during one-dimensional unloading in laboratory triaxial tests ($\Delta\varepsilon_v<0$; $\Delta\varepsilon_h=0$), where:

$$\mu_0'=\frac{(\Delta\sigma_v'/\Delta\sigma_h')}{1+(\Delta\sigma_v'/\Delta\sigma_h')} \qquad \{3\}$$

and $\Delta\sigma'_v/\Delta\sigma'_h$ is the measured effective stress path gradient after reversal.

Expressions {1} and {2} provide an incrementally conservative elastic formulation, written in terms of the tangent moduli and explicitly including the effect of the current void ratio, e , in soil stiffness.

3.2.2 Hysteretic Behavior

The description of non-linear behavior during unloading and reloading is also described by separate components for shear and volumetric response.

In modeling the response due to vertically propagating shear waves, only non-linear behavior during shear is required for 1-D problems. The perfectly hysteretic response is based on the incremental, isotropic relations between effective stress and elastic strain rates. For a load cycle in

stress space, the perfectly hysteretic model describes a closed symmetric hysteresis loop in the stress-strain response of the material, using a formulation that is piecewise continuous (i.e. the moduli vary smoothly) between stress reversal points. Table 3.1 summarizes the equations used to formulate the perfectly hysteretic MIT-S1 model for horizontal cyclic shearing of a soil that is consolidated at a constant mean effective stress level, σ'.

The ratio of shear to bulk moduli (for the specific case of $\sigma' = \sigma'_{rev}$), during shearing is given by:

$$\frac{2G}{K} = \left(\frac{2\,G_{max}}{K_{max}}\right)\frac{1}{1+\omega\,\xi_s} \qquad \{4\}$$

where ξ_s is a non-dimensional distance in stress space which describes changes in the mean effective stress and stress ratio relative to conditions at the stress reversal point (τ_{rev}). For horizontal shear analysis, this distance is:

$$\xi_s = \left|\frac{\tau - \tau_{rev}}{\sigma'}\right| \qquad \{5\}$$

ω is a constant that relates the swelling behavior and is selected from measurements of K_0 versus OCR during unloading. This parameter ω can be determined directly from the effective stress path in one-dimensional unloading:

$$\omega = \sqrt{\frac{3}{2}}\,\frac{(1+2K_{0NC})}{(1-K_{0NC})^2}\left[K_{0NC} - 1 + \frac{2\,G_{max}}{K_{max}}\left(\frac{1+2K_{0NC}}{3} - \frac{1}{OCR_1}\right)\right] \qquad \{6\}$$

where: K_{0NC} the lateral stress coefficient of the normally consolidated deposit, and

OCR_1 the overconsolidation ratio (σ'_p / σ'_v) at $K_0 = 1$.

The stress reversal point is defined from the direction of the strain rates (Hardin & Drnevich, 1972), based on the observation that the non-linearity of the soil is most appropriately described in terms of strain history. The tangent bulk modulus during one-dimensional unloading of a granular soil is described by:

$$\frac{K}{p_a} = \frac{e}{(1+e)\,\rho_r}\left(\frac{\sigma'}{p_a}\right) \qquad \{7\}$$

$$\rho_r = \frac{(1+\omega_s \xi_s)}{C_b}\left(\frac{\sigma'}{p_a}\right)^{2/3} \qquad \{8\}$$

where ρ_r is the current (tangential) slope of the hydrostatic swelling curve in a log$e$ - logσ' space diagram and ω_s describes small strain non-linearity during undrained shear.

3.3 Evaluation of Model Input Parameters

The *dimensionless* material parameters needed to evaluate the stress strain behavior of a soil deposit under cyclic loading using the MIT-S1 model, which can be measured directly or estimated with similar procedures for both sands and clays, are summarized below:

i. K_{0NC}, is the coefficient of lateral earth pressure at rest. It can be directly measured from K_0 consolidation or from oedometer tests. It can also be estimated from empirical formulae (i.e., $K_{0NC} = 1 - \sin\varphi'_{cs}$; Jaky, 1948; Mesri & Hayat, 1993), with φ'_{cs} being the friction angle at large strain conditions (critical state) in triaxial compression. For sands, this parameter is well-bounded with values $\varphi'_{cs} = 33.6° \pm 2.5°$. For practical applications, and in the light of the uncertainties of the present analysis, the author has assumed $K_0 = K_{0NC}$ and $K_0 = 0.5$.

ii. μ'_0 , is the elastic Poisson's ratio immediately after load reversal, and controls the ratio of small strain elastic moduli (i.e. 2 G_{max} /K_{max}). It is determined from the initial slope of the stress path during 1-D swelling. For uncemented materials, the expected range of μ'_0 is narrow with typical values $\mu'_0 = 0.20 - 0.25$ for both clays and freshly deposited sands.

iii. ω describes the variation of the elastic Poisson's ratio accompanying changes in the stress ratio (equation {6}). Common values of ω are found to be $\omega = 1.0 \pm 0.5$ for both clays and sands (Pestana, 1994).

iv. C_b defines the elastic bulk modulus at small strain levels (i.e. K_{max} at stress reversal). For clean uniform sands, average values of C_b are in the range 800 ± 100. For clays, on the other hand, the parameter C_b decreases as the plasticity index increases. For low plasticity clays, Pestana & Whittle (1994) report typical values of $C_b = 400 - 500$.

v. ω_s describes the small-strain non-linearity in shear and it is evaluated through the analysis of shear modulus degradation with strain level.

3.4 EVALUATION OF SECANT SHEAR MODULUS REDUCTION CURVES

The MIT-S1 model formulation was next specialized and used to develop analytical expressions for the secant shear modulus (G_{sec}) in terms of the maximum cyclic strain (γ_c), based on the definition of the tangential shear modulus $G_{tan}=d\tau/d\gamma$ (Table 3.1). For the evaluation of the shear modulus degradation curves, only the analytical expression of the backbone curve (τ_{rev} = 0, γ_{rev} = 0) is needed:

$$\gamma(\tau)=\frac{1}{3}C\,C_1C_2\tau^3+\frac{1}{2}C\left(C_1+C_2\right)\tau^2+C\,\tau \qquad \{9\}$$

where:

$$C=\frac{2e}{1+e}\,\frac{1+\mu_0'}{1-2\mu_0'}\,\frac{1}{3C_b}\,\frac{1}{\sigma'}\left(\frac{\sigma'}{p_a}\right)^{2/3} \qquad \{10\}$$

$$C_1=\frac{\omega_s}{\sigma'}\ ;\ C_2=\frac{\omega}{\sigma'}$$

are parameters with constant value for a given soil and level of confining pressure. The backbone curve is then defined as follows:

$$\tau(\gamma)=\frac{\left[\left(A+2C_1C_2B^{1/2}\right)C^2\right]^{1/3}}{2C\,C_1C_2}+\frac{C\left(C_1^2-C_2^2\right)}{2C_1C_2\left[\left(A+2C_1C_2B^{1/2}\right)C^2\right]^{1/3}}-\frac{C_1+C_2}{2C_1C_2} \qquad \{11\}$$

where:

$$A=12C_1^2C_2^2\gamma+3C\,C_1C_2\left(C_1+C_2\right)-C\left(C_1^3+C_2^3\right)$$

$$B=\left(6C_1C_2\right)^2\gamma^2+\left[18C\,C_1C_2\left(C_1+C_2\right)-6C\left(C_1^3+C_2^3\right)\right]\gamma+10C^2C_1C_2-3C^2\left(C_1^2+C_2^2\right)$$

Finally, the secant shear modulus can be written as a function of the maximum strain level:

$$G(\gamma_c)=\frac{\tau(\gamma_c)}{\gamma_c} \qquad \{12\}$$

For a given soil type, i.e. provided that the soil model parameters remain constant, this modulus differs for each level of confining pressure.

Four input constants are necessary to define the backbone curve given by equation {12}. However, default values for three of these parameters (μ'_0, C_b, ω) can be assumed without significant lack of accuracy, and only the constant ω_s must be specified for a given soil type. The proposed equations will then generate modulus degradation and damping curves, for all void ratios, e, and confining pressures, σ'.

Figure 3.1 shows a comparison between the shear modulus reduction curves predicted by the proposed formulation and the experimental data presented by Laird & Stokoe (1993), using $\omega_s = 2.40$. Results are found to be in very good agreement for all tests with $\sigma' = 28$ to 1800 kPa.

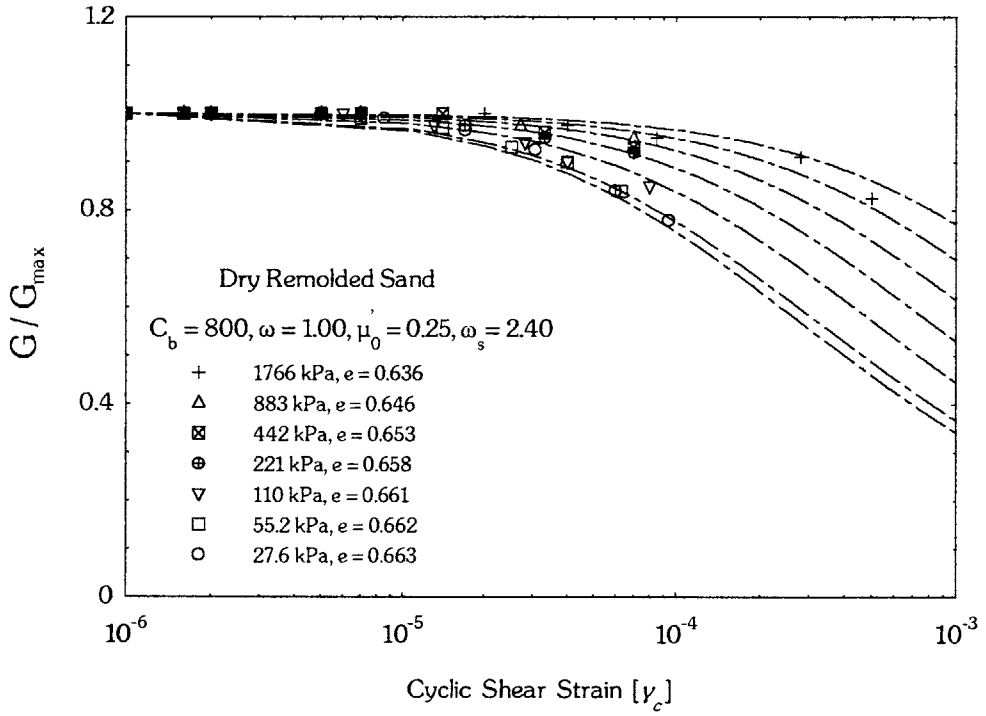

Figure 3.1 Comparison of Measured Degradation Curves for Remolded Sand Specimens with proposed model predictions.

3.5 Material Damping using MIT-S1 Model

Starting from the analytical expression for the backbone curve in the previous section, the theoretical value of material damping (ξ) can also be derived as a function of maximum cyclic shear strain (γ_c) for different levels of mean effective stress (σ'_0). For this purpose, the area within the hysteresis loop must be evaluated. It is convenient to introduce the auxiliary variables shown in Fig. 3.2.

$$\tau' = \frac{\tau + \tau_c}{2} \quad , \quad \gamma' = \frac{\gamma + \gamma_c}{2} \qquad \{13\}$$

These denote a shift of the origin of the coordinates to the lower-left reversal point, and a scaling of the coordinates by a factor 0.5. Therefore, areas measured in the transformed coordinate system are one-quarter the areas in the actual shear stress-strain coordinate system.

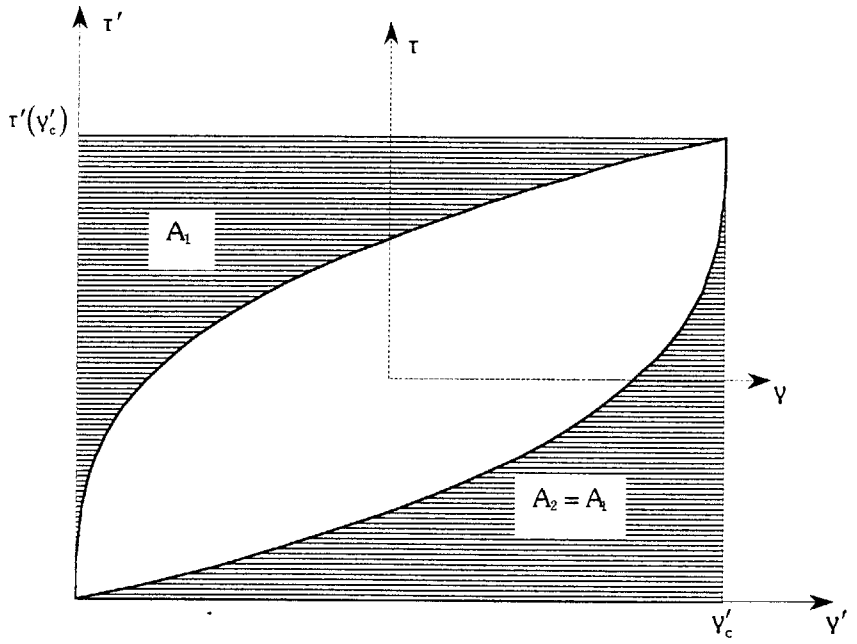

Figure 3.2 Integration of hysteresis loop to assess material damping.

The shaded area above the loop can be obtained (in local coordinates) as:

$$A_1 = \int_0^{\tau_c} \gamma' \, d\tau' = \int_0^{\tau_c} \left[\frac{1}{3} C\, C_1 C_2 \left(\tau'\right)^3 + \frac{1}{2} C \left(C_1 + C_2\right)\left(\tau'\right)^2 + C\left(\tau'\right) \right] d\tau' = \tag{14}$$

$$= \frac{1}{12} C\, C_1 C_2 \left(\tau_c\right)^4 + \frac{1}{6} C \left(C_1 + C_2\right)\left(\tau_c\right)^3 + \frac{1}{2} C \left(\tau_c\right)^2$$

Therefore, using this transformation, the area within the hysteresis loop is given by:

$$\Delta E = 4 \left[\tau_c \cdot \gamma_c - 2\, A_1 \right] \tag{15}$$

Using the fundamental definition, the resulting material damping is:

$$\xi(\gamma_c) = \frac{1}{2\pi}\frac{\Delta E}{G(\gamma_c)\cdot\gamma_c^{\,2}}$$
$$= \frac{2}{\pi}\left[1 - G(\gamma_c)\cdot\left(\frac{1}{6}CC_1C_2(\tau_c)^2 + \frac{1}{3}C(C_1+C_2)(\tau_c) + C\right)\right] \quad \{16\}$$

where $G(\gamma_c)$ is the secant modulus associated with the strain amplitude γ_c, and $\tau(\gamma_c) = \tau_c$ is defined in equation {11}, for $\gamma = \gamma_c$. The results are also summarized in Table 3.1.

Figure 3.3 shows very good agreement between the damping predicted by equation {16} at different levels of confinement ($\dot{\sigma}_0$ = 0 to 1766 kPa), with the experimental data on dry remolded sand specimens.

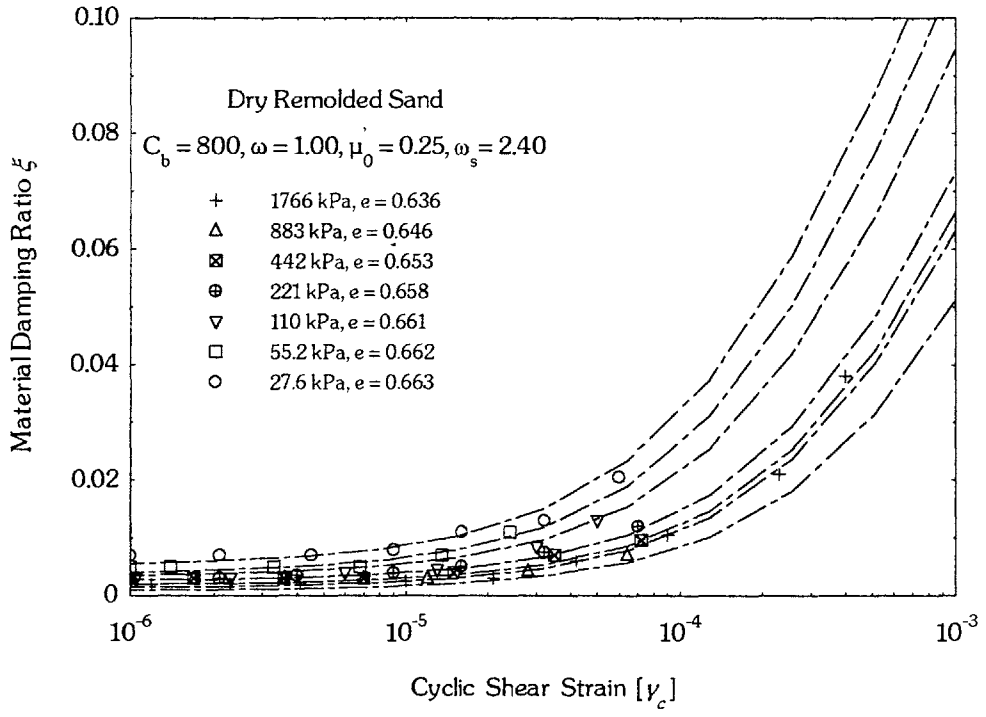

Figure 3.3 Comparison of Experimental Material Damping on Dry Remolded Sand Specimens and proposed model at different levels of confining pressure.

3.6 MIT-S1 Compression Model

Figure 3.4 summarizes the characteristic features of the compression model for cohesionless soils proposed by Pestana (1994). The model describes the recoverable and irrecoverable strain components during hydrostatic compression over a wide range of densities and confinig pressures. Sand specimens compressed from different initial formation densities

approach a unique response at high stress levels, referred to as Limiting Compression Curve (LCC). The behavior in the LCC regime can be described by a linear relationship in a log$e$ - logσ' space, defined by the slope, ρ_c, referred to as soil matrix compressibility, and the reference stress at a unit void ratio, σ'_r.

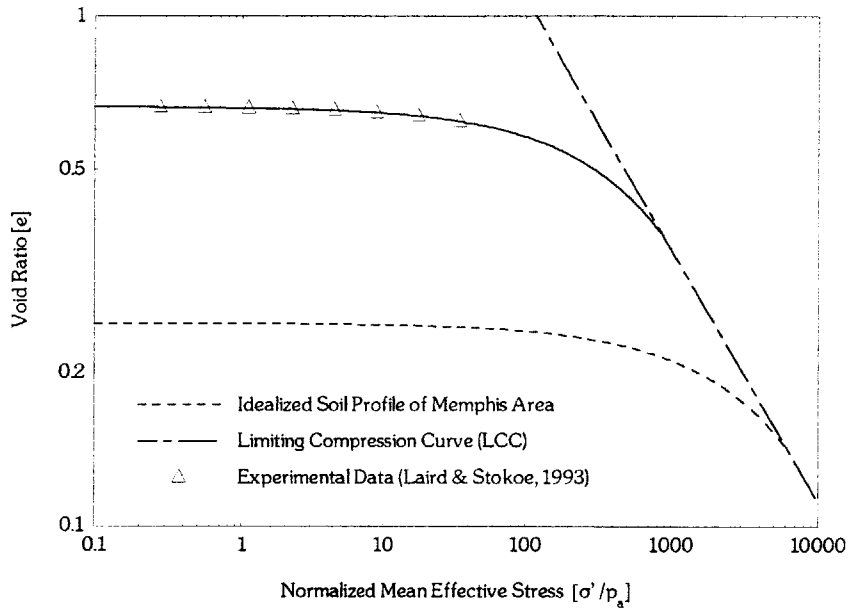

Figure 3.4 Void ratio as function of mean effective stress

The model describes irrecoverable, plastic strains, which develop thoughout first loading and represents mechanisms ranging from particle sliding and rolling at low stresses, to crushing, which is the principal component of deformation for LCC states. The behavior in the transitional regime is controlled primarily by the formation density. The proposed model makes two assumptions:

i. The incremental volume strains can be subdivided into elastic and plastic components:

$$d\varepsilon = d\varepsilon^e + d\varepsilon^p \qquad \{17\}$$

ii. The tangent bulk modulus, K, for loading can be written as a separable function of the current void ratio, e, and the mean effective stress, σ'.

The variation of void ratio with confining pressure is given by:

$$\ln\left(\frac{e}{e_0}\right) = -\frac{1}{2/3 \cdot C} \cdot \left(\frac{\sigma'}{p_a}\right)^{2/3} \quad ; \text{for first loading} \qquad \{18a\}$$

$$\ln(e) = \exp\left(-\frac{1}{C} \cdot \ln\left(\frac{\sigma'}{\sigma_r'} \right) \right) \quad \text{; for the Limiting Compression Curve Regime (LCC)} \qquad \{18b\}$$

where e_0 is the void ratio at $\sigma' = 0$; σ'_r is a 'reference stress' defined at $e = 1.00$; and $C = 1 / \rho_c$, with ρ_c being the slope of the Limiting Compression Curve in $\log e$ - $\log \sigma'$ space.

The MIT-S1 compression model assumes that the soil particles are incompressible and that there is free drainage of pore fluid within the soil skeleton. The selection of a general functional form for K (equation {7}), and the linearization of LCC behavior (equation {18b}), lead to a conceptual framework for describing hydrostatic compression of freshly deposited cohesionless soils.

There are two conceptual limits on the formulation of the MIT-S1 compression model, arising primarily from the basic assumptions of the particle compressibility and pore fluid drainage. In particular:

i. σ'_{lim} , an upper limit on effective stress, where compressibility of the solid particles is significant; and

ii. e_{lim} , a lower limit where the void space becomes discontinuous and assumptions of free drainage are no longer valid.

3.7 EXAMPLE OF APPLICATION

An idealized soil profile of depth 1000m and mass density varying from 2.12 ton/m^3 at the surface to 2.21 ton/m^3 at 1000m depth, is subjected to an earthquake prescribed at the outcropping of rock. Two simulations are carried out in which the input motions are, respectively, the 1995 Kobe (Japan) and the 1989 Loma Prieta (California) earthquakes, both scaled to a maximum acceleration of 0.05g. The soil parameters are chosen identical to the remolded sand specimens from Laird & Stokoe (1993). The variation of void ratio (and mass density) of the profile with depth was chosen to match the soil properties in Memphis, Tennessee, as reported by Abrams & Shinozuka (1997).

Table 3.2 lists the dimensionless input parameters for this model. These are used both to estimate the small strain ($\gamma = 10^{-6}$) shear modulus G_{max} and to determine the modulus degradation and damping curves. The variation of the shear wave velocity with depth is depicted in Figure 3.5, along with the reported profile for the Memphis area (Abrams & Shinozuka, 1997). The

fundamental shear-beam frequency of the soil for this profile is 0.156 Hz, and there are some twenty resonant modes in the 0-5 Hz frequency range.

C_b	800
ω	1
μ'_0	0.25
ω_s	2.4
e_0	0.25
σ'_{rev} / p_a	6051
C	2.26

Table 3.2 Input parameters for MIT-S1 model

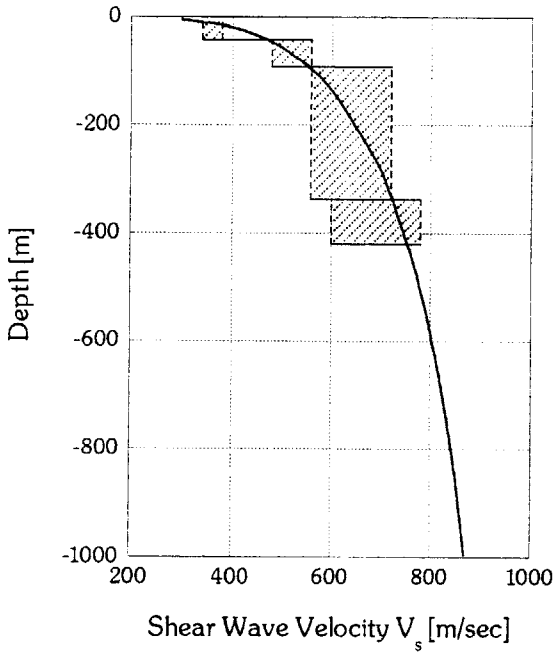

Figure 3.5 Soil profile used for 1-D soil amplification simulation (measured data from Memphis area by Abrams & Shinozuka, 1997)

The variation of void ratio with the mean effective stress is taken from the original formulation for the MIT-S1 model for cohesionless soils (Pestana & Whittle, 1995).

The dynamic response of the profile at the surface is calculated using the computer code LAYSOL (Kausel, 1992), which is based on a continuum formulation of the wave propagation problem in the frequency-wavenumber domain. The soil profile is divided into 100 homogeneous layers of 10m thickness each, whose material properties are inferred from Fig. 3.5 (taking the values at the center of the layers).

Figures 3.6 and 3.7 present the simulation results for the Kobe and Loma-Prieta earthquakes respectively. The time histories of these earthquakes are shown at the top in part (a) of these figures. Parts (b) exhibit the simulated motions at the free surface, while parts (c) depict the corresponding Fourier amplitude spectra. The left hand side shows the results obtained with the proposed pressure dependent model formulation (reduced MIT-S1 model), while the right hand side displays those for the standard Seed-Idriss model for cohesionless soils. For convenience, both sets of figures are drawn to the same scale. Inspection of these figures reveals several important differences between the standard and proposed models:

- The new model produces generally larger amplifications.
- The high-frequency components suffer much less filtering.
- The duration of strong motion as well as total response duration are longer

All three items above are caused primarily by the decrease in damping with confining pressure, and therefore, with depth.

The figures also show a characteristic 1.6 sec delay in initiation of the response at the surface. This is consistent with the travel time of shear waves between the basal rock and the surface with an average velocity of 600 m/s (as can be inferred from the 1/6 Hz resonant frequency and the 1000 m thickness). Hence, the simulations do satisfy causality. In addition, the reader should observe that while the response was obtained by Fourier-inversion of the frequency response functions, the time histories do not suffer from wraparound (i.e. the ' dog bites tail phenomenon). In other words, the coda of the response does not spill into its beginning, as could have been expected for the lightly damped system with long natural period being considered here. These desirable characteristics are accomplished with the' complex exponential window method described by Kausel & Roesset (1992).

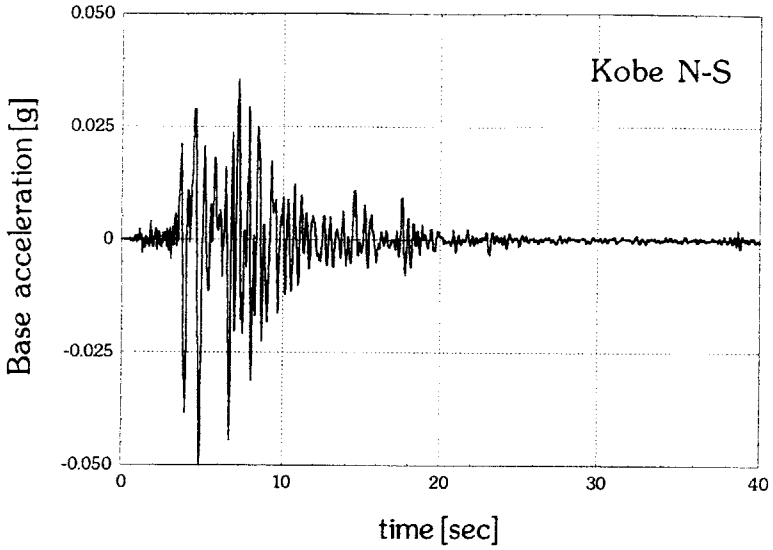

(a)

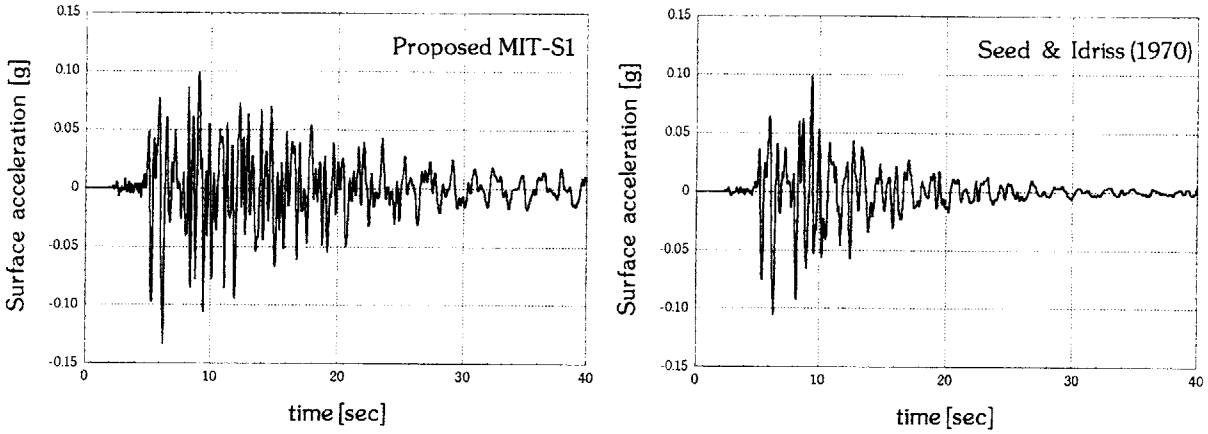

(b)

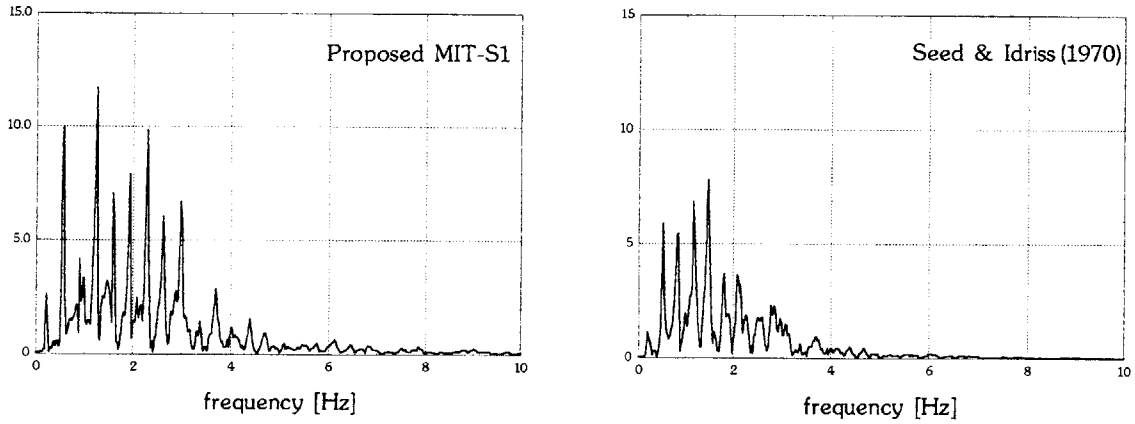

(c)

Figure 3.6 Simulation of wave propagation in deep soil deposit for Kobe earthquake: (a) Input motion, (b) surface response, and (c) Fourier Spectra

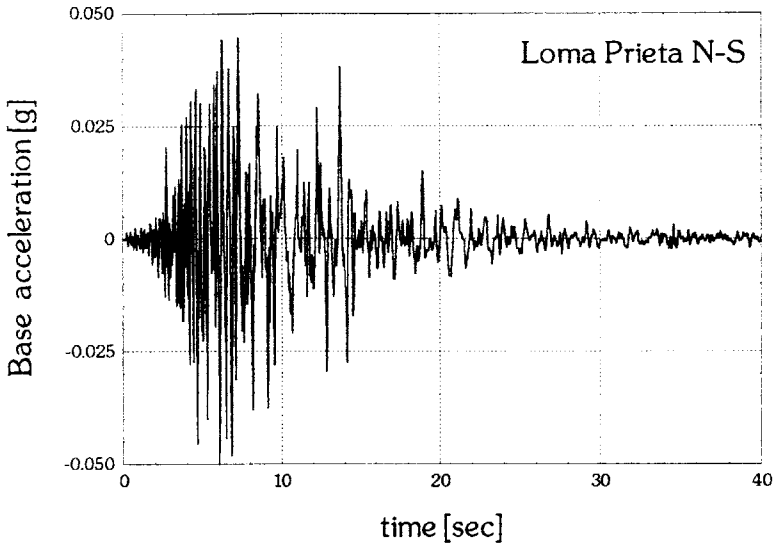

(a)

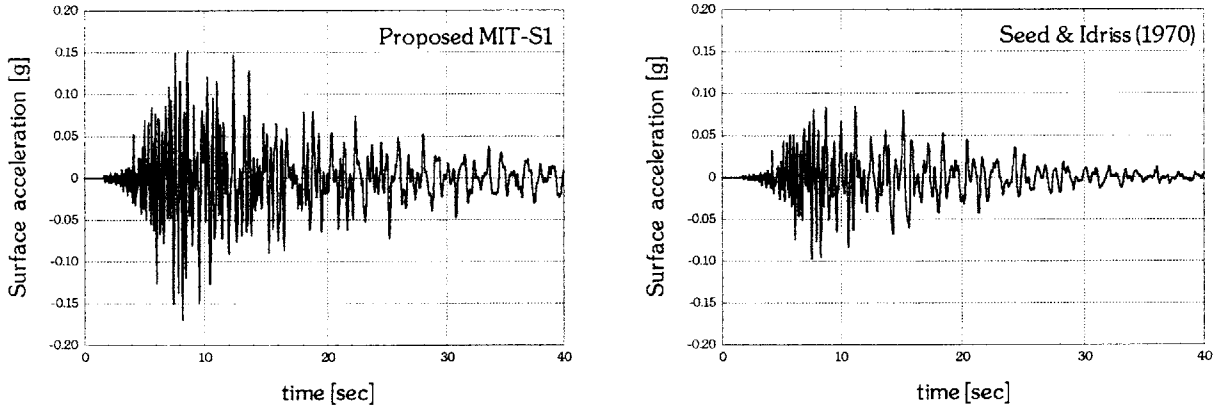

(b)

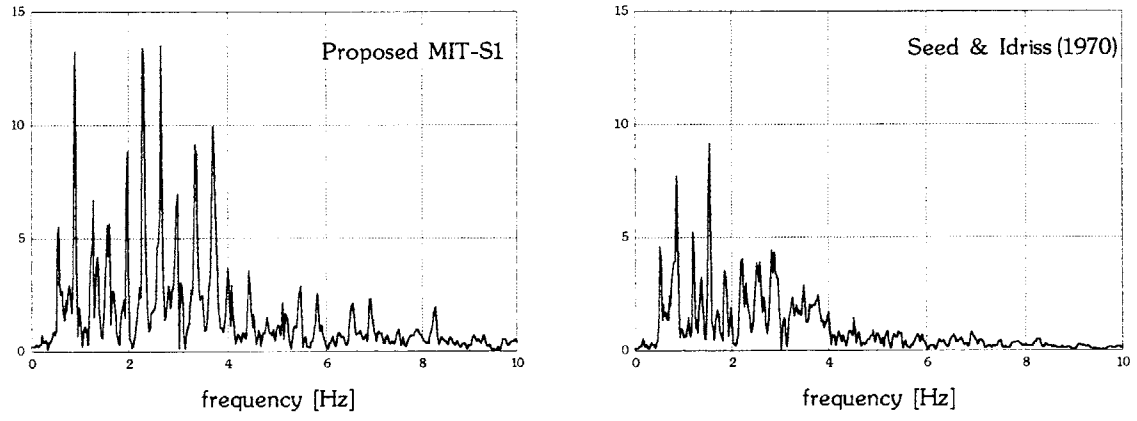

(c)

Figure 3.7 Simulation of wave propagation in deep soil deposit for Loma-Prieta earthquake: (a) Input motion, (b) surface response, and (c) Fourier Spectra

3.8 CONCLUSIONS

This chapter presented a simple four-parameter model for the dynamic shear moduli and damping characteristics of granular soils when they deform in shear only. This model is based on the MIT-S1 generalized plasticity model proposed earlier by Pestana and Whittle (1995). Its four parameters can readily be measured in the laboratory, or estimated from existing data. The shear moduli and damping values predicted by the proposed model were found to be in excellent agreement with experimental results obtained by Laird and Stokoe (1993) over a wide range of confining pressures.

The proposed formulation takes into account the effect of confining pressure on soil parameters and hysteretic behavior, and therefore, permits proper consideration of the hysteretic characteristics of the ground with depth. As demonstrated with two simulations for a 1 km deep site, the dependence of the dynamic moduli on confining pressure can be an important consideration in the analysis of soil deposits for earthquake effects.

The simulations indicate that when the confining pressure is taken into account, the elasticity of the soil steadily increases with depth. The refinement introduced by the pressure-dependant characterization of the soil in turn alleviates significantly one of the alleged shortcomings of the standard equivalent-linear model, which is that it unrealistically wipes out the high-frequency components of motion when used for moderately deep to very deep soil profiles.

3.9 REFERENCES

Abrams, D.P. & Shinozuka, M. (1997)." Loss Assessment of Memphis Buildings" , *Technical Report NCEER-97-0018.*

Constantopoulos, I.V., Roesset, J.M. & Christian, J.T. (1973). "A comparison of linear and nonlinear analyses of soil amplification". *5th World Conference on Earthquake Engineering*, Rome

Dobry, R., Ladd, R.S., Yokel, F.Y., Chung, R.M. & Powell, D. (1982). "Prediction of pore water pressure buildup and liquefaction of sands during earthquakes using the cyclic strain method", *NBS Building Science Series 138*, National Bureau of Standards, Gaithersburg, Maryland

Hardin, B. O. (1965). "The nature of damping in sands", *Journal of Soil Mechanics and Foundation Engineering Division*, ASCE, Vol. 91, No. SM1, February, pp. 33-65.

Hardin, B. O. & Drnevich, V. P. (1970)." Shear modulus and damping in soils: I. Measurement and parameter effects, II. Design equations and curves" , *Technical Reports UKY 27-70-CE 2 and 3*, College of Engineering, University of Kentucky, Lexington, Kentucky.

Hardin, B. O. & Drnevich, V. P. (1972a)." Shear modulus and damping in soils: Measurement and parameter effects" , *Journal of Soil Mechanics and Foundation Engineering Division*, ASCE, Vol. 98, No. SM6, June, pp. 603-624.

Hardin, B. O. & Drnevich, V. P. (1972b)." Shear modulus and damping in soils: Design equations and curves" , *Journal of Soil Mechanics and Foundation Engineering Division*, ASCE, Vol. 98, No. SM7, pp. 667-692.

Houlsby, G.T. (1965).'' The use of a Variable Shear Modulus in Elastic-Plastic Models for Clays'' , *Computers and Geotechnics*, Vol. 1, No. 1, pp. 3-21.

Iwasaki, T., Tatsuoka, F. & Takagi, Y. (1978). "Shear Moduli of Sands under Cyclic Torsional Shear Loading", *Soils and Foundations*, Vol. 18, No. 1, pp. 39-56.

Jaky, J. (1948). "Pressure in Silos", *2nd ICSMFE*, Vol. 1, pp. 103-107.

Kausel, E. (1992)." LAYSOL: A computer program for the dynamic analysis of layered soils" .

Kausel, E. and Roesset, J.M. (1992)." Frequency domain analysis of undamped systems" , *Journal of Engineering. Mechanics*, ASCE, **118** (4), pp. 721-734

Lade, P.V. & Nelson, R.B. (1987).'' Modeling the Elastic Behavior of Antigranulocytes-Materials'' , *International Journal for Numerical and Analytical Methods in Geomechanics*, Vol. 11, No. 5, pp. 521-542.

Laird, J. P. & Stokoe, K. H. (1993)." Dynamic properties of remolded and undisturbed soil samples tested at high confining pressures" , *Geotechnical Engineering Report GR93-6*, Electrical Power Research Institute.

Loret, B. & Luong, M.P. (1982).'' Double Deformation Mechanism for Sand' , *Proc. 4th Int. Conf. Num. Meth. and Advances in Geomechanics*, Edmonton, Alberta.

Mesri, G. & Hayat, T.M. (1993). "The Coefficient of Earth Pressure at Rest", *CGJ*, Vol. 30, No. 4, August, pp. 647-666.

Ng T.T. & Dobry, R. (1992).'' A Non-linear Numerical Model for Soil Mechanics'' , *International Journal for Numerical and Analytical Methods in Geomechanics*, Vol. 16, No. 4, pp. 247-263.

Ng T.T. & Dobry, R. (1994).'' Numerical Simulations of Monotonic and Cyclic Loading of Granular Soil' , *Journal of Geotechnical Engineering*, ASCE, Vol. 120, No. 2, pp. 388-403.

Civil Engineering, University of Texas at Austin, August.

Pestana, J.M. (1994)." A unified constitutive model for sands and clays" , *ScD Thesis*, Department of Civil Engineering, Massachusetts Institute of Technology.

Pestana, J. M. & Whittle, A. J. (1994)." Model Prediction of Anisotropic Clay Behavior due to Consolidation Stress History" , *Proc. 8th Int. Conf. Comp. Meth. and Advances in Geomechanics*, Morgantown, Virginia.

Pestana, J. M. & Whittle, A. J. (1995)." Predicted effects of confining stress and density on shear behavior of sand' , *Proc. 4th Int. Conf. Computational Plasticity*, Barcelona (Spain), **2**, pp. 2319-2330.

Pestana, J. M. & Whittle, A. J. (1995)." Compression model for cohesionless soils" *Geotechnique* **45**, (4), pp. 611-631.

Shibata, T. & Soelarno, D. S. (1975)," Stress strain characteristics of sands under cyclic loading" , *Proc.. Japanese Society of Civil Engineering*, **239**, pp. 57-65.

Whittle, A.J. (1987), "A constitutive model for Overconsolidated Clays with Application to the Cyclic Loading of Friction Piles", *Sc. M. Thesis*, MIT, Cambridge, MA

PERFECTLY HYSTERETIC MODEL USED IN MIT-S1
(FOR ONE - DIMENSIONAL ANALYSIS)

DIMENSIONLESS DISTANCE MEASURE (in stress space)

$$\xi_s = \left| \frac{\tau - \tau_{rev}}{\sigma'} \right|$$

where τ, τ_{rev} are the current stress and the stress at the reversal point, respectively. For the definition of the backbone curve $\tau_{rev} = 0$.

DEFINITION OF TANGENTIAL ELASTIC MODULI

$$\frac{K}{p_a} = \frac{e}{(1+e)\,\rho_r}\left(\frac{\sigma'}{p_a}\right); \quad \text{where } \rho_r = \frac{(1+\omega_s \xi_s)}{C_b}\left(\frac{\sigma'}{p_a}\right)^{2/3}$$

$$\frac{2G}{K} = \left(\frac{2G_{max}}{K_{max}}\right)\frac{1}{1+\omega\,\xi_s} \quad \text{for } \sigma' = \sigma'_{rev}; \quad \text{where } \frac{2G_{max}}{K_{max}} = 3\left(\frac{1-2\mu_0'}{1+\mu_0'}\right)$$

where C_b and μ_0' are elastic parameters; ω and ω_s are material constants introduced to characterize the hysteresis.

DEFINITION OF BACKBONE CURVE - SECANT SHEAR MODULUS

$$\tau(\gamma) = \frac{\left[\left(A + 2C_1C_2B^{1/2}\right)C^2\right]^{1/3}}{2C\,C_1C_2} + \frac{C\left(C_1^2 - C_2^2\right)}{2C_1C_2\left[\left(A + 2C_1C_2B^{1/2}\right)C^2\right]^{1/3}} - \frac{C_1 + C_2}{2C_1C_2}$$

where:

$$A = 12\,C_1^2\,C_2^2\,\gamma + 3C\,C_1C_2\left(C_1 + C_2\right) - C\left(C_1^3 + C_2^3\right)$$

$$B = \left(6C_1C_2\right)^2\gamma^2 + \left[18\,C\,C_1C_2\left(C_1 + C_2\right) - 6C\left(C_1^3 + C_2^3\right)\right]\gamma + 10\,C^2C_1C_2 - 3C^2\left(C_1^2 + C_2^2\right)$$

$$C = \frac{2e}{1+e}\,\frac{1+\mu_0'}{1-2\mu_0'}\,\frac{1}{3C_b}\,\frac{1}{\sigma'}\left(\frac{\sigma'}{p_a}\right)^{2/3}; \quad C_1 = \frac{\omega_s}{\sigma'}; \quad C_2 = \frac{\omega}{\sigma'}$$

and C, C_1 and C_2 have constant value for each level of mean effective stress σ'.

Table 3.1 Derivation of Modulus Degradation and Damping Curves from Perfectly Hysteretic Formulation used in MIT-S1

PERFECTLY HYSTERETIC MODEL USED IN MIT-S1
(FOR ONE - DIMENSIONAL ANALYSIS)

MATERIAL DAMPING RATIO

$$\xi(\gamma_c) = \frac{2}{\pi}\left[1 - G(\gamma_c)\cdot\left(\frac{1}{6}C\,C_1C_2\,(\tau_c)^2 + \frac{1}{3}C\,(C_1 + C_2)(\tau_c) + C\right)\right]$$

where:

$G(\gamma_c)$	is the secant modulus associated with the strain amplitude γ_c
$\tau(\gamma_c) = \tau_c$	is the shear stress associated with the strain amplitude γ_c
C, C_1 and C_2	have constant value for each level of mean effective stress σ'.

Table 3.1(cont) Derivation of Modulus Degradation and Damping Curves from Perfectly Hysteretic Formulation used in MIT-S1

INPUT MATERIAL PARAMETERS FOR MIT-S1
(FOR ONE - DIMENSIONAL ANALYSIS)

COHESIONLESS SOILS (SANDS)

PARAMETER [Symbol]	PHYSICAL CONTRIBUTION [Meaning]	TEST TYPE	MEAN VALUE
ρ_c	Compressibility of Sands at large stresses [LCC regime]	Hydrostatic/Compression Test (Triaxial or Oedometer)	-
σ'_r / p_a	Reference Stress at unity Void Ratio		-
K_{0NC}	K_0 at the LCC regime	K_0 Oedometer or K_0 Triaxial	0.50
μ'	Poisson's Ratio at Load Reversal		0.25
ω	Non-linear Poisson's Ratio (1-D unloading stress path)		1.00
ω_s	Small Strain non-linearity in Shear	Undrained / Drained Triaxial Shear Tests	2.5 ± 0.5
C_b	Small Strain Stiffness at Load Reversal	Resonant Column Bender Elements	800

COHESIVE SOILS (CLAYS)

PARAMETER [Symbol]	PHYSICAL CONTRIBUTION [Meaning]	TEST TYPE	MEAN VALUE
ρ_c	Compressibility of Normally Consolidated [NC] Clay	Hydrostatic/Compression Test (Triaxial, Oedometer or CRS apparatus)	0.22 ± 0.05
K_{0NC}	K_0 for NC Clay	K_0 Oedometer or K_0 Triaxial	0.50
μ'_0	Poisson's Ratio at Stress Reversal controlling 2 G_{MAX}/K_{MAX}		0.25
ω	Non-linear Poisson's Ratio (1-D unloading stress path)		1.00
ω_s	Small Strain non-linearity in Shear	Undrained Triaxial Shear Tests	-
C_b	Small Strain Stiffness at Load Reversal	Shear Wave Velocity / Resonant Column	450

Table 3.3 Input Material Parameters for one – dimensional MIT-S1 model formulation, for cohesionless and cohesive soils

ONE – DIMENSIONAL MIT–S1 COMPRESSION MODEL

COHESIONLESS SOILS (SANDS)

For first loading

$$\ln\left(\frac{e}{e_0}\right) = -\frac{1}{2/3 \cdot C} \cdot \left(\frac{\sigma'}{p_a}\right)^{2/3}$$

For the LCC Regime

$$\ln(e) = \exp\left(-\frac{1}{C} \cdot \ln\left(\frac{\sigma'}{\sigma_r'}\right)\right)$$

where: e_0 is the void ratio at $\sigma' = 0$,

σ'_r is a 'reference stress' defined at $e = 1.00$, and

$C = 1 / \rho_c$ with ρ_c being the slope of the LCC, in log$e$ - logσ' space.

COHESIVE SOILS (CLAYS)

- Empirical Correlations for Compressibility of Normally Consolidated Clay

$$C_c = 2.303\ \rho_c\, e_0 \left[1 - \left(\frac{0.4}{e_0}\right)^2\right]$$

$$C_c = \frac{a\, w_L}{100}\left[1 - \left(\frac{20}{w_L}\right)^2\right]$$

where: $C_c = de / d\log(\dot{\sigma})$ Compression Index

w_L [%] Liquid Limit

a Empirical Constant

- Data Compilations

SOIL	Cc	SOIL	Cc
NC Medium Sensitive Clays	0.2 - 0.5	Mexico City Clay (MH)	7 - 10
Chicago Silty Clays (CL)	0.15 - 0.3	Organic Clays (OH)	› 4
Boston Blue Clay (CL)	0.3 - 0.5	Organic Silt, Clayey Silts (ML - MH)	1.5 - 4
Canadian Leda Clays (CL - CH)	1 - 4	San Fransisco Bay Mud (CL)	0.4 - 1.2

Table 3.4 One – dimensional compression MIT-S1 model formulation, for unified approach of cohesive and cohesionless soils

CHAPTER 4

REPRESENTATION OF STRESS - STRAIN RELATIONS IN CYCLIC LOADING

4.1 INTRODUCTION

Soils do not exhibit linear elastic behavior except at very small strains (less than 10^{-5}, in general). In this range the nonlinear effects while present, have little influence and can hardly be assessed because it is difficult to measure such small strains and stresses accurately.

At larger strains, such as the ones induced by relatively strong earthquakes, experimental data (Hardin & Drnevich, 1972a, 1972b; Seed & Idriss, 1969; Thiers & Seed, 1968) show that the stress-strain relationships for soils deviate from linearity, and, therefore, nonlinear effects cannot be ignored. Certain features of this relationship, whilst complicated, can be identified from available experimental data:

i. The hysteretic stress stress-strain behavior of soils is nonlinear and strain-dependent.
ii. The loops exhibit a sudden change in slope when the strain changes direction.
iii. The unloading and reloading branches of the loops appear geometrically similar when measured from the reversal point of strain.
iv. The tangent modulus upon reversal of strain is approximately the same for both the unloading and reloading parts of the loop, and is approximately equal to the initial modulus.
v. The area enclosed by each loop is the energy loss per cycle, and is independent of strain rate.

Modeling of soil behavior under cyclic or random loading conditions may be made so that the model can duplicate the deformation characteristics in the range of strains under consideration. When soil behavior is expected to stay within the small strain range (i.e. below the elastic threshold), the use of an elastic model is justified and the shear modulus is a key parameter to properly model the soil behavior.

When a given problem is associated with the medium range of strain, approximately below the level of 10^{-3}, the soil behavior becomes elastoplastic and the shear modulus tends to

decrease as the shear strain increases. At the same time, energy dissipation occurs during cycles of load application. The energy dissipation in soils is mostly rate - independent and of hysteretic nature, and the damping ratio can be used to represent the energy absorbing properties of soils. Since the strain level concerned is still small enough not to cause any progressive change in soil properties, the shear modulus and damping ratio do not change with the progression of cycles in load application. This kind of behavior is called *non-degraded hysteresis* type. Such steady-stage soil characteristics can be represented to a reasonable degree of accuracy by use of the linear viscoelastic theory. The shear modulus and damping ratio, determined as functions of shear strain, are the key parameters to represent soil properties in this medium strain range. The most useful analytical tool accommodating these strain - dependent but cycle - independent soil properties would be the equivalent linear method based on the viscoelastic concept. Generally, the linear analysis is repeated, by stepwise changing the soil parameters until a strain - compatible solution is obtained. The seismic response analysis performed for horizontally layered soil by use of the computer program SHAKE (Schnabel et al., 1972) is a typical example of an analytical tool that can be successfully used to clarify the soil response in the medium range of strain.

For the shear strain level larger than about 10^{-2}, soil properties tend to change appreciably not only with shear strain but also with the progression of cycles. This kind of behavior is termed *degraded hysteresis* type. The manner in which the shear modulus and damping change with cycles is considered to depend upon the manner of change in the effective confining stress during irregular time histories of shear stress application. When the law of changing effective stress is established, it is then necessary to have constitutive law in which stress - strain relations can be specified at each step of loading, unloading and reloading phases. One of the concepts most commonly used at present for this purpose is what is referred to as the Masing law. For analysis of a soil response accommodating such a stress - strain law covering large strain levels near failure, it is necessary to employ a numerical procedure involving the step - by - step integration technique.

In what follows, the methods of modeling soil behavior will be discussed and the soil model used for the present analysis will be described.

4.2 THE LINEAR VISCOELASTIC MODEL

When the level of cyclic shear strain is still small, of the order of 10^{-3} and 10^{-4}, the cyclic behavior of soils can be represented to a reasonable degree of accuracy by means of a constitutive model based on the classical theory of linear viscoelasticity. In this model, the stress - strain relation is assumed linear, but the energy dissipating characteristics of soils can be logically taken into account. It has been shown that there always exists a certain degree of damping in soils and it plays an important role in determining motions in soil deposits during earthquakes. Thus this model has frequently been used to represent soil behavior even in the slightly nonlinear range where damping has important effects.

4.2.1 CYCLIC STRESS - STRAIN RELATIONSHIP

Before discussing the stress - strain law for a specific viscoelastic model, the general form of expression relating the viscoelastic stresses and strains is introduced.

Let the stress and strain in any mode of deformation, such as triaxial, simple shear or torsional shear be denoted as τ and γ. Let a sinusoidally reciprocating shear stress:

$$\tau = \tau_a \sin(\omega t) \qquad \{1\}$$

be applied to a body exhibiting viscoelastic response, where τ_a is the amplitude, t is the time, and ω stands for the angular frequency or circular frequency. As a result of the shear stress application, shear strain with the same frequency will be produced, accompanied by a time delay as:

$$\gamma = \gamma_a \sin(\omega t - \delta) \qquad \{2\}$$

where γ_a is the amplitude and δ stands for the angle of phase difference indicating that the time lag in strain response, which is conveniently represented by τ / γ, is not only a function of amplitude ratio τ_a / γ_a, but also a function of the phase angle difference δ.

Making use of the complex variables method, we denote herein:

$$\tau_R = \tau_a \cos(\omega t) \qquad \{3\}$$

$$\gamma_R = \gamma_a \cos(\omega t - \delta) \qquad \{4\}$$

and it may be stated further that if a viscoelastic body is subjected to an input stress expressed in a form of complex variables as $\bar{\tau} = \tau_R + i\tau$, then the resulting response in strain

would be $\bar{\gamma} = \gamma_R + i\,\gamma$, where i is the unit imaginary number and $\bar{\tau}$ and $\bar{\gamma}$ are the stress and strain in complex variables. We therefore have:

$$\bar{\tau} = \tau_a\, e^{i\omega t} \qquad \{5\}$$

$$\bar{\gamma} = \gamma_a\, e^{i(\omega t - \delta)} \qquad \{6\}$$

The strain versus stress response can be described by the ratio $\bar{\tau}/\bar{\gamma}$, which is explicitly written as:

$$\frac{\bar{\tau}}{\bar{\gamma}} = \frac{\tau_a}{\gamma_a} e^{i\delta} = \frac{\tau_a}{\gamma_a}\left(\cos\delta + i\sin\delta\right) = \mu + i\,\mu' = \mu^* \qquad \{7\}$$

where μ and μ' are called *elastic* modulus and *loss* modulus, respectively, and μ^* is named *complex* modulus. The elastic modulus is a parameter indicative of elastic or instantaneous power and loss modulus represents the energy dissipating characteristics of the viscoelastic. Finally we have:

$$\frac{\tau_a}{\gamma_a} = \sqrt{\mu^2 + \mu'^2} = \left|\,\mu^*\,\right| \qquad \{8a\}$$

$$\tan\delta = \frac{\mu'}{\mu} = n \qquad \{8b\}$$

where n is a parameter called *loss coefficient* which is indicative of energy loss or damping characteristics. From equation {8a} and {8b}, the absolute value of the complex modulus μ^* is shown to indicate the shear modulus of the material.

It is to be noted here that the material parameters μ and μ' need not necessarily be real constants, but could be a function of the angular frequency ω. Therefore the moduli μ and μ', as defined in equation {7} are regarded as the most general expression, and consequently can take any form expressed as a function of frequency. Once a functional form is specified to these moduli, the viscoelastic behavior of the material can be described in a more tangible manner. Several methods for specifying these moduli have been proposed, either on the basis of direct experiments or on the basis of spring-dashpot models.

4.2.2 Hysteretic Stress – Strain Curve

Describing the stress – strain behavior of a viscoelastic body, the pair of equations {1} and {2} can be viewed as a stress – strain relation, correlated through a tracking parameter ωt. Therefore, by eliminating the parameter ωt, a single relation as follows is obtained:

$$\left(\frac{\tau}{\tau_a}\right)^2 - 2\cos\delta\left(\frac{\gamma}{\gamma_a}\right)\left(\frac{\tau}{\tau_a}\right) + \left(\frac{\gamma}{\gamma_a}\right)^2 - \sin^2\delta = 0 \qquad \{9\}$$

This is regarded as a second order equation with respect to τ / τ_a. Solving with reference to the definition of μ and μ', one obtains:

$$\tau = \mu\gamma \pm \mu' \sqrt{\gamma_a^2 - \gamma^2} \qquad \{10\}$$

An alternative expression is obtained by decomposing the right − hand side of equation {10} in two parts, namely:

$$\begin{aligned} &\tau = \tau_1 + \tau_2 \\ &\tau_1 = \mu\gamma \qquad \{11\} \\ &\left(\frac{\tau_2}{\mu'\gamma_a}\right)^2 + \left(\frac{\gamma}{\gamma_a}\right)^2 = 1 \end{aligned}$$

Therefore, the actual value of shear stress can be graphically represented as the addition of a straight line with slope μ (τ_1) and an ellipse (τ_2). The result of this manipulation is an ellipse with inclined axis, as shown in Fig. 4.1.

As indicated in Fig. 4.1, the inclined ellipse cut the ordinate at a shear stress point of $\mu' \cdot \gamma_a$. Therefore, the value of μ' may be taken as a measure to indicate a degree of flatness in the shape of the ellipse. The greater the value of μ', the rounder the ellipse indicating that the energy loss or damping is bigger, whereas the smaller the value of μ', the thinner the ellipse and, hence, the smaller the damping during cyclic loading.

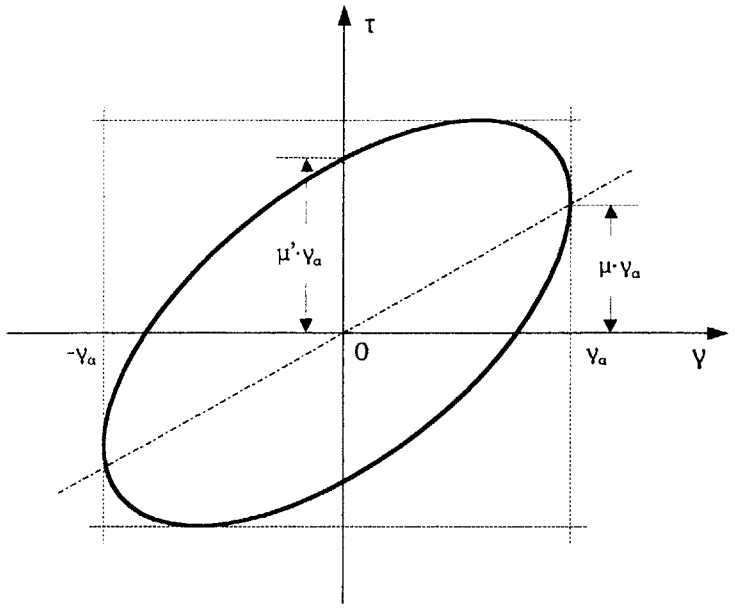

Figure 4.1 Shear stress - strain hysteresis loop of a viscoelastic material

In order to quantify the damping characteristics, the amount of energy dissipated in one cycle of load application is initially calculated. The energy loss per cycle is equal to the area enclosed by the hysteresis loop shown in Fig. 4.1, and it can be readily evaluated using the well - known formula of an ellipse:

$$\Delta W = \int \tau \, d\gamma = \mu' \pi \gamma_a^2 \qquad \{12\}$$

Next we consider the maximum elastic energy stored in a unit volume of a viscoelastic body. The stored energy is defined by the elastic component of the shear stress τ_1. Therefore, using eq. {11}, the energy is expressed as follows:

$$W = \frac{1}{2} \tau_1 \gamma_a = \frac{1}{2} \mu \gamma_a^2 \qquad \{13\}$$

As a measure of the damping characteristics, the ratio of energy loss per cycle to the maximum stored energy is evaluated, and the loss coefficient, n, is thereafter calculated as follows:

$$\frac{\Delta W}{W} = \frac{\mu' \pi \gamma_a^2}{\frac{1}{2} \mu \gamma_a^2} = 2\pi \frac{\mu'}{\mu}$$

$$n = \frac{1}{2\pi} \frac{\Delta W}{W} = \frac{\mu'}{\mu} = \tan\delta \qquad \{14\}$$

The above procedure may be used most conveniently to calculate the loss coefficient, even in case of nonlinear hysteresis curves where the linear viscoelasticity is no longer exactly applicable.

4.2.3 Model Representation by the Spring - Dashpot System

The viscoelastic behavior of a body discussed above has been also examined by using spring - dashpot systems. In this type of model, the elastic property is represented by a spring and the damping characteristics are represented by a dashpot, connected in parallel or in series, as illustrated in Figure 4.2.

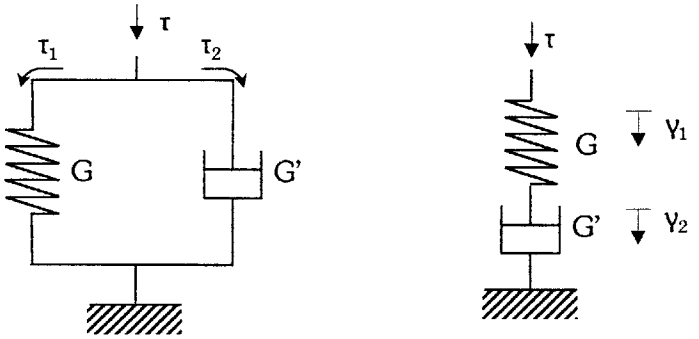

(a) Kelvin Model (b) Maxwell Model

Figure 4.2 Typical viscoelastic models

Even if it is well known that the energy loss can occur from numerous different internal mechanisms in a deforming body, the dashpot can represent energy loss characteristics due only to the viscosity, that is, the damping generated in proportion to the velocity or time rate of deformation. This kind of energy loss is referred to as *rate - dependent damping*. In case of cyclic loading, the *rate dependency* is manifested in such a way that the deformation depends upon frequency.

- Kelvin model

The most widely used model is the Kelvin model, consisting of a spring and a dashpot connected in parallel, as shown in Fig. 4.2 (a). In this model, while the strain γ is imposed equally to two elements, the stress τ is divided in two parts: One carried by the spring, τ_1 and the other borne by the dashpot, τ_2. Therefore, according to equation {11}, the total stress is evaluated as follows:

$$\tau = G\gamma + G' \frac{d\gamma}{d\tau} \qquad \{15\}$$

- Maxwell model

This model consists of a spring and a dashpot connected in series, as shown in Fig. 4.2 (b). In this model, the stress τ is carried commonly but the strain γ consists of two parts: γ_1 coming from the deformation of the spring γ_2 resulting from the dashpot deformation. Therefore, the stress - strain relationship for the Maxwell model is evaluated as follows:

$$\frac{\tau}{G'} + \frac{1}{G}\frac{d\tau}{dt} = \frac{d\gamma}{dt} \qquad \{16\}$$

Evaluating the loss coefficient for each one of the aforementioned viscoelastic models, it can be proven that:

$$\begin{aligned} n = \tan\delta &= \frac{G'\omega}{G} \qquad \text{Kelvin Model} \\ n = \tan\delta &= \frac{G}{\omega G'} \qquad \text{Maxwell Model} \end{aligned} \qquad \{17\}$$

Therefore, the damping evaluated by means of the two models is frequency dependent, with the Kelvin model loss coefficient increasing and the Maxwell model loss coefficient decreasing with increasing frequency in cyclic loading.

4.3 THE NON - LINEAR CYCLE INDEPENDENT MODEL

When the amplitude of shear strain is still small, the response of soils does not change with the progression of cycles and therefore the modulus and damping properties remain the same throughout the duration of cyclic stress application. However, the level of shear strain is assumed to be large enough to produce a nonlinear hysteresis loop in the cyclic stress – strain relationship. This type of soil behavior seems to be manifested when the induced shear strain is within the range approximately between 10^{-5} and 10^{-3}.

Modeling the stress – strain nonlinear soil behavior, two types of curves need to be specified. In particular, one is associated with monotonic loading and the other constitutes a cyclic loop. The former is referred to as *backbone* curve or *skeleton* curve and the latter is called a *hysteresis* loop. As an extension to the nonlinear case, it may be mentioned that the skeleton curve and the hysteresis loop indicate respectively, the elastic property and energy dissipating characteristics, which are nonlinear. Due to this feature, the skeleton curve is not a straight line nor does the hysteresis loop have rounded corners.

In constructing a nonlinear cyclic stress – strain relation, two basic functions need to be specified, one for the backbone curve and the other for the hysteresis loop. The backbone curve can be expressed by the following relationship:

$$\tau = f(\gamma) \qquad \{18\}$$

which is obtained from monotonic loading tests on soils. For the load reversal occurring at point (γ_a, τ_a), the equation of the stress – strain curve for the subsequent unloading is given as:

$$\frac{\tau - \tau_a}{2} = f\left(\frac{\gamma - \gamma_a}{2}\right) \qquad \{19\}$$

The unloading branch of the stress – strain curve as defined above implies that a half part of the hysteresis curve is obtained by two – fold stretching of the skeleton curve and by translating its one end to the point of the stress reversal. Similarly, for reloading occurring at point $(-\gamma_a, -\tau_a)$, the stress – strain curve for the reloading branch is now given by:

$$\frac{\tau + \tau_a}{2} = f\left(\frac{\gamma + \gamma_a}{2}\right) \qquad \{20\}$$

It is shown that the reloading branch defined by equation {20} intersects the backbone curve at the initial point of stress reversal. Thus the pair of curves defined by equations {19} and {20} constitute a complete closed loop representing the nonlinear hysteresis curve in the cyclic loading. The rule for constructing the unloading and reloading branches as above using a skeleton curve is called the *Masing rule*.

The characteristics of hysteretic stress-strain behavior of soils, which have been summarized above and have been experimentally observed, are similar to observations made by *Masing*, who studied the plastic deformations of metals under uniaxial simple cyclic loading

conditions and observed their hysteretic behavior. Their hysteretic stress-strain behavior, known as Masing's Principles, has the following characteristics:

i. The non-linearity of the material is plastic, with the charactesistic that at each change in direction of loading, the stiffness of the material returns momenarily to its initial stiffness.

ii. Under uniform cyclic loading of constant amplitude, a steady-state stress-strain behavior is obtained (stabilized loops), provided the hysteretic damping is sufficient to attenuate any transient effects within a few cycles.

iii. For stabilized loops under uniform cyclic loading conditions, the unloading and reloading branches of the stabilized loops are of the same form as the spine except for an enlargement of two in strain.

iv. The damping or energy loss is independent of the rate of strain and is entirely hysteretic.

By analogy with the reasoning in the linear viscoelastic model, the nonlinear deformation characteristics are normally represented by the secant modulus, defined as the slope of the straight line connecting the origin and the point of strain amplitude on the backbone curve (see Chapter 3). In the same fashion as in the viscoelastic model, the damping ratio, ξ, is defined as:

$$\xi = \frac{1}{4\pi}\frac{\Delta W}{W} \qquad \{21\}$$

where according to Masing's rule:

$$W = \frac{1}{2}\gamma_a f(\gamma_a)$$
$$\Delta W = 8\left[\int_0^{\gamma_a} f(\gamma)\,d\gamma - W\right] \qquad \{22\}$$

Using equations {21} and {22}, the damping ratio is defined as follows:

$$\xi = \frac{2}{\pi}\left[\frac{2\int_0^{\gamma_a} f(\gamma)\,d\gamma}{\gamma_a \cdot f(\gamma_a)} - 1\right] \qquad \{23\}$$

It should be noted herein that both parameters controlling the nonlinear deformation characteristics of soils, namely the shear modulus G and material damping ξ, are expressed as a function of the strain amplitude γ_a , as the derivation of the formulae is based on the backbone curve. For a constitutive model expressing the shear strain in terms of shear stress ($\gamma = \gamma(\tau)$), the damping ratio would be defined as follows:

$$\xi = \frac{2}{\pi}\left[1 - \frac{2\int_0^{\tau_a}\gamma(\tau)\,d\tau}{\tau_a \cdot \gamma(\tau_a)}\right] \qquad \{24\}$$

Several models have been suggested to reproduce the nonlinear stress - strain characteristics of soils. They generally fall into two categories.

1. Models with multi-linear stress - strain relationship.
2. Models with curvilinear stress - strain relationship.

These models are briefly presented in the following sections.

4.3.1 Multi-Linear Stress - Strain Models

4.3.1a Elastoplastic Models

These systems are described by a stress - strain or load - deflection relationship similar to the one plotted in Figure 4.3a. During loading up to a yield value τ_y the system exhibits a constant stiffness G. If loading (or rather straining) continues, the system exhibits zero stiffness. The same behavior characterizes the model during unloading. Under forced vibration conditions the system dissipates energy as indicated by the non-zero hysteresis loop area. Under free vibrations though (i.e. the system is initially displaced beyond the elastic threshold and successively released, undergoing free oscillations), energy is not dissipated. The elastoplastic model has been primarily used in load - deformation studies with finite elements and finite difference methods.

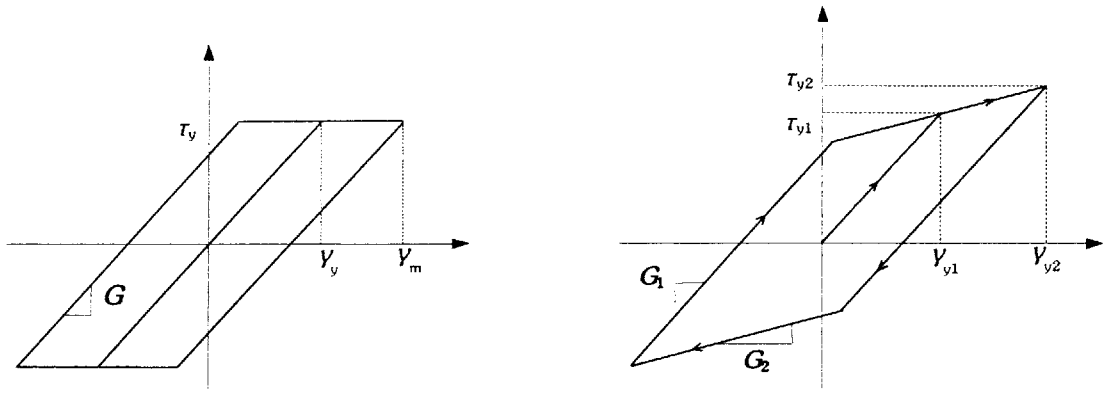

(a) (b)

Figure 4.3 Shear stress - strain relationship of: (a) An elastoplastic spring and, (b) A bilinear spring

4.3.1b Bilinear and Multilinear Models

The load - deflection relationship as shown in Fig. 4.3b is typical of these systems. During loading up to a yield value τ_{y1} the system has initial stiffness G_1 and, for further loading beyond the yield point, the stiffness becomes G_2 until the next yield point, τ_{y2}, is reached. The same sequence occurs during unloading.

In particular, the actual continuous curve of the force - deflection relationship is approximated by several straight-line segments. Hence this system more closely represents the idealized curve than either the elastic or the elastic– perfectly plastic systems do.

For the present analysis, a multilinear model is used to simulate the inelastic soil behavior under cyclic and arbitrary loading. The model is more extensively analyzed in subsequent section.

4.3.2 CURVILINEAR STRESS - STRAIN MODELS

4.3.2a Hyperbolic Model

Considering the stress - strain curve of soils, it is bounded by two straight lines, namely the tangent G_0 (the elastic modulus) at small strains, and the horizontal asymptote at large strains indicating the strength of soils τ_f, as illustrated in Fig. 4.4.

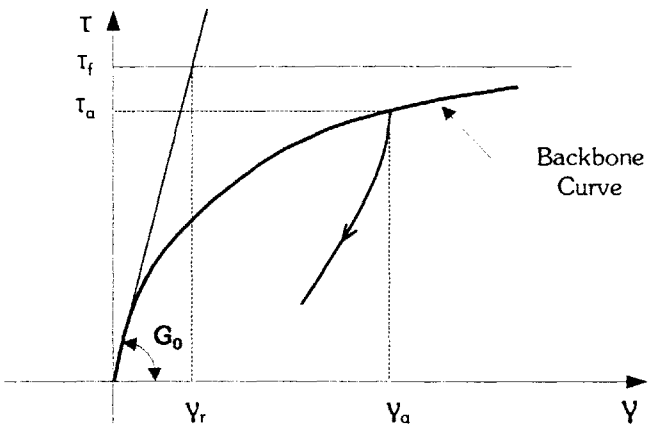

Figure 4.4 Hyperbolic stress - strain relationship - Definition of reference strain

The stress - strain curve bounded by these two straight lines may be expressed in differential form as:

$$\frac{d\tau}{d\gamma} = G_0\left(1-\frac{\tau}{\tau_f}\right)^n \qquad \{25\}$$

where n is an arbitrary number. This expression indicates that the tangent to the stress - strain curve takes a value of G_0 at $\tau = 0$ and decreases with increasing stress until it becomes zero at $\tau = \tau_f$. Except of the case of $n = 1$, equation {25} can be integrated, as follows, so as to satisfy the condition $\gamma = 0$ when $\tau = 0$,

$$\gamma = \frac{\gamma_r}{n-1}\left[\frac{1}{\left(1-\frac{\tau}{\tau_f}\right)^{n-1}}-1\right] \qquad \{26\}$$

where a new parameter is introduced, γ_r , referred to as reference strain and defined as follows:

$$\gamma_r = \frac{\tau_f}{G_0} \qquad \{27\}$$

The reference strain indicates a strain that would be attained at failure stress, if a soil were to behave elastically.

Defining the shear stress in terms of the shear strain, equation {26} can be written as follows:

$$\frac{\tau}{\tau_f} = \frac{1}{\left[1 + (n-1)\frac{\gamma}{\gamma_r}\right]^{\frac{1}{n-1}}} \qquad \{28a\}$$

which, for the special case of n = 1, is reduced to the following expression:

$$\frac{\tau}{\tau_f} = 1 - e^{-\frac{\gamma}{\gamma_r}} \qquad \{28b\}$$

The stress - strain curve defined by equation {25}, produces a constant damping ratio of $2/\pi$ as an upper limit, when the strain becomes large. This can be readily proved by modifying equation {23} as follows:

$$\left(1 + \frac{\pi}{2}\xi\right)\gamma_a f(\gamma_a) = 2\int_0^{\gamma_a} f(\gamma)\, d\gamma \qquad \{29\}$$

If the damping ratio is assumed to take constant value ξ_0 at large strains, equation {29} can be differentiated as follows:

$$\left(1 - \frac{\pi}{2}\xi_0\right) f(\gamma_a) = \left(1 + \frac{\pi}{2}\xi_0\right)\gamma_a f'(\gamma_a) \qquad \{30\}$$

Introducing equations {25} and {26} into equation {30} with $\gamma = \gamma_a$ and $\tau = \tau_a$, one obtains:

$$1 - \frac{\pi}{2}\xi_0 = \frac{\gamma_r}{n-1}\frac{G_0}{\tau_0}\left(1 + \frac{\pi}{2}\xi_0\right)\left[\left(1 - \frac{\tau_a}{\tau_f}\right) - \left(1 - \frac{\tau_a}{\tau_f}\right)^n\right] \qquad \{31\}$$

When the strain is very large, τ_a becomes equal to τ_f and the right - hand side of equation {31} vanishes. Therefore $\xi_0 = 2/\pi$.

This limit value of material damping can be also obtained as follows. From equation {29}, we have:

$$1 + \frac{\pi}{2}\xi = 2\,\frac{\int_0^{\gamma} f(\gamma)\,d\gamma}{\gamma \cdot f(\gamma)} \qquad \{32\}$$

In Figure 4.5, the numerator and denominator of the RHS of equation {32} are plotted, and the limit value of the ratio, as the shear strain becomes sufficiently large, is unity.

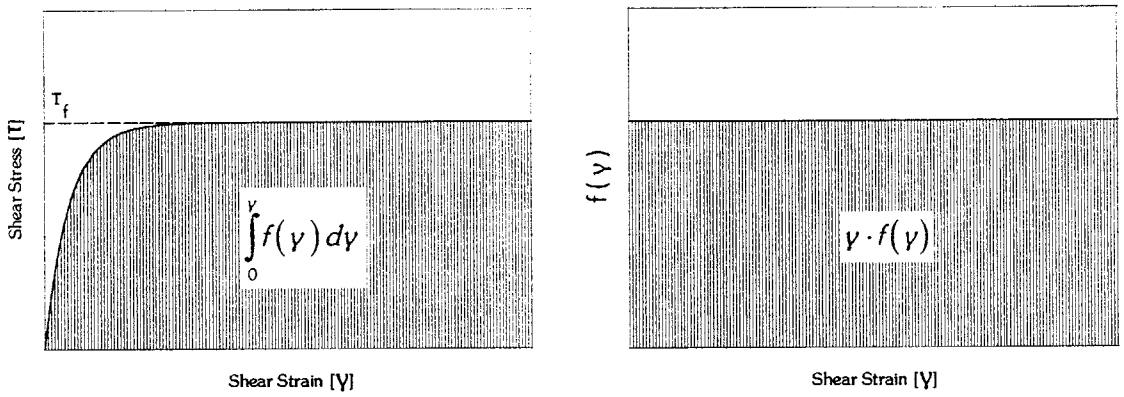

Figure 4.5 Schematic illustration of the large strain limit value of material damping ratio

Therefore, from equation {32} we obtain:

$$\lim_{\gamma \to \infty} \frac{\int_0^{\gamma} f(\gamma)\,d\gamma}{\gamma \cdot f(\gamma)} = 1 \qquad \{33\}$$

$$\lim_{\gamma \to \infty} 1 + \frac{\pi}{2}\xi = 2 \qquad \text{and} \qquad \lim_{\gamma \to \infty} \xi = \xi_0 = \frac{2}{\pi}$$

The stress - strain curve for the hyperbolic model can be directly obtained from equation {26}, by introducing $n = 2$:

$$\tau = \frac{G_0\,\gamma}{1 + \frac{\gamma}{\gamma_r}} \qquad \{34\}$$

This equation has been extensively used to represent the stress – strain relations for variety of soils. The hyperbolic model has also been used to specify the hardening rule in the theory of plasticity (Venmeer, 1978).

The expression for the secant modulus in the cyclic loading is obtained from equation {32} as follows:

$$\frac{G}{G_0} = \frac{1}{1 + \gamma_a/\gamma_r}, \qquad G = \frac{\tau_a}{\gamma_a} \qquad \{35\}$$

It is can be readily noted that the secant modulus is reduced to half the initial shear modulus when the shear strain becomes equal to the reference strain.

Applying Masing's rule to the skeleton curve given by equation {34}, the damping ratio of the hyperbolic model evaluates to:

$$\xi = \frac{4}{\pi}\left[1 + \frac{1}{\gamma_a/\gamma_r}\right]\left[1 - \frac{\ln(1+\gamma_a/\gamma_r)}{\gamma_a/\gamma_r}\right] - \frac{2}{\pi} \qquad \{36\}$$

In the hyperbolic model as specified above, there are two parameters G_0 and τ_f which define the model. In some cases, it is difficult to specify both the strain – dependent shear modulus and damping ratio by means of only two parameters. Particularly inconvenient is the fact that, once the reference strain γ_r is specified from the stress – strain characteristics of the secant shear modulus, the value of strain – dependent damping ratio is automatically determined, and there is no choice for any parameter to be adjusted so as to provide a good fit to experimentally obtained damping data.

Usually the model representation is satisfactory in the range of small strains, yet it tends to deviate from actual soil behavior with increasing shear strains, thereby overestimating the damping ratio.

4.3.2b Davidenkov and Ramberg - Osgood Models

The hyperbolic relationship, in spite of the fact that it adequately represents part of a cycle, has certain shortcomings:

i. It models only the loading part of a given cycle.

ii. The parameters for the relationship have to be changed for each cycle.

iii. It does not have "memory", and hence unloading cannot be handled uniquely by the same relationship unless the parameters are changed continually.

Therefore, it would be desirable to use a relationship that is relatively smooth and continuous at yielding and yet is general enough to describe yielding behavior between the extremes of linear elastic and elastic– perfectly plastic material.

Constitutive soil models satisfying Masing's Principles belong to one of two general classes, namely the Davidenkov (D) class models and the Ramberg-Osgood (RO) models. The major difference between these two classes is that for the D class models, strain is the independent variable, while for the RO class models, stress is the independent variable. The D class models have received little attention in the field of seismic analysis of rate - independent yielding systems, although they are probably best suited for this purpose. This arises from the fact that strains or displacements are normally obtained from the numerical solution of equations of motion, and they are then used as the independent variable in the constitutive model.

However, the RO class models have been used in the past to model the nonlinear hysteretic stress - strain behavior of such systems under seismic loading conditions despite the shortcomings that arise from the use of stress as independent variable. In what follows, the RO class model principles will be briefly presented.

In the original formulation of the Ramberg-Osgood model, for a spring representing a soil element, the stress - strain relation for the backbone curve is given by:

$$\frac{\gamma}{\gamma_y} = \frac{\tau}{\tau_y}\left[1 + \alpha\left|\frac{\tau}{\tau_y}\right|^{r-1}\right] \qquad \{37\}$$

where τ_y and γ_y are shear stress and shear strain, respectively, to be appropriately chosen, and α and r are constants. Thus, the RO model contains four parameters that can be adjusted to achieve a best fit to experimental data. The most widely used way to specify the quantities τ_y and γ_y is to equate them to the shear strength τ_f and the reference strain γ_r respectively, as suggested Idriss et al. (1978) and Hara (1980). Therefore, equation {37} can be rewritten as follows:

$$\tau = \frac{G_0\,\gamma}{1 + \alpha\left|\frac{\tau}{\tau_f}\right|^{r-1}} \qquad \{38\}$$

The expression for the strain – dependent modulus for the cyclic loading condition, as well as for the damping ratio, can be obtained by setting $\gamma = \gamma_a$ and $\tau = \tau_a$:

$$\frac{G}{G_0} = \frac{1}{1 + a\left|\frac{G}{G_0}\cdot\frac{\gamma_a}{\gamma_r}\right|^{r-1}}$$

$$\xi = \frac{2}{\pi}\frac{r-1}{r+1}\cdot a \cdot \frac{\left|\frac{G}{G_0}\cdot\frac{\gamma_a}{\gamma_r}\right|^{r-1}}{1 + a\left|\frac{G}{G_0}\cdot\frac{\gamma_a}{\gamma_r}\right|^{r-1}} \qquad \{39\}$$

One of the drawbacks of the RO model is the fact that the shear strain γ_a increases in proportion to τ_a when the shear strain becomes large, as it can be readily seen by equation {38}. In view of the possible range of the parameter r supposedly taking a value between 2 and 4, the quantity τ_a tends to increase indefinitely with increasing shear strain, which is inconsistent with the real behavior of soils. One of the ways of overcoming this contradiction would be to set a rule for determining the parameter a so that in no case the shear stress τ_a exceeds the value of τ_f corresponding to failure.

With respect to the determination of the parameter r, it would be reasonable to take into account the damping characteristics of soils. Combining equations {39} and eliminating the shear strain ratio γ_a / γ_r, the parameter r could be evaluated if the values of ξ and G / G_0 at a certain strain level are known.

The main disadvantage of the models analyzed in this section is that their use cannot be arbitrarily extended to more complicated cyclic loading conditions because these classes of models are not physical models of rate independent yielding systems. This shortcoming can be readily seen, when the system is subjected to a steady – state cyclic strain time history, containing two reversal points in addition to the extreme reversal points during a cycle. Due to the presence of the two additional reversal points, an additional smaller hysteresis loop is expected in the overall hysteretic stress – strain behavior. The important feature of these models without memory capacity of intermediate reversal periods, is that the overall hysteresis loops are not stable under the given strain time history and in fact, for continued cyclic loading, the stress increases without bound. The explanation of this behavior is that the

D and RO class models only consider the most recent reversal point, and hence unload and reload without regard to reversal points prior to the most recent one.

4.3.2c Parallel Series Model

The two classes of models described in Section 4.3.2b were developed on a purely phenomenological basis and are consistent with the experimentally observed stress - strain behavior of rate - dependent yielding systems under one-dimensional simple cyclic loading conditions. Their main disadvantage is that they cannot be arbitrarily extended to more complicated loading conditions because these classes of models are not physical models of rate− independent yielding systems.

In particular, the D and RO class models consider only the most recent reversal points. Hence, the model always unload and reload without regard to load reversal points prior to the most recent one, a fact which, in the light of experimental laboratory data, is unrealistic (see Appendix II).

Numerous laboratory data confirm that the soil tested under arbitrary loading has a "memory", i.e. its performance depends on all previous load reversal points and follow the loading curve associated with the appropriate load reversal point. After the strain has increased past the last extreme strain at which there was a load reversal, the loading curve resumes the initial backbone curve.

The shortcomings of D and RO models have been analyzed by Jennings (1964), Cundall (1975) and Finn et al. (1975). Both Jennings and Finn limited the arbitrary cyclic stress - strain behavior by upper and lower bounds if the present strain fell between previously established minimum and maximum strains. The bounds chosen were the loading and unloading curves corresponding to these minimum and maximum strains, respectively. Beyond these extremes, the backbone curve defines the stress - strain behavior.

Realizing the shortcomings of the phenomenological D and RO models described above, it is anticipated that a model representing the physical behavior of rate-independent yielding systems would probably be much more satisfactory for arbitrary cyclic loading conditions. The simplest physical model for such systems is obviously an elastoplastic model, described by a stress-strain or load-deflection relationship shown in Fig.4.3a.

This model comprises a spring with shear stiffness, k, in series with a Coulomb unit with critical slipping stress, τ_y (Figure 4.6a). It can be seen that this model satisfies Masing's

Principles and also has a "memory capacity", i.e. it inherently remembers the last yield point from which unloading occurred.

By using a large number of elastoplastic springs in parallel, as shown in Fig. 4.6b, any non-linear characteristic of a stress-strain relationship, derived from test results, may be simulated as closely as desired by selecting appropriate values of stiffness and Coulomb resistance for as many elements as necessary. In this case, the continuous backbone curve is approximated by a series of straight segments, as shown in Fig.4.7 and the approximation becomes more accurate, as the number of springs increases.

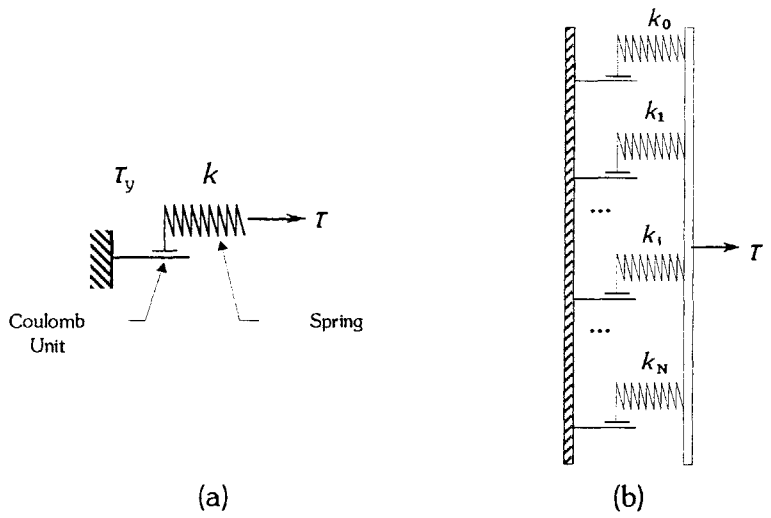

Figure 4.6 Schematic Representation of an: (a) Elastoplastic Model,and (b) Elastoplastic parallel series model.

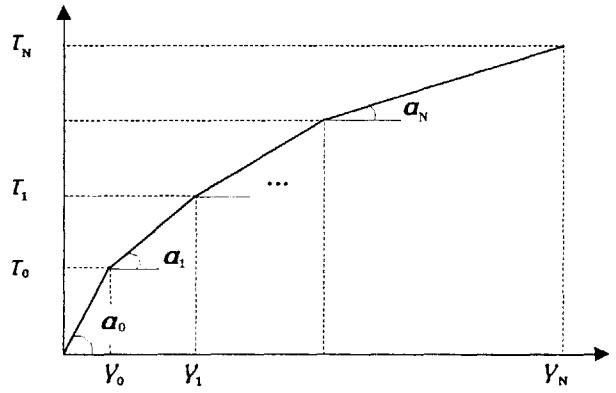

Figure 4.7 Multi - linear approximation of the backbone curve

If finite number of springs is used, the tangent stiffness, $\tan(\alpha_j)$, is defined as following:

$$\begin{aligned}
\tan(\alpha_0) &= k_0 + k_1 + \ldots + k_N \\
\tan(\alpha_1) &= \quad k_1 + \ldots + k_N \\
&\ldots \\
\tan(\alpha_N) &= \quad k_N
\end{aligned} \qquad \{40\}$$

Therefore, from equation {40}, the spring stiffness k_j is defined as follows:

$$k_j = \tan(\alpha_j) - \tan(\alpha_{j+1}) \qquad \{41\}$$

Defining τ_j as the yield shear stress corresponding to the yield shear strain γ_j, the secant stiffness is successively evaluated as:

$$G_j = \frac{\tau_j}{\gamma_j} \qquad \{42\}$$

Therefore, the tangent stiffness can be expressed in terms of the secant stiffness, as follows:

$$\tan(\alpha_j) = \frac{\tau_j - \tau_{j-1}}{\gamma_j - \gamma_{j-1}} = \frac{G_j\gamma_j - G_{j-1}\gamma_{j-1}}{\gamma_j - \gamma_{j-1}} = \frac{\left(\frac{\gamma_j}{\gamma_{j-1}}\right) G_j - G_{j-1}}{\left(\frac{\gamma_j}{\gamma_{j-1}}\right) - 1} \qquad \{43\}$$

Choosing $\gamma_j = z^j \gamma_0$, and introducing it into equation {43}, the expression for tangent stiffness is now reduced to:

$$\tan(\alpha_j) = \frac{z\, G_j - G_{j-1}}{z - 1} \qquad \{41\}$$

In terms of shear stress - strain behavior, with N being the number of elastoplastic elements in parallel, the backbone curve is described by:

$$\tau = \sum_{i=1}^{N} \frac{k_i}{N} \cdot \gamma + \sum_{i=n+1}^{N} \frac{\tau_{yi}}{N} \qquad \{44\}$$

where: k_i the shear modulus of the i^{th} element

τ_{yi} the critical slipping stress of the i^{th} element

n the number of elements which remain elastic

τ the shear stress on the backbone curve obtained for a given shear strain, γ

Using the parallel series model described above for rate-independent yielding systems, such as soils, the shear stress-strain relationship under arbitrary cyclic loading conditions can be accurately represented, provided that it is updated with the appropriate reversal point coordinates as the solution marches in time.

In what follows, the parallel series model shall be used for the performance of true incremental non-linear analyses (see Chapters 5,6). For consistency, the shear stiffness of the discrete elements is defined using stress - strain characteristics of the modified MIT-S1 model (see Chapter 3), and the material damping ratio is evaluated by integration of the shear stress-strain hysteresis loop.

Consequently, results obtained by means of the nonlinear analysis are compared with these obtained using the equivalent linear wave propagation analysis.

4.4 REFERENCES

Chen, W. F. & Mizuno, E. (1990). "Nonlinear Analysis in Soil Mechanics: Theory and Implementation", *Developments in Geotechnical Engineering*, Vol. 53, Elsevier Science Publishers B.V.

Constantopoulos, I. V. (1973). "Amplification Studies for a Nonlinear Hysteretic Soil Model", *Research Report* R73-46, Massachusetts Institute of Technology, September

Dames & Moore, Science Applications Inc. (1978). " Study of Nonlinear Effects on One - Dimensional Earthquake Response" , prepared for *Electric Power Research Institute*, Projects 615-1,-2

Daniel, A. W. T., Harvey, R. C. and Burley, E. (1975). "Stress – Strain Characteristics of Sand", Technical Note, *Journal of the Geotechnical Division*, ASCE, Vol. 101, No. GT5, May, pp. 508-512

Das, B. M. (1993). "Principles of Soil Dynamics", PWS-KENT Publishing Company, Boston, MA

Dobry, R. (1971). "Soil Properties and the One-Dimensional Theory of Earthquake Amplification", *Research Report* R71-18, Massachusetts Institute of Technology

Drnevich, V. P., Hall, J. R. & Richard, F. E. Jr. (1967)." Effects of Amplitude of Vibration on the Shear Modulus of Sand" , *Proc. International Symposium on Wave Propagation and Dynamic Properties of Earth Materials*, New Mexico, pp. 189-199

Finn, W. D. L., Lee, K. W. & Martin, G. R. (1975)." Stress-Strain Relations for Sand in Simple Shear" , *ASCE National Convention*, Denver, Colorado, November, Meeting Reprint 2517

Hall, J. R. Jr. & Richard, F. E. Jr. (1963)." Dissipation of Elastic Wave Energy in Granular Soils" ,*Journal of the Soil Mechanics and Foundation Division*, ASCE, Vol. 98, No. SM6, November, pp. 27-56

Hardin, B.O. & Drnevich, V. P. (1972a)." Shear Modulus and Damping in Soils: I. Measurement and Parameter Effects" , *Journal of the Soil Mechanics and Foundation Division*, ASCE, Vol. 98, No. SM6, June, pp. 603-624

Hardin, B.O. & Drnevich, V. P. (1972b). " Shear Modulus and Damping in Soils: II. Design Equations and Curves" , *Journal of the Soil Mechanics and Foundation Division*, ASCE, Vol. 98, No. SM7, Juiy, pp. 667-692

Idriss, I. M., Dobry, R., Doyle, E. H. and Singh, R. D. (1976). " Behavior of Soft Clays under Earthquake Loading Conditions" , *Proc. Offshore Technology Conference*, Paper No. OTC 2671, May

Ishihara, K. (1996). "Soil Behavior in Earthquake Geotechnics", *Oxford Science Publications*, Oxford Science Press, Walton Street, Oxford OX2 6DP

Iwan, W. D. (1967). " On a class of Models for the Yielding Behavior of Continuous and Composite Systems" , *Journal of Applied Mechanics*, Vol. 34, No. 3, September, pp. 612-617

Jennings, P. C. (1964). "Response of a General Yielding Structure". *Journal of the Engineering Mechanics Division*, ASCE, Vol. 90, EM2

Joyner, W. B. & Chen, A. T. F. (1975). " Calculation of Non-linear Ground Response in Earthquakes" , *Bulletin of the Seismological Society of America*, Vol. 65, No. 5, October, pp. 1315-1336

Keydner, R. L.& Zelasko, J. S. (1963)." A Hyperbolic Stress – Strain Formulation for Sands" , *Proc. 2nd Pan American Conference on Soil Mechanics and Foundation Engineering*, Vol. 1, Brazil

Konder, R. L. (1963)." Hyperbolic Stress-Strain Response: CohesiveSoils" ,*Journal of the Soil Mechanics and Foundation Division*, ASCE, Vol. 89, No. SM1, February, pp. 115-143

Krizek, R. J. & Franklin, A. G. (1968)." Energy Dissipation in a Soft Clay" , *Proc. International Symposium on Wave Propagation and Dynamic Properties of Earth Materials*, University of New Mexico, pp. 797-807

Masing, G. (1926)." Eigenspannungen und Verfestigung beim Messing" , *Proc. 2nd International Congress of Applied Mechanics*, Zurich, pp. 332-335

Ramberg, W. & Osgood, W. R. (1943). " Description of Stress – Strain Curves by Three Parameters" , *Technical Note 902*, NACA, July

Seed, H. B. & Idriss, I. M. (1970)." Soil Moduli and Damping Factors for Dynamic Response Analyses" , Report No. EERC 70-10, *Earthquake Engineering Research Center*, University of California, Berkeley, December.

Shibuya, S., Mitachi, T. & Muira, S. (1994). "Pre-failure Deformation of Geomaterials", *Proc. International Symposium on Pre-Failure Deformation Characteistics of Geomaterials*, Sapporo, Japan, September.

Silver, M. L. & Seed, H. B. (1971). " Deformation Characteristics of Sands under Cyclic Loading" , *Journal of the Soil Mechanics and Foundations Division*, ASCE, Vol. 97, No. SM8, August, pp. 1081-1098

Thiers, G. R. and Seed, H. B. (1968)." Cyclic Stress – Strain Characteristics of Clay" ,*Journal of the Soil Mechanics and Foundation Division*, ASCE, Vol. 60, No. 5, October, pp. 1625-1651

Weissman, G. F. & Hart, R. R. (1961). " The Damping Capacity of Some Granular Soils" , *Symposium of Soil Dynamics*, Special Technical Publication No. 305, American Society for Testing and Materials, pp. 15-19

Whitman, R. V. (1970). " Evaluation of Soil Properties for Site Evaluation and Dynamic Analysisof Nuclear Plants" , *Seismic Design for Nuclear Plants*, R. J. Hanson (ed.), MIT Press, Cambridge, Massachusetts

CHAPTER 5

FREQUENCY DEPENDENT SHEAR MODULUS AND DAMPING

5.1 INTRODUCTION

In many cases, the ground motions developed near the surface of a soil deposit during an earthquake may be attributed primarily to the upward propagation of shear waves from an underlying rock formation. If the ground surface, the rock surface and the boundaries between the layers are essentially horizontal, and the soil deposit is homogeneous, the lateral extent of the soil deposit has no influence on the response, and the deposit may be considered as a series of layers extending to infinity in all horizontal directions. In such cases, the ground motion at the surface, induced by a horizontal excitation at the base of the deposit, is the result of shear deformations in the soil, and the deposit may be represented by a one-dimensional shear beam model.

For soil deposits with essentially horizontal boundaries, the analytical determination of the effect of soil conditions on the characteristics of the motion at the surface can be conducted along two methods (Roesset and Whitman, 1969; Seed, 1969):

i. The solution of the wave equation in which each soil layer is considered to be a linearly viscoelastic material.

ii. The idealization of the deposit by a lumped mass system, with the masses connected by shear springs whose force - deflection properties are defined by the stress - strain relationship of the corresponding layer of the soil.

In the first case it is generally more convenient to carry out the solution in the frequency domain, using the Fourier Transform. In the second case the solution can be performed in the time domain using modal superposition analysis or direct, step by step, integration of the equations of motion (see Chapter 6).

While it is theoretically possible to perform true incremental analysis, in which the properties of the soil are varied according to the load path and instantaneous levels of strain, such procedures are seldom used in practice. Instead, approximate linear solutions are

obtained by an iterative scheme originally proposed by Seed and Idriss (1969). Each iteration assumes constant values of soil properties during the earthquake, but the properties are chosen at the beginning of each iteration so as to be consistent with the levels of strain computed in the previous iteration. These levels of strain are usually measured by a characteristic strain, which is either the peak or the root mean square value of the principal shearing strain.

While the linear theory and iterative solution do not provide exact solutions and have a limited range of application, they provide acceptable results for engineering purposes. However, the iterative algorithm can diverge when large amplitude of motion is specified at or near the surface of a deep deposit of soft soil. According to Kausel & Roesset (1984), the failure of the iterations to converge is the result of a number of factors:

i. The soil may be required to transmit a higher level of motion than it can accommodate. There is necessarily a limit to the stress that can be sustained by a layer of soil.

ii. The soil may be required to transmit too much energy at high frequencies. The motion specified at the free surface may have a frequency content inconsistent with the properties of the soil and particularly with the damping.

Typical transfer functions at the surface of two homogeneous strata of 10m and 100m depth, overlying rigid bedrock are shown in Figure 5.1. The soil deposits have the same stiffness properties (V_s = 100 m/sec) and the same value of linear hysteretic damping, namely $\xi = 0.05$. The fundamental frequencies of the strata are $f_1 = 2.5$ Hz and $f_1 = 0.25$ Hz respectively. As it can be readily seen, the deep soil deposit tends to wipe out the high frequency components of the excitation, a fact which cannot be ignored when studying the soil amplification of deep soft soil deposits.

iii. The assumption of linear hysteretic damping, independent of frequency is only an approximation. Since material damping is a function of amplitude, high frequencies associated with small amplitude cycles of vibration may have substantially less damping than the predominant frequencies of the layer.

In what follows, a general rule for frequency dependent damping and shear modulus is developed using general characteristics of various accelerograms, and the performance of the frequency dependent linear hysteretic model is then compared with the true nonlinear analysis results (see Chapter 6).

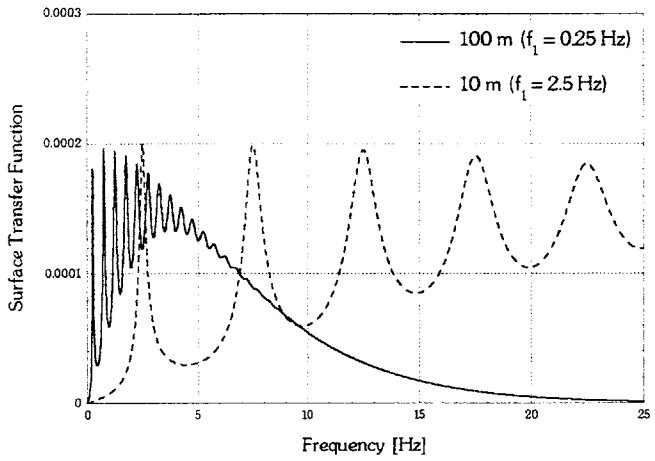

Figure 5.1 Transfer functions at the surface of two soil deposits overlying rigid bedrock

5.2 Frequency Dependent Damping - Sinusoidal Excitation

In order to illustrate qualitatively the frequency dependence of the shear modulus and damping, two sets of excitations are initially used, consisting of a combination of two single-frequency harmonics.

For the simulations performed, the soil is represented by the parallel series model, as described in Section 4.3.2c, where the spring stiffnesses and yield forces are evaluated using the modified MIT-S1 model (see Chapter 3). Table 5.1 presents the selected values of the parameters needed for MIT-S1, and the resulting values of spring stiffnesses and yield forces are shown in Figure 5.2.

Soil Parameter	
C_b	800
ω	1.00
μ'_0	0.25
ω_s	2.40
e_0	0.50
σ' / p_a	1.00
K_0	0.50

Table 5.1 Typical Soil Parameters for Non-Linear Masing Soil using Modified MIT-S1 model

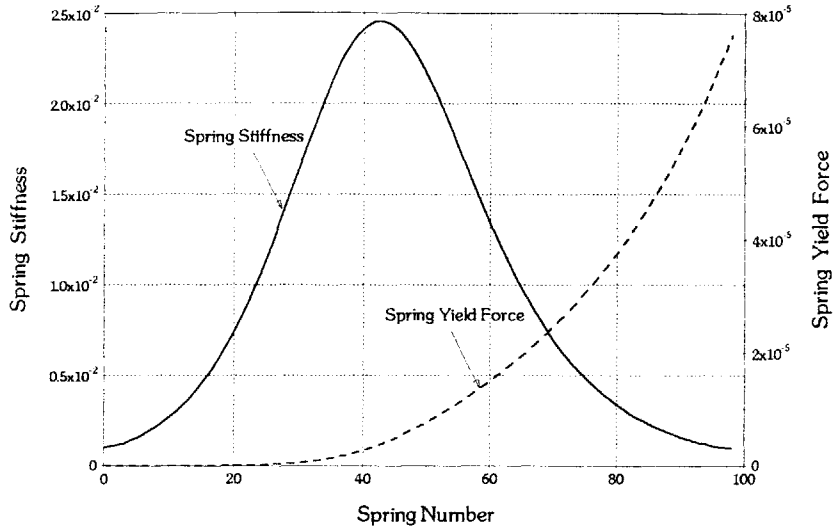

Figure 5.2 Stiffness and Yield Force of elastoplastic springs in parallel, using modified MIT-S1 model

This model is subsequently used to illustrate the frequency dependence of damping and shear modulus, as it can accurately represent the shear stress – strain hysteresis loop, including the change in stiffness at reversal point.

The analysis is performed directly in the time domain, using a Fortran computer code (see Appendix III.1). As the solution marches in time, the elastoplastic springs (see Section 4.3.1a) become successively plastic, and each individual spring dissipates energy equal to:

$$E_d^i = 4\,\tau_y^i\left(\gamma_{max}^i - \gamma_y^i\right) = 4\,k_i\,\gamma_y^i\left(\gamma_{max}^i - \gamma_y^i\right) \qquad \{1\}$$

where: k_i the stiffness of the i^{th} element,

τ_y^i the critical slipping stress of the i^{th} element,

γ_{max}^i the maximum shear deformation of the i^{th} element, and

γ_y^i the yield shear deformation of the i^{th} element.

In both multi-frequency excitations used for the simulation, the low amplitude component, $\gamma_2(t)$, is assigned four times the frequency of the high amplitude component, $\gamma_1(t)$. The superposition of the two harmonic motions is subsequently scaled to the amplitude of the low frequency component. In particular:

$$\left.\begin{aligned}\gamma_1(t) &= \gamma_1 \sin(\omega t)\\ \gamma_2(t) &= \gamma_2 \sin(4\omega t)\end{aligned}\right\} \quad \gamma(t) = \frac{\gamma_1}{\gamma_{max}}\left[\gamma_1 \sin(\omega t) + \gamma_2 \sin(4\omega t)\right] \qquad \{2\}$$

Results are presented in Figure 5.3a and b for amplitude ratios of the two components being $\gamma_1 / \gamma_2 = 2$ and $\gamma_1 / \gamma_2 = 4$ respectively.

As it can be readily seen, the dominant hysteresis loop corresponds to the low frequency component, whilst the energy dissipated due to the presence of the high frequency component is substantially lower and the shear modulus is higher.

Successively, the true inelastic energy dissipated is evaluated in the time domain for the two excitations. Results are shown in Figure 5.4, where the decreased hysteresis loop area in the second simulation is visualized through the reduced ability of the system to dissipate energy.

Therefore, the use of common damping ratio and shear modulus reduction factor for both harmonic motions would be unrealistic, underestimating the stiffness and overestimating the ability of the model to dissipate energy.

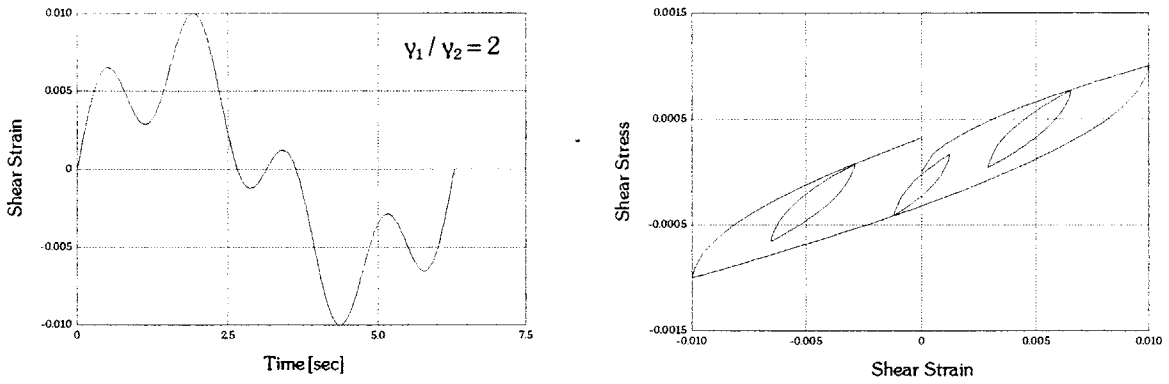

Figure 5.3a Shear strain time history and hysteresis loop of simulation using nonlinear model of elastoplastic springs in parallel, with $\gamma_1 / \gamma_2 = 2$

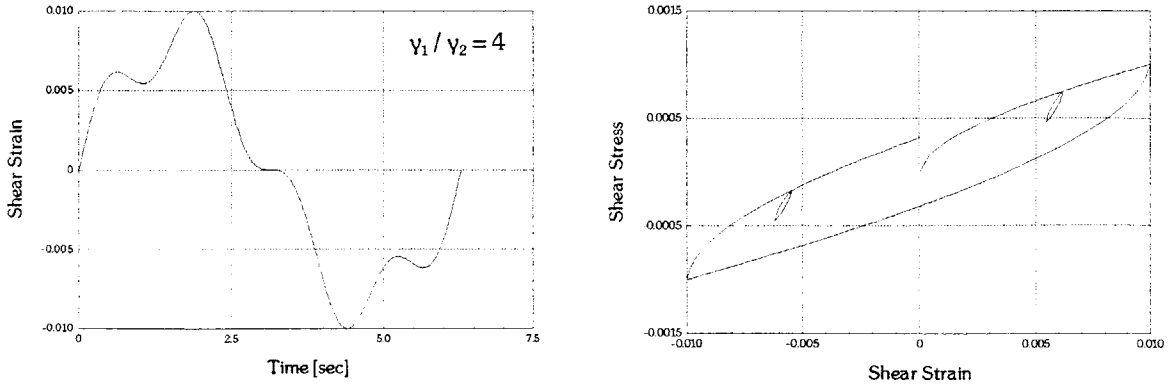

Figure 5.3b Shear strain time history and hysteresis loop of simulation using nonlinear model of elastoplastic springs in parallel, with $\gamma_1 / \gamma_2 = 4$

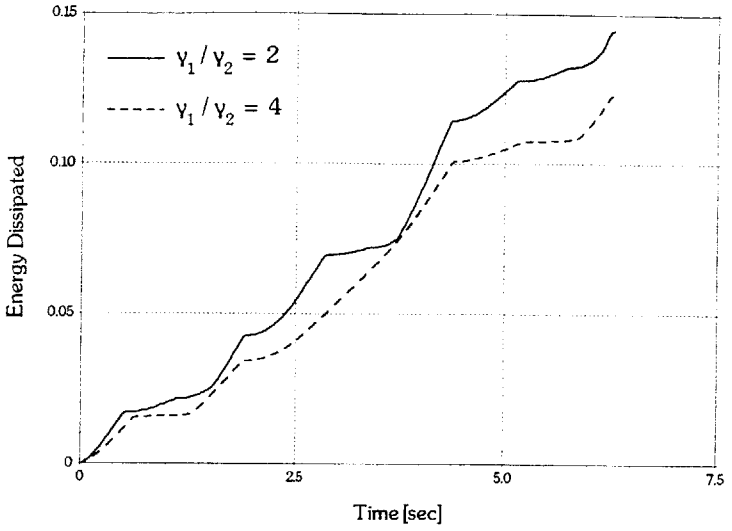

Figure 5.4 Inelastic Energy Dissipated in cyclic motion by a set of elastoplastic springs in parallel.

5.3 Frequency Dependent Damping – Arbitrary Loading

Using the parallel series model described above, the frequency dependence of damping and shear modulus is now evaluated for arbitrary loading, i.e. an earthquake excitation. The energy dissipated by the frequency - dependent linearly - hysteretic model is then compared with the true energy dissipated by the nonlinear Masing soil model.

For the simulations performed, the excitation is a strain time history, obtained by integration of a real accelerogram. The acceleration time history was integrated once and then scaled to the desired value of strain, taking advantage of the fundamental property of wave propagation, that the particle velocity is proportional to the strain.

In particular, for $u(x,t)$ being the solution of the one-dimensional wave equation and c the wave propagation velocity corresponding to the type of stress wave of interest (here shear wave velocity), we have:

$$u = f\left(t - \frac{x}{c}\right) \qquad \{3\}$$

Differentiating equation {3} with respect to t, the particle velocity is evaluated as follows:

$$\frac{\partial u}{\partial t} = \frac{\partial u}{\partial \tau}\frac{\partial \tau}{\partial t} = \frac{\partial u}{\partial \tau} = \dot{u} = \dot{f} \qquad \{4\}$$

where: $\tau = t - \frac{x}{c}$

Successively, differentiating equation {3} with respect to x, the shear strain is evaluated as follows:

$$\gamma = \frac{\partial u}{\partial x} = \frac{\partial u}{\partial \tau}\frac{\partial \tau}{\partial x} = -\frac{1}{c}\frac{\partial u}{\partial \tau} = -\frac{1}{c}\dot{f} \qquad \{5\}$$

Therefore, combining equations {4} and {5}, the shear strain (and shear stress) is proportional to the particle velocity.

The distribution of the shear modulus reduction factor and damping in the frequency domain, for the linear -hysteretic model, was evaluated by calculating the Fourier Transform of the strain time history, scaling it to the maximum shear strain and successively assigning for each discrete frequency values of modulus reduction and damping using the MIT-S1 model (see Chapter 3, equations {12} and {16}).

For consistency, the nonlinear springs of the Masing soil were evaluated using the same soil model, with the characteristics described in Section 5.2.

5.3.1 Energy Dissipated - Linear Hysteretic Model

The energy dissipated for the frequency - dependent model was evaluated in the frequency domain. In particular, the Fourier transform of the shear strain time history is defined as:

$$\gamma(t) = \frac{1}{2\pi}\int_{-\infty}^{\infty}\gamma(\omega)\, e^{i\omega t}\, d\omega \qquad \{6\}$$

In analogy, the Fourier transform of the shear stress time history is:

$$\tau(t) = \frac{1}{2\pi}\int_{-\infty}^{\infty}\tau(\omega)\, e^{i\omega t}\, d\omega \qquad \{7\}$$

where: $\tau(\omega) = G\left[1 + 2\,i\;\xi(\omega)\,\mathrm{sgn}(\omega)\right]\gamma(\omega)$,

$\gamma(\omega)$ the Fourier transform of the shear strain time history, and

$\xi(\omega)$ the frequency dependent damping.

Therefore, the instantaneous power is given by the expression:

$$P(t)=\tau(t)\,\dot{\gamma}(t)=\left(\frac{1}{2\pi}\right)^2\int_{-\infty}^{\infty}\int_{-\infty}^{\infty}\tau(\omega')\,\gamma(\omega'')\,i\omega''\,e^{i(\omega'+\omega'')t}\,d\omega\,d\omega'' \qquad \{8\}$$

Successively, the total energy dissipated by the linear - hysteretic model is evaluated as:

$$E_d=\int_{-\infty}^{\infty}P(t)\,dt=\int_{-\infty}^{\infty}\left[\left(\frac{1}{2\pi}\right)^2\int_{-\infty}^{\infty}\int_{-\infty}^{\infty}\tau(\omega')\,\gamma(\omega'')\,i\omega''\,e^{i(\omega'+\omega'')t}\,d\omega\,d\omega''\right]dt \qquad \{9\}$$

Using the congruence $\frac{1}{2\pi}\int_{-\infty}^{\infty}e^{i(\omega'+\omega'')t}\,dt=\delta(\omega'+\omega'')$,the energy dissipated is:

$$E_d=\frac{1}{2\pi}\int_{-\infty}^{\infty}\tau(-\omega)\,\gamma(\omega)i\omega\,d\omega \qquad \{10\}$$

Defining the complex conjugate $\tau(-\omega)=\tau^*(\omega)$, and substituting in equation {10} the Fourier transform of the shear stress from equation {7}, the energy dissipated is finally given by the following equation[1]:

$$E_d=\frac{1}{2\pi}\int_{-\infty}^{\infty}\tau^*(\omega)\cdot\gamma(\omega)\,i\,\omega\,d\omega=\frac{G}{2\pi}\int_{-\infty}^{\infty}i\left[1-2i\xi(\omega)\,\mathrm{sgn}(\omega)\right]\omega\,\gamma^*\gamma\,d\omega=$$

$$=\underbrace{\frac{Gi}{2\pi}\int_{-\infty}^{\infty}\omega\,|\gamma|^2\,d\omega}_{\text{antisymmetric}}+\underbrace{\frac{2G}{2\pi}\int_{-\infty}^{\infty}\omega\,\mathrm{sgn}(\omega)\,\xi(\omega)\,|\gamma|^2\,d\omega}_{\text{symmetric}}=\frac{2G}{\pi}\int_{0}^{\infty}\omega\,\xi(\omega)\,|\gamma|^2\,d\omega \qquad \{11\}$$

---

[1] Note.-If damping was constant with frequency, the energy dissipated could be expressed directly in the time domain. Using equation {7}, the shear stress is defined in the time domain as follows:

$$\tau(t)=G\left[\,\gamma(t)+2\,\xi\,\hat{\gamma}(t)\right]$$

where: $\hat{\gamma}(t)=\frac{1}{2\pi}\int_{-\infty}^{\infty}\left[i\,\mathrm{sgn}(\omega)\right]\gamma(\omega)\,e^{i\omega t}\,d\omega$ is the Hilbert Transform of $\gamma(t)$.

Therefore, the power and the energy dissipated as a function of time would be evaluated as follows:

$$P(t)=\tau\,\dot{\gamma}=G\left(\gamma+2\,\xi\,\hat{\gamma}\right)\dot{\gamma}$$

$$E_d(t)=2\,\xi\,G\int_0^t\hat{\gamma}\,\dot{\gamma}\,dt$$

With T being the duration of motion, the average power dissipated is defined as follows:

$$\overline{P} = \frac{E_d}{T} \qquad \{12\}$$

The RMS value of the shear strain, is obtained as an integral (summation) in the time and frequency domain as following:

$$\gamma_{RMS}^2 = \frac{1}{T}\int_0^T \gamma^2\, dt = \frac{1}{T}\frac{1}{2\pi}\int_{-\infty}^{\infty} |\gamma|^2\, d\omega = \frac{1}{T\pi}\int_0^{\infty} |\gamma|^2\, d\omega \qquad \{13\}$$

Considering that for a pure harmonic motion, the RMS value of the shear strain is $\gamma_{peak} = \sqrt{2}\ \gamma_{RMS}$, we define:

$$\gamma_{peak}^2 = 2\ \gamma_{RMS}^2 \qquad \{14\}$$

and therefore the maximum energy stored is evaluated as follows:

$$E_s = \frac{1}{2} G\, \gamma_{peak}^2 = G\, \gamma_{RMS}^2 = \frac{G}{\pi T}\int_0^{\infty} |\gamma|^2\, d\omega \qquad \{15\}$$

From equations {11} and {15}, the equivalent energy ratio is defined as the following integral ratio in the frequency domain:

$$\xi = \frac{1}{4\pi}\frac{E_d}{E_s} = \frac{1}{4\pi}\frac{\frac{2G}{\pi}\int_0^{\infty} \omega\ \xi(\omega)\, |\gamma|^2\, d\omega}{\frac{G}{\pi T}\int_0^{\infty} |\gamma|^2\, d\omega} = \frac{\int_0^{\infty} \omega\ \xi(\omega)\, |\gamma|^2\, d\omega}{\omega_0 \int_0^{\infty} |\gamma|^2\, d\omega} \qquad \{18\}$$

where: $\omega_0 = \frac{2\pi}{T} = \Delta\omega$

5.3.2 ENERGY DISSIPATED - NONLINEAR PARALLEL SERIES MODEL

The energy dissipated for the nonlinear parallel series model was successively evaluated directly in the time, as described in Section 5.2 for the sinusoidal loading. In particular, using the notation introduced in 4.3.2c, the tangent and spring stiffnesses are evaluated as follows:

$$G_{tan} = \frac{d\tau}{d\gamma} = G'\gamma + G \qquad \text{Tangent Stiffness}$$

$$\frac{dG_{tan}}{d\gamma} = \frac{d^2\tau}{d\gamma^2} = G''\gamma + 2G' \qquad \{19\}$$

$$k = -\left(\frac{d^2\tau}{d\gamma^2}\right) = -\frac{dG_{tan}}{d\gamma} \qquad \text{Spring Stiffness}$$

Therefore, the energy dissipated for an infinite number of elastoplastic springs is evaluated as the integral (for the present analysis, finite number of springs was used):

$$E_d = 4\int_0^{\gamma_{max}} k\gamma\left(\gamma_{max} - \gamma\right)d\gamma$$

$$= -4\int_0^{\gamma_{max}} \left(\frac{dG_{tan}}{d\gamma}\right)\gamma\left(\gamma_{max} - \gamma\right)d\gamma$$

$$= -4\left\{\gamma_{max}\int_0^{\gamma_{max}} \left(\frac{dG_{tan}}{d\gamma}\right)\gamma\, d\gamma - \int_0^{\gamma_{max}} \left(\frac{dG_{tan}}{d\gamma}\right)\gamma^2\, d\gamma\right\}$$

$$= 4\left\{G_{tan}\,\gamma^2\Big|_0^{\gamma_{max}} - 2\int_0^{\gamma_{max}} G_{tan}\,\gamma\, d\gamma - \gamma_{max}G_{tan}\,\gamma\Big|_0^{\gamma_{max}} + \gamma_{max}\int_0^{\gamma_{max}} G_{tan}\, d\gamma\right\}$$

$$= 4\left\{\gamma_{max}\int_0^{\gamma_{max}} \frac{d\tau}{d\gamma}d\gamma - 2\int_0^{\gamma_{max}} \frac{d\tau}{d\gamma}\gamma\, d\gamma\right\}$$

$$= 4\left\{2\int_0^{\gamma_{max}} G\gamma\, d\gamma - G\,\gamma_{max}^2\right\}$$

After performing the algebraic operations and substituting from equation {19} the tangent and secant moduli, the energy dissipated is calculated as:

$$E_d = 4\left\{ 2\int_0^{\gamma_{max}} G\,\gamma\,d\gamma - G\,\gamma_{max}^2 \right\} \qquad \{20\}$$

Successively, the energy stored is evaluated as follows:

$$E_s = \frac{1}{2} G\,\gamma_{max}^2 \qquad \{21\}$$

Combining equations {20} and {21}, the hysteretic damping ratio, ξ, is calculated as follows:

$$\xi = \frac{1}{4\pi}\frac{E_d}{E_s} = \frac{2}{\pi}\left\{ \frac{2\int_0^{\gamma_{max}} G\,\gamma\,d\gamma}{G\,\gamma_{max}^2} - 1 \right\} = \frac{2}{\pi}\left\{ \frac{\int_0^{\gamma_{max}} \tau\,d\gamma}{\frac{1}{2}\tau\,\gamma_{max}} - 1 \right\} \qquad \{22\}$$

5.3.3 Example of Application

In what follows, the performance of the frequency-dependent linear-hysteretic model is compared to the exact nonlinear solution, using the parallel series model. Both models were coded in FORTRAN, and the computer code can be found in Appendix III.1. For the simulation, the Kobe N-S accelerogram was used, the integral of which was scaled to γ_{max} = 0.001 and γ_{max} = 0.05.

Results are shown in Figures 5.5 and 5.6 successively. For each simulation, the following items are presented:

(a) the shear strain time history,

(b) the shear stress - strain hysteresis loop (nonlinear model),

(c), (d) the frequency dependent damping and shear modulus reduction factor, and

(e) comparison of the energy dissipated, evaluated using the two models.

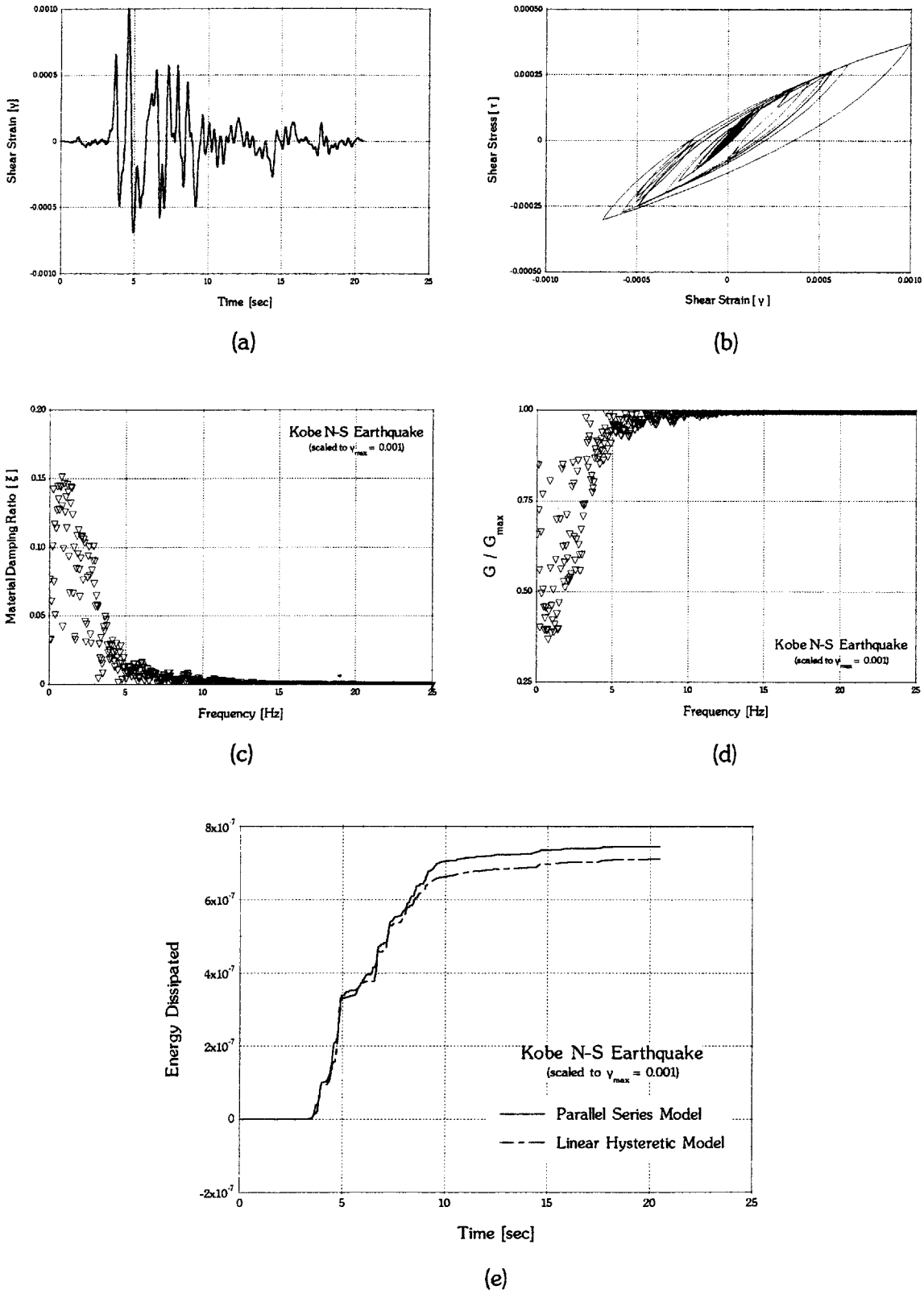

Figure 5.5 Comparison of the Linear-Hysteretic Frequency-Dependent Model with the Nonlinear Parallel Series Model for the Kobe N-S earthquake (γ_{max} = 0.001)

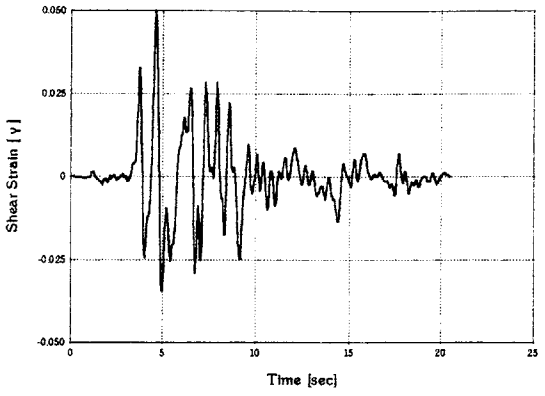

(a)

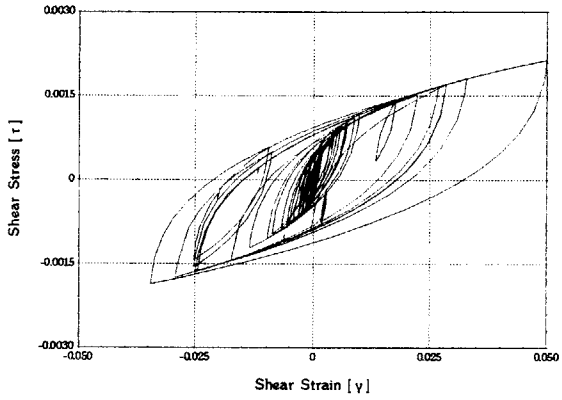

(b)

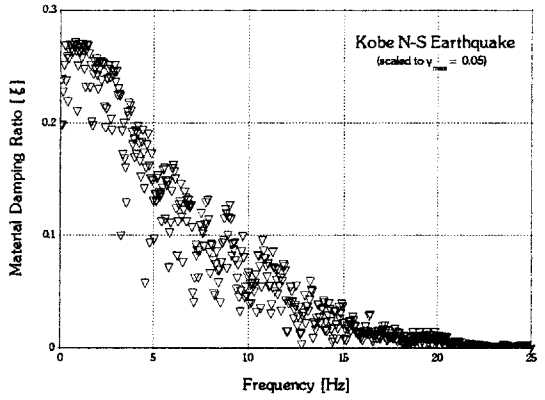

(c)

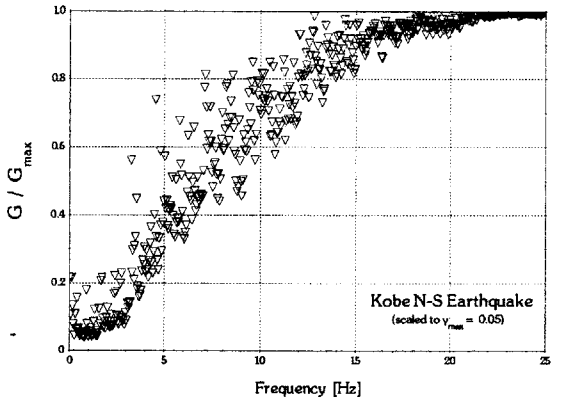

(d)

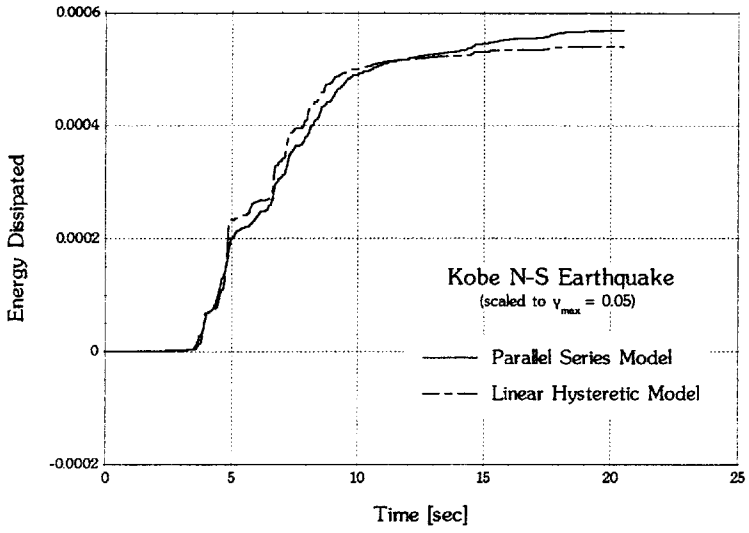

(e)

Figure 5.6 Comparison of the Linear-Hysteretic Frequency-Dependent Model with the Nonlinear Parallel Series Model for the Kobe N-S earthquake ($\gamma_{max} = 0.05$)

As it can be readily seen, results of the frequency dependent linear hysteretic model are in very good agreement with the nonlinear parallel series model. As it was expected, the distribution of shear modulus reduction factor and damping in the frequency domain shows that the model has a stiffer response and therefore dissipates less energy due to the high frequency components of the excitation.

In what follows, a general rule for the distribution of strain in the frequency domain is developed. By this approximation, an attempt to avoid errors arising from numerical instabilities due to the spikes characterizing the exact Fourier transform, and on the same time to accelerate the time required for the solution of the wave propagation problem, using the linear-hysteretic, frequency-dependent damping model, is made.

5.4 SMOOTHED STRAIN DISTRIBUTION IN THE FREQUENCY DOMAIN

In order to develop a general rule for the distribution of strain in the frequency domain, various accelerograms were used, namely Helena, Golden Gate, Kobe, Pacoima Dam, Loma Prieta, Olympia, San Fernando, Parkfield and El Centro.

The strain time history was successively approximated, by integrating the acceleration time histories once, and scaling them to the desired maximum strain value, according to the rationale described in Section 5.3.

Figure 5.7 shows the Fourier transform of the strain time histories obtained as described above and successively scaled to the same mean value in the frequency range 0 - 5 Hz. As it can be readily seen, the distribution of the strain in the frequency domain for all the earthquakes under consideration was approximately the same and therefore, a smoothed curve could approximate within desired degree of accuracy, the exact distribution.

The smoothed curve to fit the strain distribution in the frequency domain was chosen to be the following:

$$\gamma = \gamma_0 \cdot \frac{\exp(-0.15 \cdot f)}{(f+1)^{0.625}} \qquad \{23\}$$

where: γ_0 maximum strain amplitude, and

f frequency [Hz].

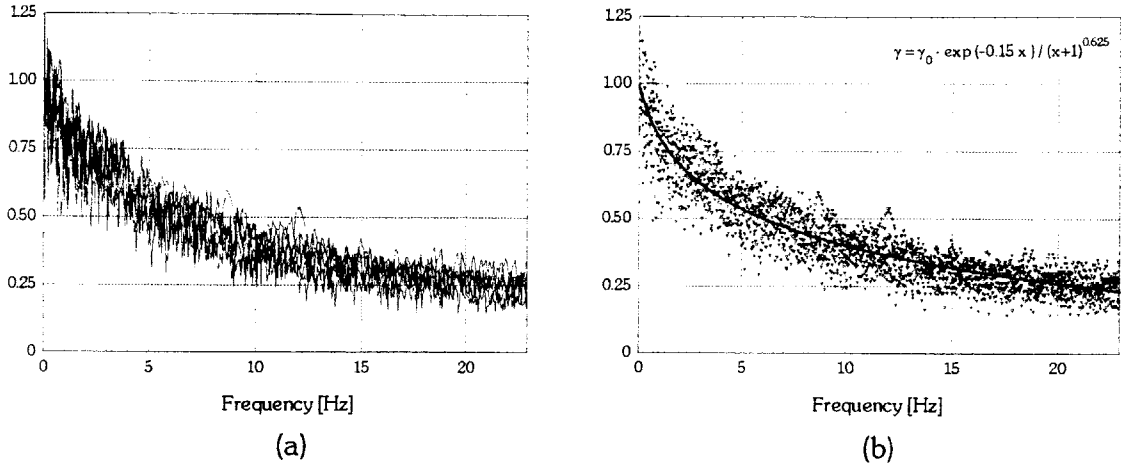

Figure 5.7 (a) Scaled Fourier transform of strain time history of various earthquakes, and (b) Smoothed approximation of given data

Using the proposed smoothed strain distribution in the frequency domain, numerical instabilities are avoided and the solution time is reduced as only the maximum value of strain is sufficient to evaluate the damping and shear modulus reduction factor in the frequency domain.

In what follows, the performance of the frequency-dependent linear-hysteretic model with smoothed strain Fourier transform is compared to the exact nonlinear solution, using the parallel series model. The FORTRAN computer code (Appendix III.1), was now modified to include the smoothed curve given by equation {23}. For the simulation, the Helena accelerogram was used, the integral of which was scaled to $\gamma_{max} = 0.001$ and $\gamma_{max} = 0.05$.

Results are found to be in very good agreement for both the low and high intensity excitations (Figures 5.8 and 5.9). For each simulation, the following items are presented:

(a), (b) the exact and approximate distribution of damping and shear modulus reduction factor in the frequency domain, and

(c) comparison of the energy dissipated, evaluated using the frequency dependent model with both exact and smoothed strain FFT, and the nonlinear parallel series model.

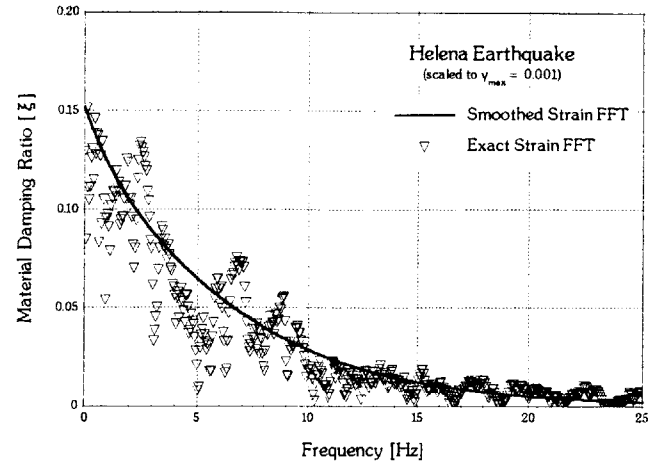

(a)

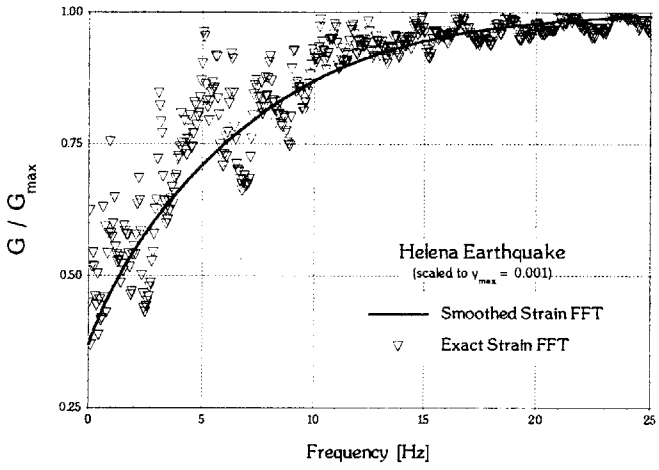

(b)

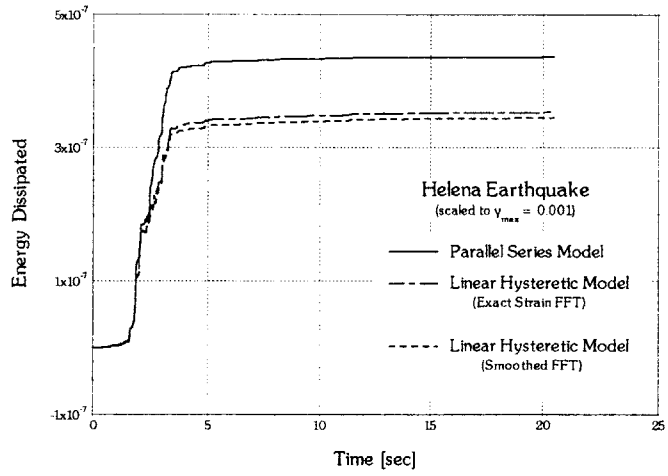

(c)

Figure 5.8 Frequency dependent damping and shear modulus reduction factor for the linear hysteretic model, and comparison of the energy dissipated evaluated using the exact, the smoothed strain FFT, and the parallel series model, for Helena earthquake scaled to $\gamma_{max} = 0.001$.

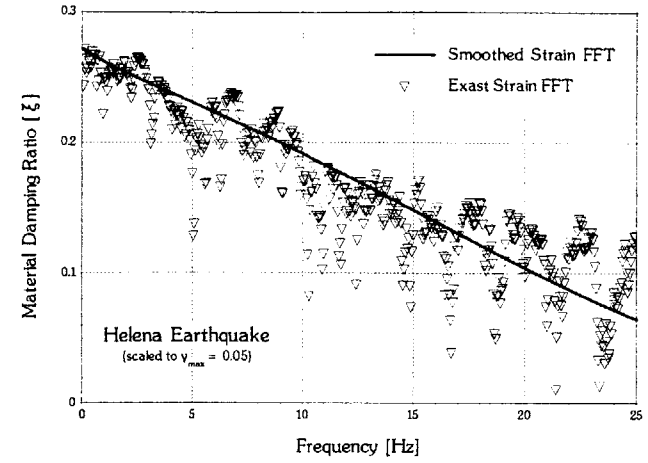

(a)

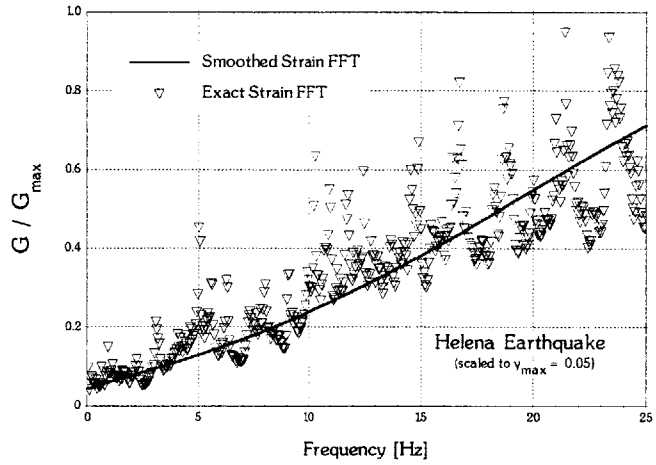

(b)

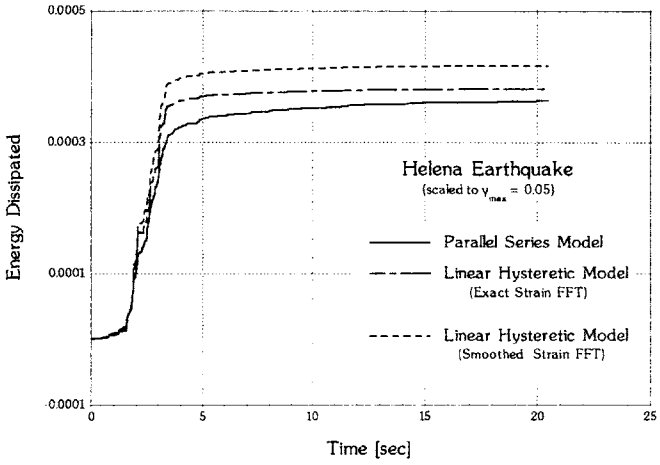

(c)

Figure 5.9 Frequency dependent damping and shear modulus reduction factor for the linear hysteretic model, and comparison of the energy dissipated evaluated using the exact, the smoothed strain FFT, and the parallel series model, for Helena earthquake scaled to $\gamma_{max} = 0.05$.

5.5 CONCLUSIONS

In this chapter, a refinement of the equivalent linear iterative procedure, namely to include frequency dependent hysteretic damping ratio and shear modulus reduction factor, was proposed. Results of the suggested linear – hysteretic frequency – dependent model have been compared to the results obtained using a nonlinear set of elastoplastic springs in parallel and are found to be in very good agreement.

Successively, an approximation of the strain distribution in the frequency domain was evaluated, to accelerate the solution and prevent numerical instabilities. Results using this approximation are found to be in agreement with the "exact" iterative procedure, within satisfying degree of accuracy.

Including the frequency dependent model into a wave propagation analysis code would lead to improved representation of the wave amplification through the continuum. In particular, for a given value of characteristic strain amplitude, the shear modulus reduction factor and damping being non-uniform in the frequency domain, would prevent the filtering of the higher frequencies, as they would be assigned lower damping and higher values of shear modulus.

The effect of including the frequency dependence of damping and shear modulus in wave propagation analysis alleviates significantly one of the alleged shortcomings of the equivalent-linear model, when used for moderately deep to very deep soil profiles.

5.6 REFERENCES

Assimaki, D., Kausel, E. & Whittle, A.J. (1999). " A Model for Dynamic Shear Modulus and Damping for Granular Soils", *Journal of Geotechnical and Geoenvironmental Engineering*, under publication

Constantopoulos, I. V. (1973). " Amplification Studies for a Nonlinear Hysteretic Soil Model", *Research Report R73-46*, Massachusetts Institute of Technology, September

Constantopoulos, I. V., Roesser, J. M. & Christian, J. T. A. (1973). " Comparison of linear and exact nonlinear analyses of soil amplification", *Proc. 5th World Conference on Earthquake Engineering*, Rome

Dames & Moore, Science Applications Inc. (1978). " Study of Nonlinear Effects on One - Dimensional Earthquake Response", prepared for *Electric Power Research Institute*, Projects 615-1,-2

Hall, J. R. Jr. & Richard, F. E. Jr. (1963). " Dissipation of Elastic Wave Energy in Granular Soils" ,*Journal of the Soil Mechanics and Foundation Division*, ASCE, Vol. 98, No. SM6, November, pp. 27-56

Iwan, W. D. (1967). " On a class of Models for the Yielding Behavior of Continuous and Composite Systems" , *Journal of Applied Mechanics*, Vol. 34, No. 3, September, pp. 612-617

Joyner, W. B. & Chen, A. T. F. (1975). " Calculation of Non-linear Ground Response in Earthquakes" , *Bulletin of the Seismological Society of America*, Vol. 65, No. 5, October, pp. 1315-1336

Kausel, E. & Roesset, J.M. (1984)." Soil Amplification: some refinements" , *Soil Dynamics and Earthquake Engineering*, Vol. 3, No.3, March, pp.116 - 123

Keydner, R. L.& Zelasko, J. S. (1963)." A Hyperbolic Stress – Strain Formulation for Sands" , *Proc. 2nd Pan American Conference on Soil Mechanics and Foundation Engineering*, Vol. 1, Brazil

Konder, R. L. (1963)." Hyperbolic Stress-Strain Response: CohesiveSoils" ,*Journal of the Soil Mechanics and Foundation Division*, ASCE, Vol. 89, No. SM1, February, pp. 115-143

Kramer, S. L. (1996)." Geotechnical Earthquake Engineering" , Prentice - Hall

Masing, G. (1926)." Eigenspannungen und Verfestigung beim Messing" , *Proc. 2nd International Congress of Applied Mechanics*, Zurich, pp. 332-335

Roesset, J.M & Whitman, R.V. (1969)." Theoretical Background for Amplification Studies" , *Research Report R69-15*, Massachusetts Institute of Technology, Soils Publication No. 231, March

Seed, H. B. (1969). " The influence of local conditions on earthquake damage" , *Proc. 7th International Conference on Soil Mechanics and Foundation Engineeering*, Mexico City, Mexico, August

Weissman, G. F. & Hart, R. R. (1961). " The Damping Capacity of Some Granular Soils" , *Symposium of Soil Dynamics*, Special Technical Publication No. 305, American Society for Testing and Materials, pp. 15-19

Whitman, R. V. (1970). " Evaluation of Soil Properties for Site Evaluation and Dynamic Analysis of Nuclear Plants" , *Seismic Design for Nuclear Plants*, R. J. Hanson (ed.), MIT Press, Cambridge, Massachusetts

CHAPTER 6

COMPARISON OF LINEAR AND EXACT NONLINEAR ANALYSIS OF SOIL AMPLIFICATION

6.1 INTRODUCTION

In the previous chapters of the present study, two major disadvantages of the equivalent linear iterative algorithm for soil amplification of deep deposits were studied in detail. In particular:

i. The shear modulus degradation and damping curves originally proposed by Seed & Idriss, 1969, and widely used in practice, are essentially the same for sands, gravels and cohesionless silts, and are independent of the cycle number considered, as well as the void ratio (or relative density), sand type and confining pressure. Laboratory experimental data provide evidence in support of some of the above simplifications, yet prove that the influence of confining pressure is significant and cannot be ignored, especially when dynamic analyses for deep soil deposits are performed.

ii. The assumption of a linear hysteretic damping, independent of frequency is only an approximation, which leads to non-realistic results when wave propagation in deep soil deposits is studied. As a result of this simplification, the high frequency components of the base excitation are artificially suppressed by the uniform distribution of hysteretic damping in the frequency domain.

Attempting to overcome the aforementioned shortcomings, two refinements to the linear iterative algorithm were introduced, namely:

i. A theoretical four - parameter soil model, derived from MIT-S1, with analytical expressions for the shear modulus reduction factor and damping versus shear strain amplitude, which depend on the soil type and the soil current state (void ratio and mean effective stress) and nonlinear characteristics (small strain nonlinearity).

ii. A frequency - dependent linear - hysteretic model, with analytical expressions for the shear modulus reduction factor and damping in the frequency domain.

In what follows, the improved proposed iterative algorithm is used for dynamic analyses of deep soil deposits, and results are compared to the true nonlinear incremental analyses performed in the time domain.

For consistency of the comparison, the properties of the nonlinear model, consisting of a series of elastoplastic springs in parallel, are derived from the stress - strain formulation of MIT-S1.

6.2 Frequency – Dependent Linear Analysis

The equivalent linear iterative algorithm used in the present study for dynamic analysis of deep soils operates as follows:

1. The soil deposit is divided in homogeneous sub-layers. For each one, the following input parameters for MIT-S1 need to be evaluated (see Chapter 3):
   a. the soil type (sand or clay),
   b. the mean effective stress acting in the middle of the stratum (calculated from the effective overburden stress and the coefficient of lateral earth pressure at rest - K_0),
   c. the current void ratio, e, (or the formation void ratio e_0, the slope of the LCC, ρ_c, and the mean effective stress), and
   d. the small strain non-linearity characteristics (described by the parameter ω_s).

   After the input parameters of the soil model are evaluated, the shear modulus degradation and damping curves are generated for each sub-layer.
2. For each homogeneous sub-layer, initial estimates of the shear modulus [G] and damping [ξ] are made, usually corresponding to the low strain values.
3. The estimated G and ξ values are used to compute the ground response, including time histories of shear strain for each sub-layer.
4. The maximum value between the fundamental frequency of the analyzed stratum and the mean frequency of the excitation velocity spectrum (which is proportional to the strain Fourier spectrum as shown in Section 5.3) is defined. Successively, the smoothed Fourier Spectrum is assigned constant value until the aforementioned frequency and decays according to the rule described in Section 5.4 thereafter.
5. The smoothed distribution of shear strain in the frequency domain is multiplied by the strain transfer function of the analyzed interface (for a layered soil deposit) and scaled to

the maximum value of shear strain in each sub-layer (see Chapter 5). The frequency corresponding to the maximum value of the scaled product (i.e. the maximum strain) is defined, and the scaled product is assigned constant value equal to the maximum until the corresponding frequency.[1]

6. Successively, each discrete frequency is assigned a value of shear modulus reduction factor and hysteretic damping, using the corresponding value of the scaled strain Fourier spectrum, constructed as described above, and the G/G_0 and ξ curves are derived for each sub-layer in step 1.
7. The iterative procedure is repeated (i.e. steps 5-7), until differences between the computed values of shear modulus and damping between two successive iterations, do not exceed a prescribed tolerance value.

The procedure described above, referring to the distribution of damping in the frequency domain, is schematically illustrated in Figure 6.1.

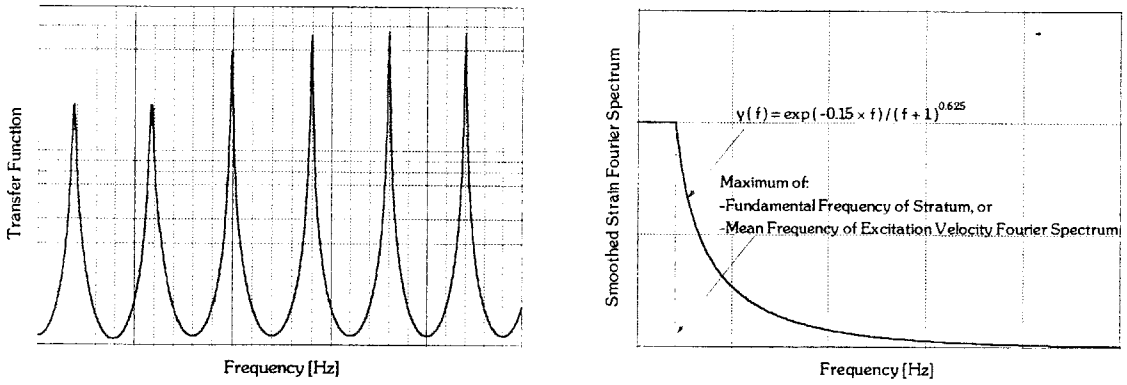

6.1a The Transfer function of the interface of interest is multiplied by the smoothed strain Fourier Spectrum

[1] Note.- The product of the smoothed strain Fourier spectrum and the transfer function at the interface under consideration, is at this point smoothed using a "smoothing window" of 0.75 Hz. The amplitude of the smoothed window was chosen such that no sharp peaks, introduced by the strain transfer functions, appear in the analysis, probably causing numerical instabilities to the solution. In addition, a wider "smoothing window", i.e. including more points, would probably assign less damping to the resonant frequencies of the stratum.

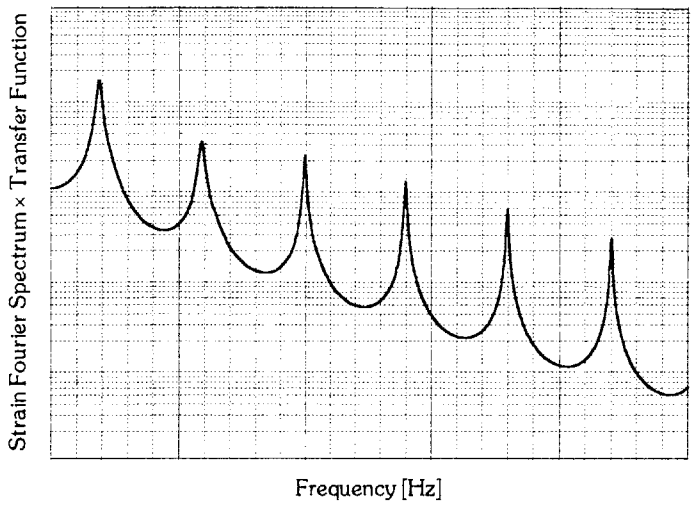

6.1b The product of the smoothed strain Fourier Spectrum and the Transfer function is then scaled to the maximum value of the strain time history, and the frequency corresponding to the maximum value of the product is defined.

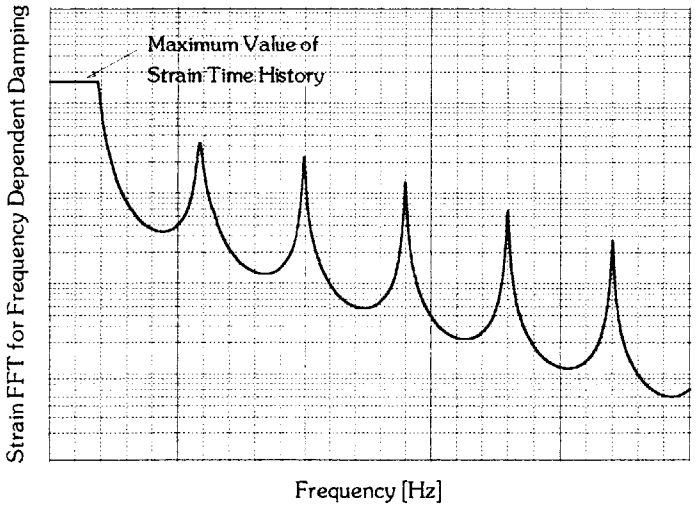

6.1c The scaled strain Fourier Spectrum is assigned constant value of the strain time history maximum until the frequency corresponding to the maximum of the product, is successively smoothed and used for the distribution of damping and shear modulus reduction factors in the frequency domain.

Figure 6.1 Frequency Dependent Damping and Shear Modulus for seismic wave propagation - Illustration of the Method.

It should be noted herein that the proposed iterative algorithm would lead to similar results with the procedure commonly used in practice, when shallow soil deposits are studied. However, the incorporation of a theoretical soil model and a frequency - dependent damping rule makes the algorithm applicable for a wider range of studies.

In addition, by introducing the distribution of damping and shear modulus reduction factor in the frequency domain, the need of defining a characteristic level of strain, which for a transient motion has not been standardized yet, is eliminated.

6.3 EXACT NONLINEAR ANALYSIS

To verify the validity of the approach described in Section 6.2, results are compared to the exact nonlinear incremental analysis. For the analysis performed herein, the soil profile was modeled as a lumped mass, multi - degree of freedom system, as shown in Figure 6.2.

The nonlinear soil elements were modeled as a set of elastoplastic springs in parallel (Masing soil), the stiffness and yield deformation of which was derived from the stress - strain formulation of the modified MIT-S1 soil model, as described in Sections 4.3.2c and 5.2.

The equations of motion were directly integrated in the time domain using the Central Difference Method.

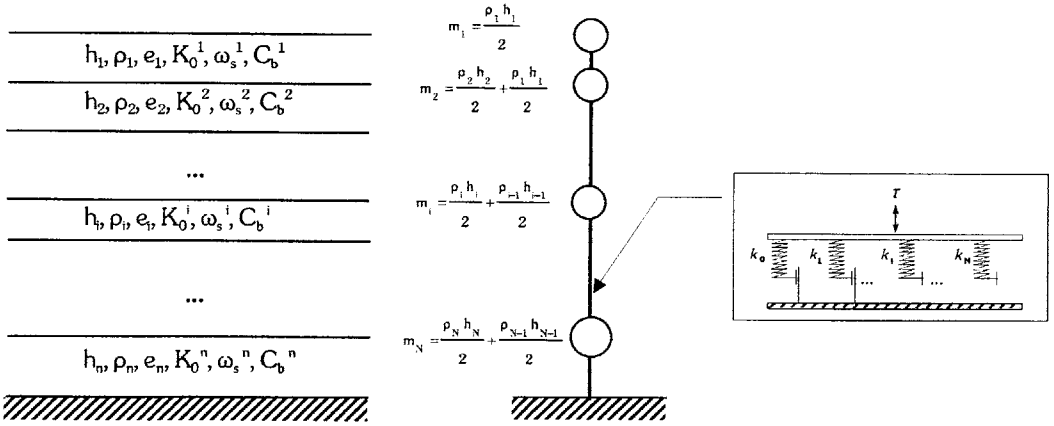

Figure 6.2 Idealization of the soil profile as a multi-degree of freedom system, for the exact nonlinear soil amplification analysis.

The FORTAN computer code used to evaluate the nonlinear seismic response of the soil profiles successively studied, can be found in Appendix III.2.

6.4 EXAMPLE OF APPLICATION

In what follows, soil amplification analyses using both approaches (Section 6.2 and 6.3) are presented. The validity of the proposed method is initially illustrated for the seismic analysis of a shallow homogeneous profile overlying rigid bedrock, and then for the deep soil profile analyzed in Section 3.7.

6.4.1 HOMOGENEOUS SHALLOW SOIL PROFILE

An idealized homogeneous profile of depth 25.00m and mass density 2.00 ton/m^3 is subjected to various excitations prescribed at the rigid bedrock. The profile is analyzed using both the equivalent - linear, frequency - pressure dependent, as well as the lumped mass nonlinear approach, as described in Sections 6.2 and 6.3 successively.

The shear wave velocity of the profile is 200 m/sec, and therefore the fundamental shear-beam frequency of the stratum is 2.00 Hz.

Table 6.1 lists the dimensionless parameters for the modified MIT-S1 soil model, which was used to estimate the material damping and shear modulus reduction factors distribution in the frequency domain.

C_b	800
ω	1
μ'_0	0.25
ω_s	2.4
K_0	0.5
e_0	0.5
C	2.03

Table 6.1 Input Parameters for MIT-S1 model

For both the equivalent linear and nonlinear analyses, the profile was divided into 10 homogeneous layers of 2.5m each. The equivalent linear dynamic analysis of the profile was carried out using the computer code LAYSOL (Kausel, 1992), based on a continuum formulation of the wave propagation problem in the frequency - wavenumber domain, which was modified to incorporate frequency dependent damping.

The profile was initially subjected to a pure sinusoidal excitation with frequency of 2.00 Hz (coinciding with the fundamental frequency of the soil deposit). Successively to the superposition of two sinusoidal motions (2.00 Hz and 8.00Hz) with the high frequency component having half the amplitude of the low frequency. Finally, the profile was subjected to various earthquake excitations of intensities varying from 0.01g, where the response was nearly elastic, to 0.5g where nonlinear effects dominate in the response of the profile.

It should be noted herein that when the nonlinear analysis is performed, the value of damping is internally adjusted according to the level of strain as the solution marches in time. On the other hand, whilst using the equivalent linear frequency dependent analysis, the same pattern of frequency dependent damping is maintained throughout the solution. The results of this approximation become apparent when observing the response of the profile to the sinusoidal excitation, where the equivalent linear solution produces more damping until the motion reaches the steady state regime.

Results are shown in Figures 6.3 - 6.6 and are found to be in very good agreement. In particular, the analysis for each excitation under consideration is presented as follows:

(a) The input motion prescribed at bedrock.

(b) The response at the top of the profile, evaluated using both the equivalent linear pressure – frequency dependent and nonlinear analysis.

(c) The distribution of material damping ratio and shear modulus reduction factors in the frequency domain, for the bottom layer of the stratum, used for the equivalent linear analysis.[2]

(d) The hysteresis loops at the bottom and middle layer of the stratum, evaluated using the nonlinear parallel series model.

It readily seen that the equivalent linear pressure – frequency dependent analysis represents the nonlinear behavior of the stratum, within acceptable degree of accuracy, even for very strong motions, where nonlinear effects dominate in the response.

[2] Note.-In the modified computer code used for the seismic response of the stratum with the frequency dependent model, material damping ratio was constrained to 0.1%, when smaller values would result following the approach described in Section 6.2.

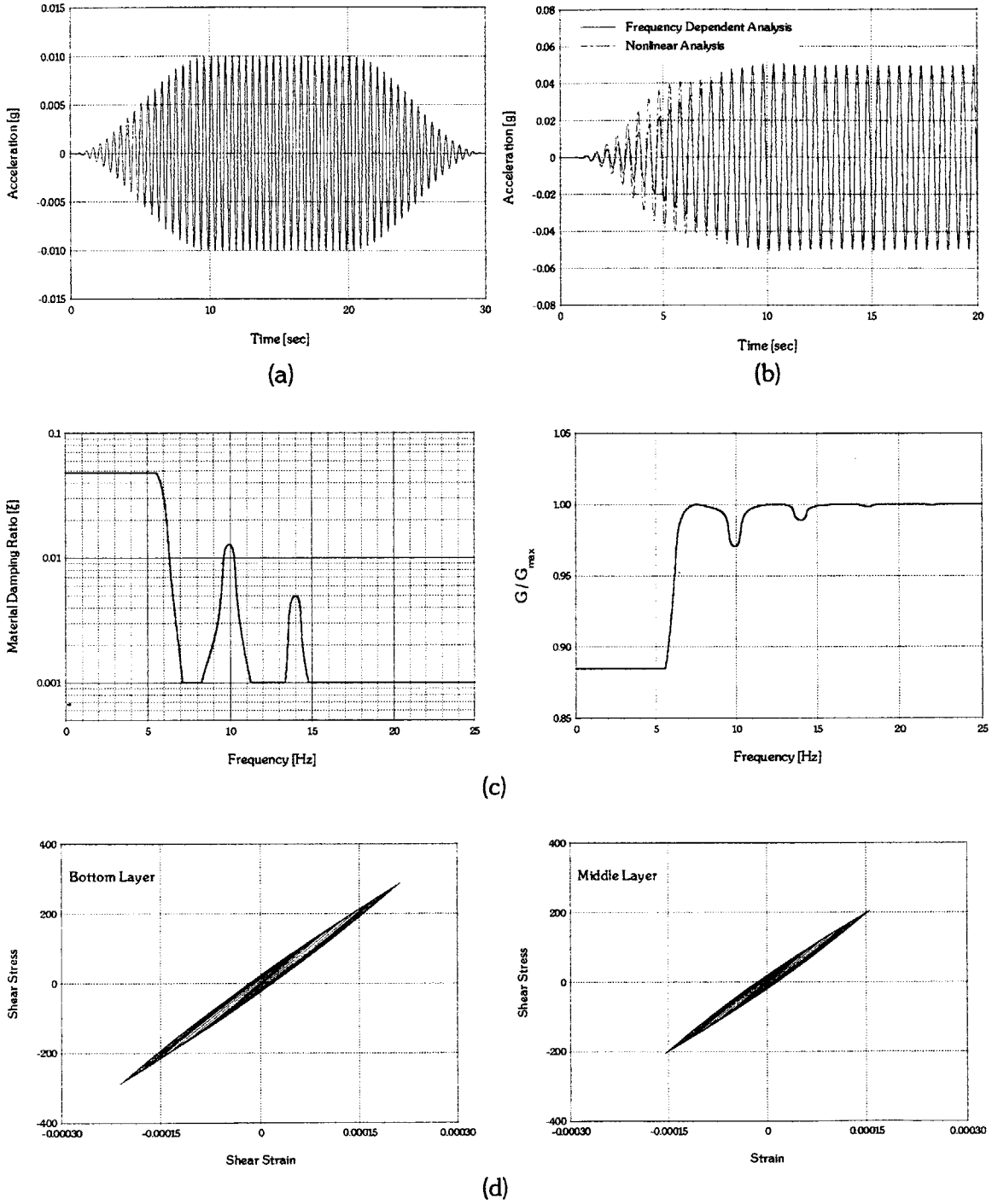

Figure 6.3 Simulation of seismic analysis of a shallow homogeneous soil deposit for a pure sinusoidal excitation [2.0 Hz], using frequency dependent and nonlinear analyses.

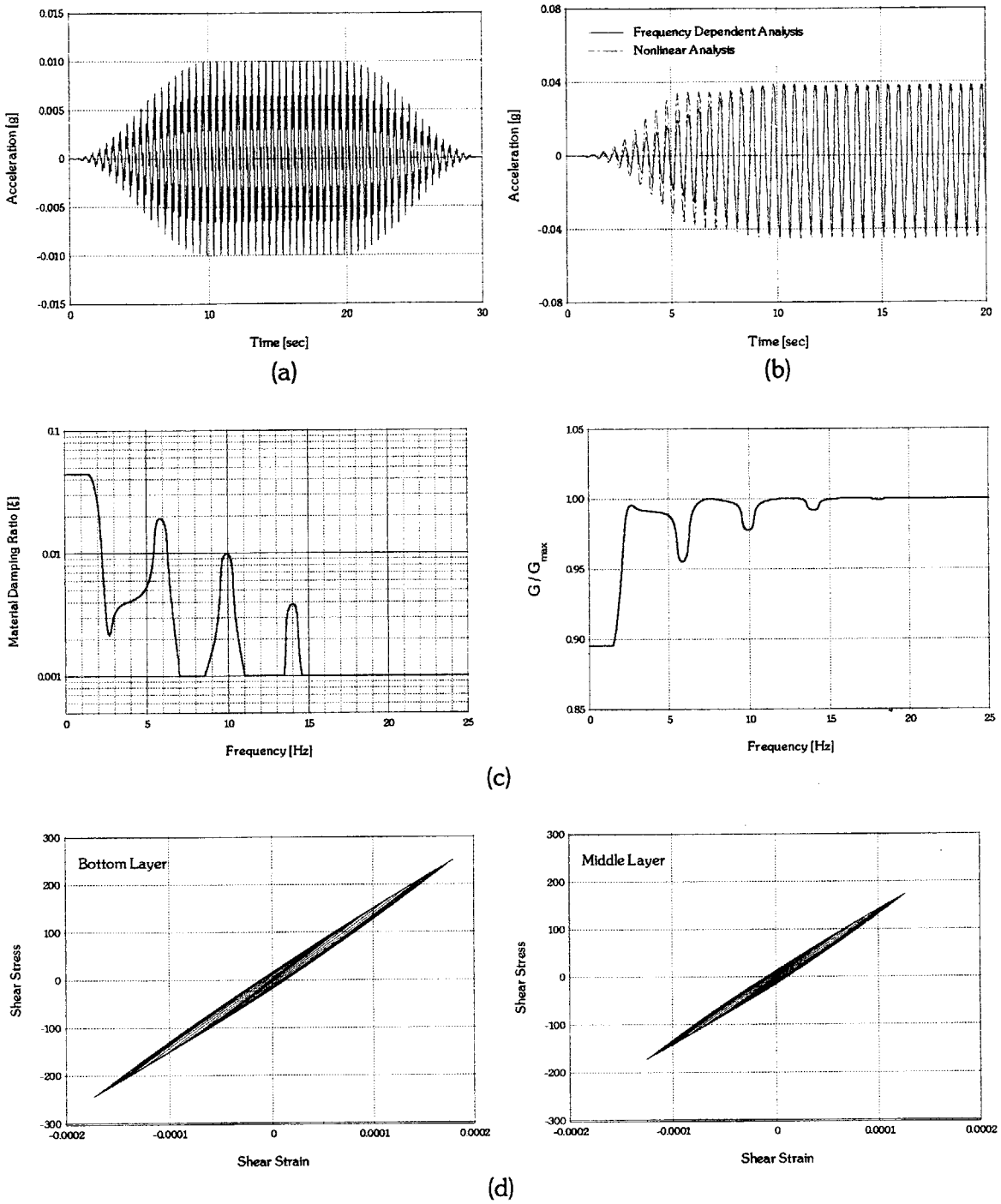

Figure 6.4 Simulation of seismic analysis of a shallow homogeneous soil deposit for the superposition of 2 sinusoidal excitations [2.0 and 8.0 Hz], using frequency dependent and nonlinear analyses.

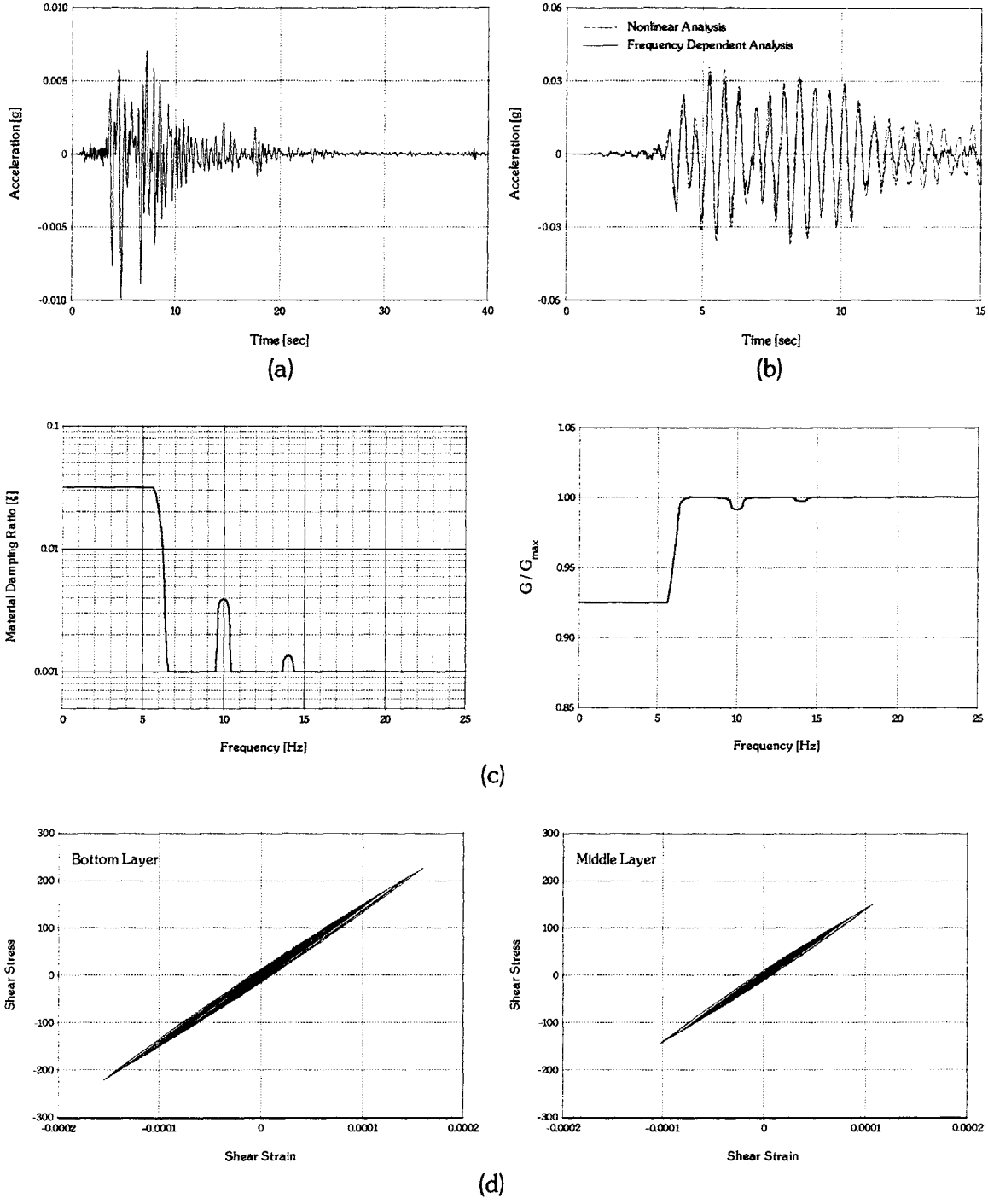

Figure 6.5a Simulation of seismic analysis of a shallow homogeneous soil deposit for the Kobe earthquake with maximum acceleration 0.01g, using frequency dependent and nonlinear analyses.

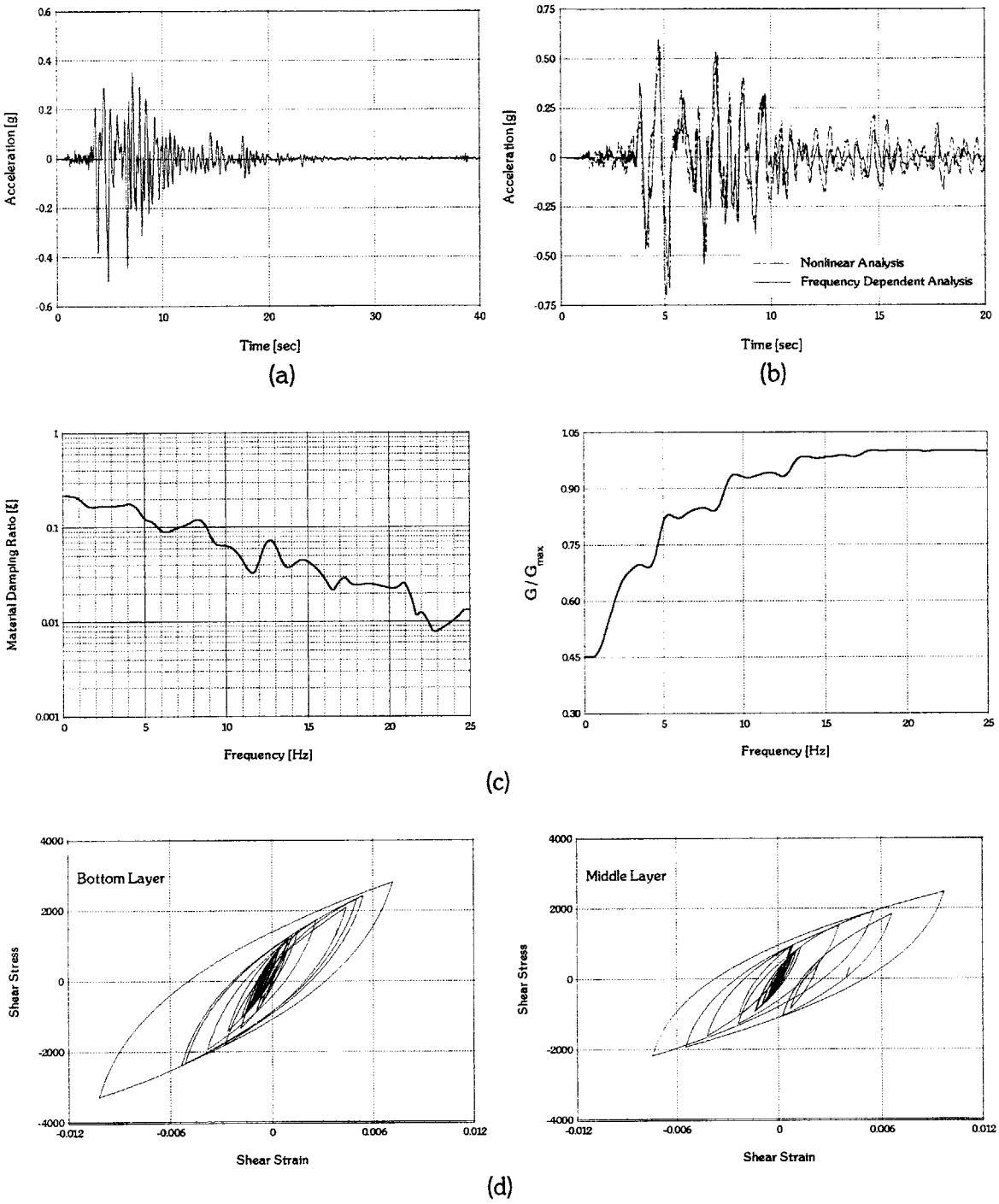

Figure 6.5b Simulation of seismic analysis of a shallow homogeneous soil deposit for the Kobe earthquake with maximum acceleration 0.5g, using frequency dependent and nonlinear analyses.

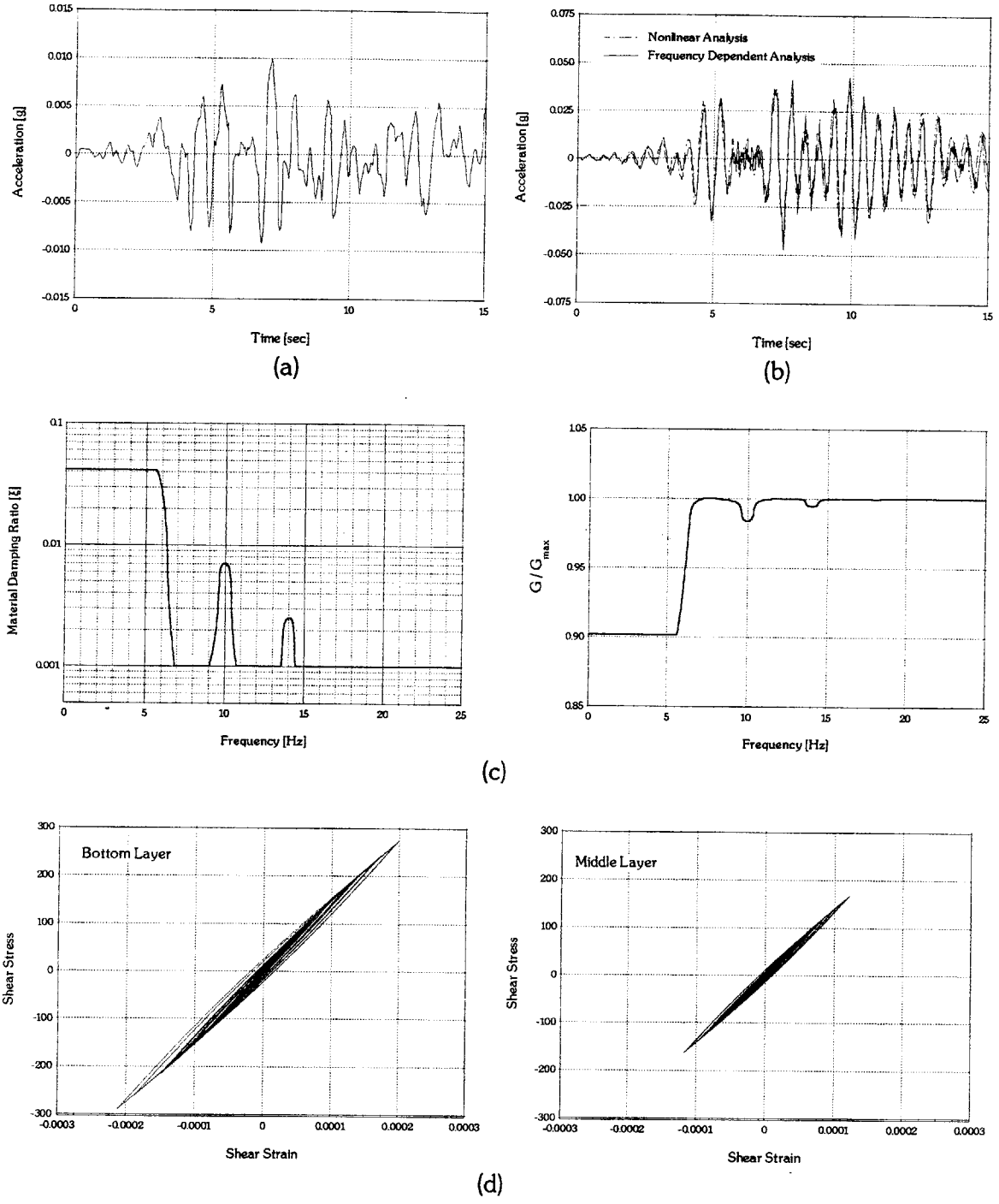

Figure 6.6a Simulation of seismic analysis of a shallow homogeneous soil deposit for the Pasadena earthquake with maximum acceleration 0.01g, using frequency dependent and nonlinear analyses.

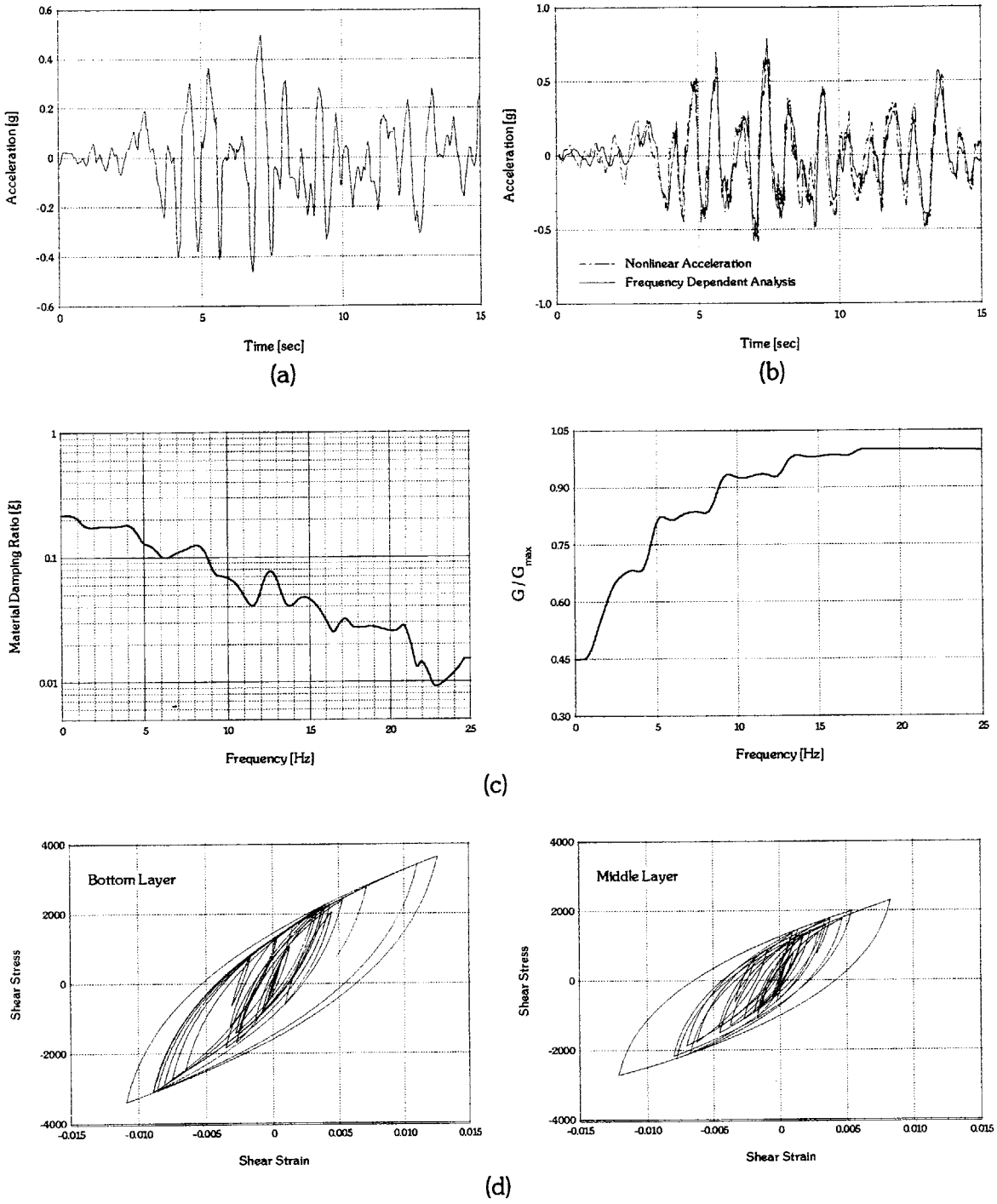

Figure 6.6b Simulation of seismic analysis of a shallow homogeneous soil deposit for the Pasadena earthquake with maximum acceleration 0.5g, using frequency dependent and nonlinear analyses.

6.4.2 DEEP SOIL PROFILE

The idealized soil profile described in detail in Section 3.7, namely of depth 1000m and mass density varying from 2.12 ton/m^3 at the surface to 2.21 ton/m^3 at 1000m depth, is subjected to an earthquake prescribed at the bedrock. The soil parameters are chosen identical to the remolded sand specimens from Laird & Stokoe (1993). The variation of void ratio (and mass density) of the profile with depth was chosen to match the soil properties in Memphis, Tennessee, as reported by Abrams & Shinozuka (1997).

Table 6.2 lists the dimensionless input parameters for this model. These are used both to estimate the small strain ($\gamma = 10^{-6}$) shear modulus G_{max} and to determine the modulus degradation and damping curves. The variation of the shear wave velocity with depth can be found in Figure 3.6, along with the reported profile for the Memphis area (Abrams & Shinozuka, 1997). The fundamental shear-beam frequency of the soil for this profile is 0.156 Hz.

C_b	800
ω	1
μ'_0	0.25
ω_s	2.4
e_0	0.25
σ'_{rev} / p_a	6051
C	2.26

Table 6.2 Input parameters for MIT-S1 model

The variation of void ratio with the mean effective stress is taken from the original formulation for the MIT-S1 model for cohesionless soils (Pestana & Whittle, 1995).

The dynamic response of the profile at the surface is calculated both by means of the equivalent linear pressure – frequency dependent, as well as the nonlinear analyses described above. For the analyses performed, the soil profile is divided into 100 homogeneous layers of 10m thickness each, whose material properties are inferred from Fig. 3.6 (taking the values at the center of the layers).

For the equivalent linear approach, the computer code LAYSOL (Kausel, 1992) was used, appropriately modified to incorporate the material damping ratio and shear modulus reduction factor distribution in the frequency domain.

The profile was subjected to various earthquake excitations of intensities varying from 0.01g, where the response was nearly elastic, to 0.5g where nonlinear effects dominate in the response of the profile.

Results are shown in Figures 6.7a-6.7c for Kobe earthquake and are found to be in very good agreement. In particular, the analysis for each excitation under consideration is presented as follows:

(a) The response at the top of the profile, evaluated using both the equivalent linear pressure– frequency dependent and nonlinear analysis.

(b) The Fourier Spectrum of acceleration time history at the surface, evaluated using both the equivalent linear pressure– frequency dependent and nonlinear analysis.

(c) The absolute value of the transfer function at the uppermost interface of the profile, obtained using the equivalent linear pressure– frequency dependent approach.

(d) The hysteresis loops at the middle layer of the stratum, evaluated using the nonlinear parallel series model.

It readily seen that the equivalent linear pressure – frequency dependent analysis represents the nonlinear behavior of such a deep stratum, within acceptable degree of accuracy, even for very strong motions, where nonlinear effects dominate in the response.

Moreover, the response of the deep profile obtained by means of the modified equivalent linear analysis, i.e. both frequency and depth dependency of shear modulus reduction factor and material damping, lead to significant less filtering of the high-frequency components of the excitation, in contrast to the equivalent linear approach used in practice, where high-frequency components would be completely wiped out.

The figures also show a characteristic 1.6 sec delay in initiation of the response at the surface. This is consistent with the travel time of shear waves between the basal rock and the surface with an average velocity of 600 m/s (as can be inferred from the 1/6 Hz resonant frequency and the 1000 m thickness). Hence, the simulations do satisfy causality. In addition, it should be observed that while the response of the equivalent linear model was obtained by Fourier-inversion of the frequency response functions, the time histories do not suffer from wraparound. In other words, the coda of the response does not spill into its beginning, as could have been expected for the lightly damped system with long natural period being considered here. These desirable characteristics are accomplished with the' complex exponential window method described by Kausel & Roesset (1992).

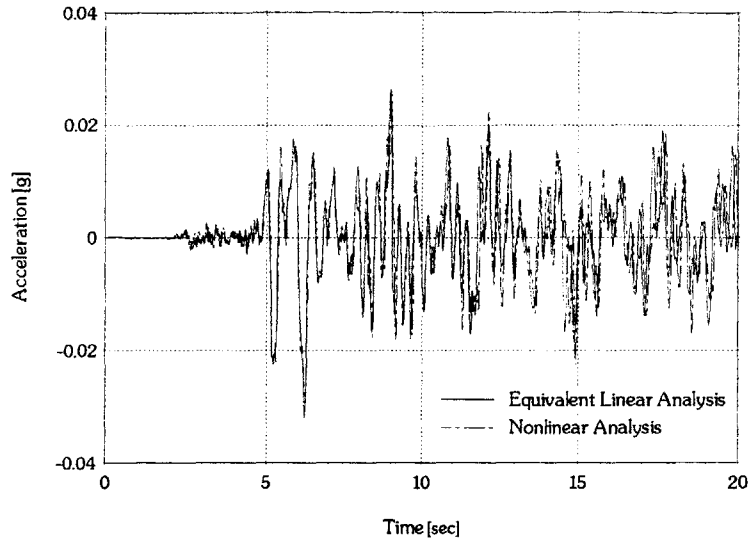

(a)

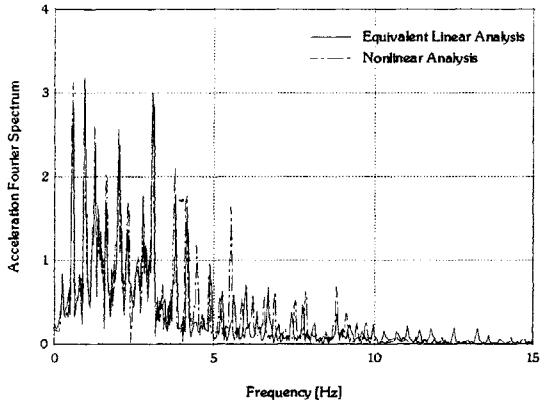

(b)

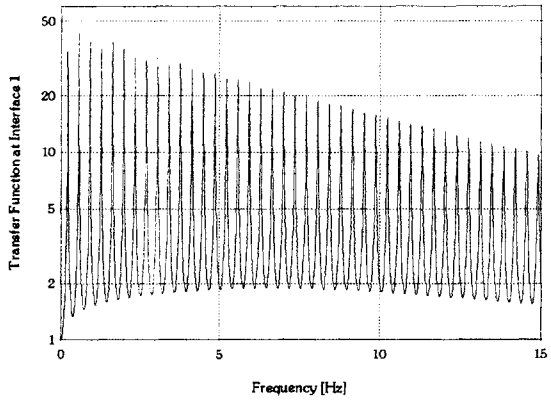

(c)

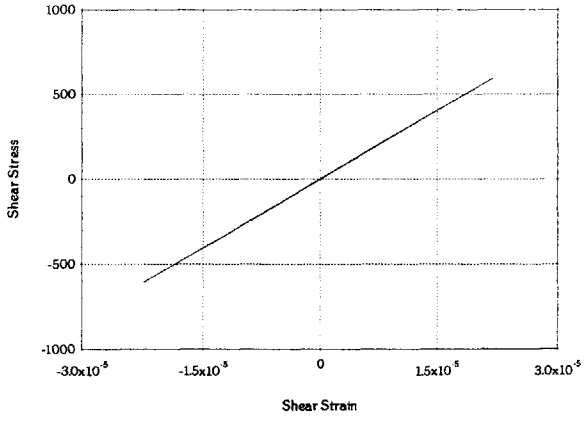

(d)

Figure 6.7a Simulation of seismic analysis of a deep (1.0 km) soil deposit for the Kobe earthquake with maximum acceleration 0.01g, using frequency dependent and nonlinear analyses.

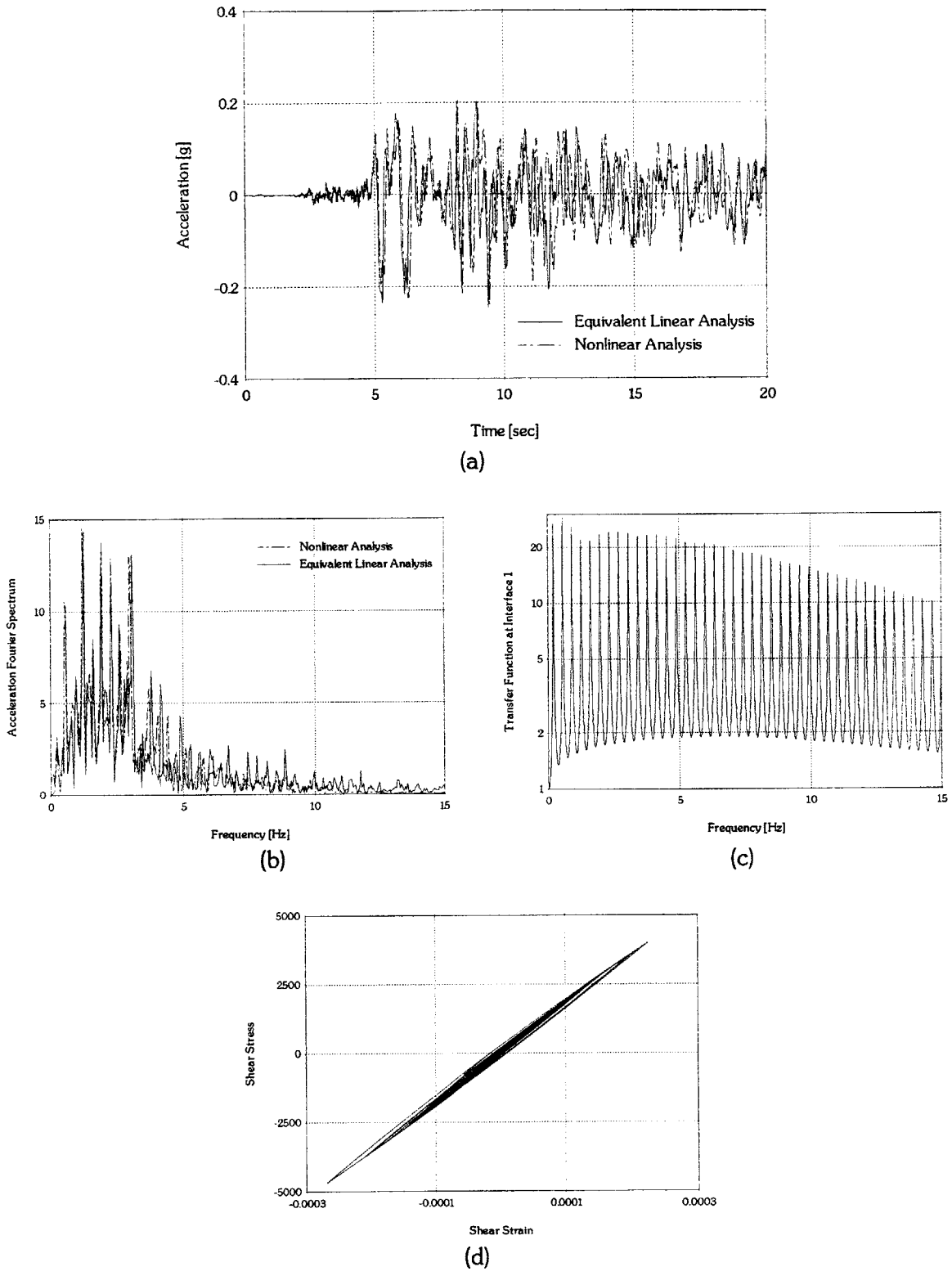

Figure 6.7b Simulation of seismic analysis of a deep (1.0 km) soil deposit for the Kobe earthquake with maximum acceleration 0.1g, using frequency dependent and nonlinear analyses.

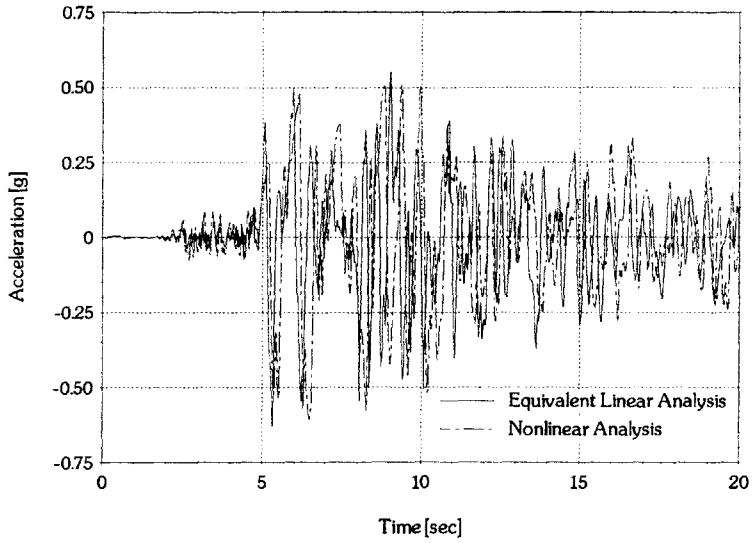

(a)

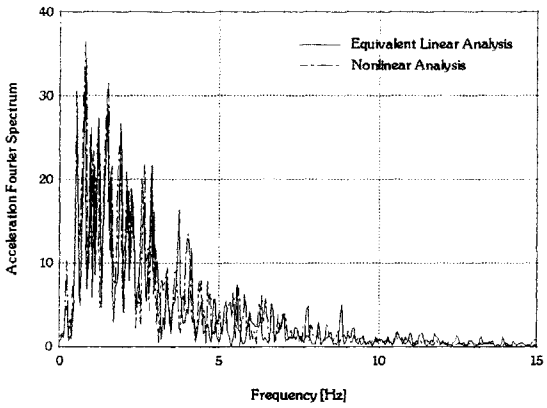

(b)

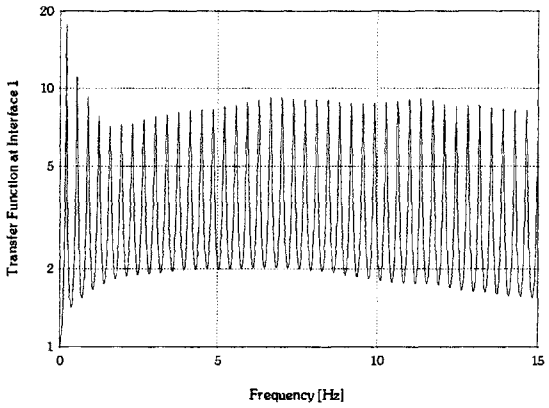

(c)

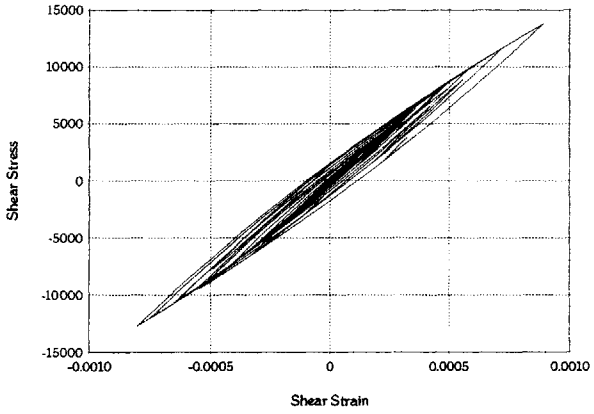

(d)

Figure 6.7c Simulation of seismic analysis of a deep (1.0 km) soil deposit for the Kobe earthquake with maximum acceleration 0.5g, using frequency dependent and nonlinear analyses.

Finally, it should be noted that for the case of the low intensity excitation, where the profile is subjected to very low shear strains, and the material damping ratio - according to the frequency- and pressure- dependent equivalent linear model - is successively minimal, no attenuation of the response amplitude is predicted by the proposed algorithm. Results of the surface response of the profile, when subjected to Kobe and Loma Prieta earthquakes, scaled to maximum acceleration 0.01g (Figures 6.8a and 6.8b), are compared with these obtained by the conventional Seed & Idriss (1970) approach.

This phenomenon, is found to be in agreement with accelerograms reported at the surface of deep basins (for example the Mississippi embayment), where the intensity of the ground motion is usually small, yet the profile characteristics (soft sediments) result to surface records of very long duration.

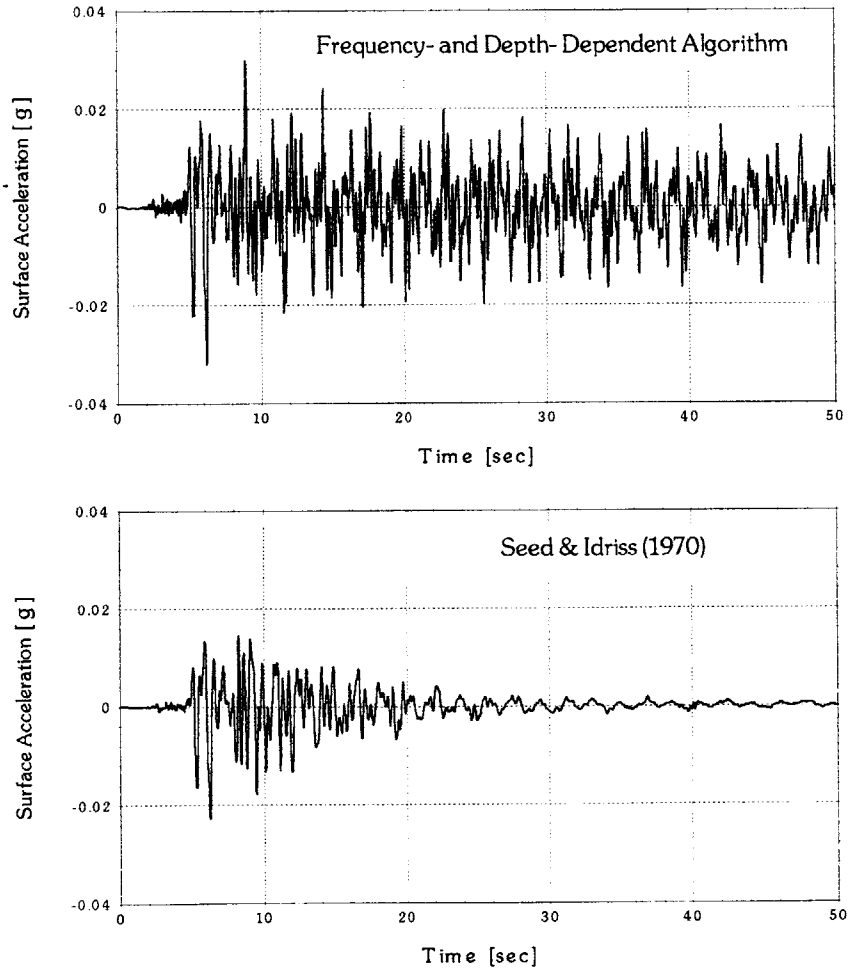

Figure 6.8a Comparison of the predicted duration of the surface response, for the Kobe earthquake scaled to maximum acceleration 0.01g.

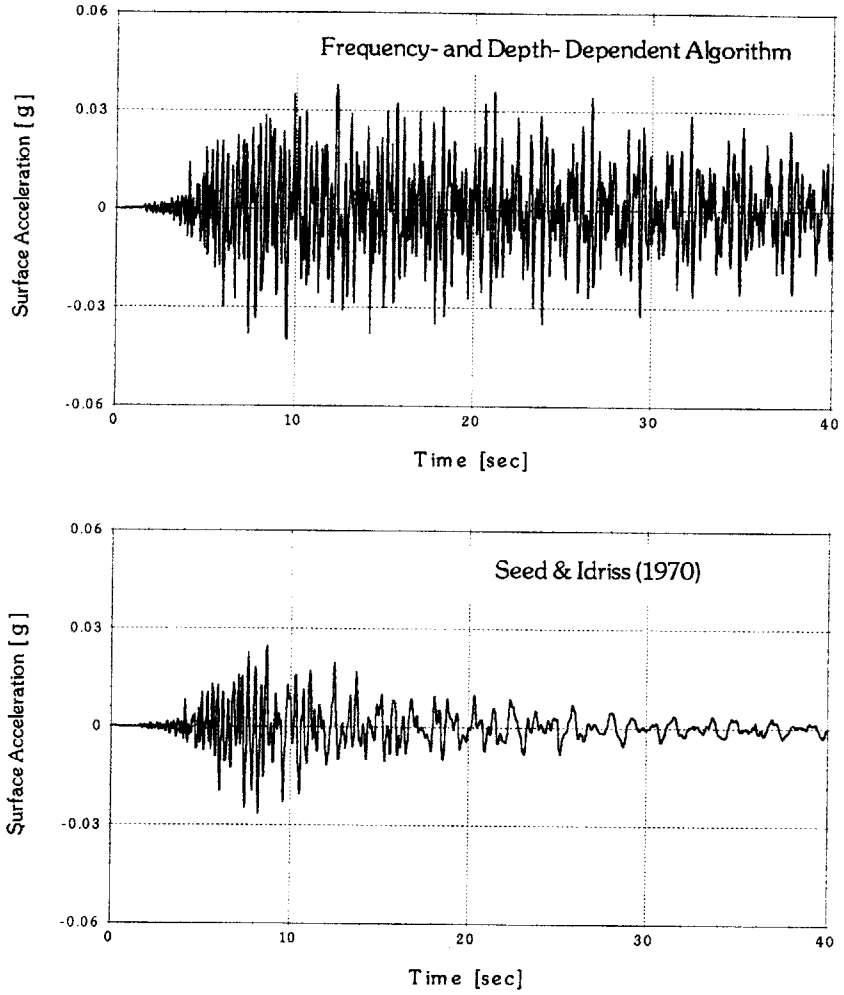

Figure 6.8b Comparison of the predicted duration of the surface response, for the Loma Prieta earthquake scaled to maximum acceleration 0.01g.

6.5 CONCLUSIONS

In this chapter, a modified equivalent-linear iterative procedure is proposed for amplification analyses of soil deposits. The proposed approach consists of a frequency- and pressure-dependent model, and was used to evaluate the seismic response of a shallow homogeneous and a deep (1.0 km) soil profiles.

Successively, results were compared to the response evaluated using" true" nonlinear incremental analysis, were the soil profile was modeled as a lumped mass, multi-degree of freedom system. The nonlinear elements were modeled as a set of elastoplastic spring is parallel (Masing soil), the stiffness and yield deformation of which was derived from the stress-strain formulation of MIT-S1 soil model.

The profiles were subjected to various excitations, with amplitudes varying from 0.01g (nearly elastic behavior) to 0.5g (very pronounced nonlinear response). Results were found to be in very good agreement, both for the shallow homogeneous as well as for the deep soil profiles.

Moreover, as it was expected, the seismic amplification analysis evaluated in the frequency – wavenumber domain, by means of a continuum formulation of the wave propagation problem, demands significantly less computational effort than the incremental analysis. In particular, a considerably lower time step is required for the conditionally stable direct integration scheme used for the present study, namely the central difference method, to allow for an accurate representation of the resonant frequencies of the profile, a fact which becomes more apparent as the depth and / or the shear wave velocity of the profile analyzed increases.

The proposed algorithm represents within acceptable degree of accuracy the nonlinear soil behavior and prevents the artificial filtering of the high-frequency components of the excitation.

6.6 REFERENCES

Assimaki, D., Kausel, E. & Whittle, A.J. (1999)." A Model for Dynamic Shear Modulus and Damping for Granular Soils", *Journal of Geotechnical and Geoenvironmental Engineering*, under publication

Constantopoulos, I. V. (1973)." Amplification Studies for a Nonlinear Hysteretic Soil Model", *Research Report R73-46*, Massachusetts Institute of Technology, September

Constantopoulos, I. V., Roesser, J. M. & Christian, J. T. A. (1973)." Comparison of linear and exact nonlinear analyses of soil amplification", *Proc. 5th World Conference on Earthquake Engineering*, Rome

Dames & Moore, Science Applications Inc. (1978)." Study of Nonlinear Effects on One - Dimensional Earthquake Response", prepared for *Electric Power Research Institute*, Projects 615-1,-2

Hall, J. R. Jr. & Richard, F. E. Jr. (1963)." Dissipation of Elastic Wave Energy in Granular Soils" ,*Journal of the Soil Mechanics and Foundation Division*, ASCE, Vol. 98, No. SM6, November, pp. 27-56

Joyner, W. B. & Chen, A. T. F. (1975)." Calculation of Non-linear Ground Response in Earthquakes" , *Bulletin of the Seismological Society of America*, Vol. 65, No. 5, October, pp. 1315-1336

Kausel,E. (1992)." LAYSOL: A computer program for the dynamic analysis of layered soils"

Kausel,E. & Roesset, J.M. (1992)." Frequency domain analysis of undamped systems using the exponential window method" , *Proc. 10th World Conference on Earthquake Engineering*, Madrid, Spain

Roesset, J.M & Whitman, R.V. (1969). " Theoretical Background for Amplification Studies" , *Research Report R69-15*, Massachusetts Institute of Technology, Soils Publication No. 231, March

Whitman, R. V. (1970). " Evaluation of Soil Properties for Site Evaluation and Dynamic Analysis of Nuclear Plants" , *Seismic Design for Nuclear Plants*, R. J. Hanson (ed.), MIT Press, Cambridge, Massachusetts

APPENDICES

APPENDIX I

ENVIRONMENTAL AND LOADING FACTORS AFFECTING DYNAMIC SOIL PROPERTIES

I.1 Introduction

A comprehensive general stress – strain relation for shear modulus and damping for soils would be very complex, simply because of the numerous parameters affecting soil behavior. One approach towards developing a general constitutive relation is to study special cases. Once these are understood, it may then be possible to link them together to formulate a generalized constitutive relation. An attempt to describe how the controlling parameters, briefly described in Chapter 2, affect the stress – strain relation of soils subjected to cyclic shear deformation (for example the vibration of horizontal soil layers due to the horizontal component of an earthquake) is made herein.

According to Hardin & Drnevich, 1972, the relative importance of the parameters affecting the dynamic properties (namely shear modulus [G] and damping [ξ]) of clean sands and cohesive soils, can be summarized in the following Table:

PARAMETER	IMPORTANCE TO*			
	Modulus		Damping	
	Clean Sands	Cohesive Soils	Clean Sands	Cohesive Soils
Strain Amplitude	V	V	V	V
Effective Mean Principle Stress	V	V	V	V
Void Ratio	V	V	V	V
Number of Cycles	R**	R	V	V
Degree of Saturation	R	V	L	U
Overconsolidation Ratio	R	L	R	L
Effective Strength Envelope	L	L	L	L
Octahedral Shear Stress	L	L	L	L
Frequency of Loading (above 0.1 Hz)	R	R	R	L
Other Time Effects (Trixotropy)	R	L	R	L
Grain Characteristics, Size, Shape, Gradation, Minearology	R	R	R	R
Soil Structure	R	R	R	R
Volume Change due to Shear Strain (for strains less than 0.5%)	U	R	U	R

* V means *Very Important*, L means *Less Important*, and R means *Relatively Unimportant*, except as might affect another parameter; Umeans relative importance is not clearly known.

** Except for saturated clean sand where the number of cycles of loading is a *Less Important* parameter.

What can be readily seen is that the strain amplitude, effective mean principle stress, and void ratio are very important for the modulus and damping in all soils, whereas overconsolidation ratio is a less important parameter for cohesive soils, and is unimportant for clean sands. The Table also shows that a parameter such as grain distribution is relatively unimportant for both modulus and damping in all soils, except from the case where it affects other parameters listed. Grain characteristics will affect both the void ratio (a very important parameter) and the effective strength envelope (a less important parameter). But if the void ratio and effective strength envelope of the soil are accounted for, then the effects of grain distribution are automatically taken into account as well, making it relatively unimportant in this context.

In what follows, cohesionless and cohesive soils are analyzed separately, and the most important parameters affecting the dynamic behavior of these two major soil categories are examined.

I.2 Cohesionless Soils

The dynamic behavior of cohesionless soils is affected by various parameters, the most important of which are the cyclic strain amplitude, mean effective principle stress (i.e. confining pressure) and void ratio, which were analyzed in detail in Chapter 2. Among the remaining parameters, the most important are:

I.2.1 Effect of Prior Straining– Number of Loading Cycles, N

The effect of prior cyclic straining in sands is significant, both for the values of initial (small strain) shear modulus, G_{max}, as well as for the values of material damping, especially in the small strain regime. The influence of number of cycles on the dynamic characteristics of cohesionless soils becomes more apparent, when the strain amplitude of prior loading cycles exceeds the plastic threshold, i.e. $\gamma_c^{\ prior} \geq 10^{-2}$ %.

In particular, the values of initial shear modulus and damping after the soil specimen has been subjected to prior cyclic loading, plot significantly higher that the "virgin" soil curves. On the other hand, the effect of number of cycles in the shear modulus reduction factor G/G_{max} depends of the drainage conditions of the loading procedure. For draining conditions, the reduction factor tends to increase (due to possible densification of the material resulting from prior loading), and for undrained conditions, the reduction factor tends to decrease n value.

The effect of prior straining on the dynamic soil properties tends to disappear for cyclic strain amplitude equal to the one used in the prior straining. At this particular amplitude, the values of G/G_{max} and ξ are about the same in the prestrained and virgin specimen, as verified by experimental data (Drnevich & Richart, 1970).

I.2.2 Degree of Saturation, S [%]

Another important factor affecting the dynamic properties of cohesionless soils is the degree of saturation. However, whilst numerous experimental data are available for fully saturated cohesionless soils, very little or no information is available on partially saturated soils. Presumably, the shear modulus degradation and damping curves developed for dry materials, are also applicable to partially saturated granular soils, under the condition that the cyclic loading will not induce excess pore water pressures. For example, the values of G and ξ for a partially saturated cohesionless silt above the ground water table could be evaluated if the effect of capillarity were taken into account, leading to an increased value of the confining pressure.

For a fully saturated soil, a differentiation between drained and undrained cyclic loading must be established. If the cyclic loading is applied slow enough and in a complete drained condition, i.e. there is no pore pressure built up due to the cyclic loading, then statements made for dry cohesionless soils are also applicable for fully saturated material, with the confining pressure now being interpreted as the effective confining pressure ($\sigma' = \sigma - u$). The reason is that, given the drainage conditions of loading, the pore water can move freely in and out of the soil, not participating in the stress - strain response nor in the energy dissipation of the material. In that case, energy is still almost exclusively dissipated due to friction at the contacts and other intergranular interactions, resembling to the mechanisms of energy dissipation of dry materials.

However, the cyclic loading conditions of interest involve rapid succession of introduced shear strain cycles, leading to a characterization of the loading as undrained. In this particular case, water cannot move freely through the soil skeleton and as a result, it participates to the stress – strain behavior along with the solid skeleton.

In this case, if the shear strain amplitude is less than the elastic threshold (i.e. approximately $\gamma_c^e = 10^{-5}$), the material damping ratio is strongly affected by the frequency of the loading, due to viscous effects arising from the interaction between the solid and fluid phases of the material. On the other hand, in this range, neither the shear strain amplitude nor

the number of cycles, affect the dynamic soil properties. If the shear strain amplitude is larger than the elastic threshold, but still smaller than the volumetric threshold (i.e. approximately $\gamma_c^v = 10^{-4}$), the role of frequency on the value of material damping becomes less important, and the value of the shear modulus reduction factor is approximately equal to the one established for the dry material.

In essence, between the two thresholds, the level of strain amplitude is important but the number of cycles not. On the other hand, if the shear strain amplitude is larger than the volumetric threshold, then the effect of frequency on the dynamic properties of the material becomes negligible, and the value of shear modulus decreases with increasing strain amplitude and number of cycles.

This phenomenon of shear modulus degradation, which can reduce the value of G to a value close to zero, is due to the built up of excess pore pressures in the soil, an extreme example of which being the phenomenon of liquefaction of saturated cohesionless soils. The value of material damping ratio, whilst pore pressure built− up occurs with increasing number of cycles, remains constant or decreases (Dobry, et al. 1982, Stokoe, et al., 1995, Vucetic, et al., 1996).

In conclusion, the behavior of saturated cohesionless soils described above indicates that there is no substantial difference between the dynamic properties of a saturated soil and a dry soil under similar confining pressure. Therefore, the effect of excess pore pressure in decreasing G/G_{max} can be explained by the corresponding reduction in effective confining pressure. However, for high frequency cyclic loading such as applied in resonant column tests, and for small cyclic strains, the material damping is higher for the saturated sand, due to viscous effects related to the relative movements involving solid phase and pore water, which essentially become insignificant at greater cyclic strains. Therefore, the difference in damping between dry and saturated soil is generally more important when high− vibration phenomena are encountered, such as machine vibrations or explosions.

I.2.3 Effect of Cementation

The cementation of a cohesionless material, either natural or artificial, increases both the small− strain shear modulus G_{max}, as well as the small− strain material damping value, ξ_{min}. Strong cementation also decreases the significance of confining pressure. It may also radically change the shapes of the modulus reduction and damping curves, by decreasing the relative importance of friction at the interparticle contacts and the freedom of movement of the

grains. In particular, the stress– strain relationship of the material becomes more linear, a fact which becomes more apparent in the small– strain regime and might even disappear at cyclic strain amplitudes large enough to destroy the cementation. At those high strain amplitudes, the dynamic properties of the cemented material may approach the uncemented values, with the shear modulus degradation curve of the remolded material even plotting lower than the equivalent uncemented.

I.3 Cohesive Soils

Probably the most important parameter affecting the dynamic behavior of cohesive soils apart from the shear strain amplitude, is the plasticity index [PI]. Parameters as the overconsolidation ratio or confining pressure play minor role in this category of soils. In what follows, various parameters apart from the Plasticity Index, namely the number of straining cycles and the geological age of the material, are further analyzed, and experimental formulae existing in the literature for the estimation of material damping and shear modulus reduction factor as a function of these parameters are briefly discussed.

I.3.1 Effect of Plasticity Index [PI]

Numerous experimental data, available in the literature, reveal the importance of plasticity index in the characterization of the dynamic properties of cohesive soils. In the early years of geotechnical earthquake engineering, the modulus reduction behavior of coarse- and fine- grained soils were treated separately (e.g., Seed & Idriss, 1970). Recent research however, has revealed a gradual transition between the modulus reduction behavior of non-plastic coarse-grained (cohesionless) soil and plastic fine-grained (cohesive) soil.

Zen et al. (1978) and Kokushu et al. (1982) first noted the influence of soil plasticity on the shape of the modulus reduction curves; the shear modulus of highly plastic soils was observed to degrade more slowly with shear strain than did low-plasticity soils. Laboratory data show that the linear cyclic threshold shear strain is greater for highly plastic soils than for soils with low plasticity. Moreover, for non-plastic cohesive soils such as non-plastic silt, the shear modulus reduction curves plot together with the non-cohesive soil curves.

After reviewing experimental results from a broad range of materials, Dobry & Vucetic (1987) and Sun et al. (1988) concluded that the shape of the modulus reduction curve is influenced more by the Plasticity Index than by the void ratio and/or the confining pressure.

Five major aspects of fine-grained soil undrained cyclic behavior being influenced by Plasticity Index can be identified. In particular, as the value of PI *increases*:

i. The low strain shear modulus G_{max} increases faster with overconsolidation ratio [OCR].

ii. The low strain shear modulus G_{max} increases faster with geological age [t_g] (see Section I.3.3).

iii. The material exhibits more elastic behavior (i.e. the shear modulus reduction curve G/G_{max} versus cyclic strain, γ_c rises).

iv. The material damping ratio [ξ] versus cyclic strain [γ_c] curve plots lower.

v. The shear modulus G degrades less after N applied cycles of amplitude γ_c.

Whilst effects (i) and (ii) relate to G_{max}, and therefore to very low strains (i.e. $\gamma_c \approx 10^{-6}$), the effects (iii)-(v) are related to the behavior at larger strains, above $\gamma_c \approx 10^{-4}$. These effects lead to the same conclusion: the soil is more linear and its stiffness degrades less at a given strain amplitude with increasing PI, i.e. the level of cyclic strain needed to induce significant nonlinear stress - strain response and stiffness degradation increases with PI.

In what follows, an attempt is being made to speculate on the possible reasons for this influence of PI from a soil - structure point of view, especially considering that index properties are determined on fully disturbed or remolded soil specimens, and yet correlate well with the cyclic response of the soil in its natural, undisturbed state. The influence of PI indicates that highly plastic soils tend to develop a microstructure that behave linearly to higher shear strains than soils with lower plasticity.

Soils of high and very high plasticity are composed of very small particles that have a relatively high surface area per unit weight of the particle [SSA]. In such soils, the number of particle contacts is also large. Consequently, the electrochemical and repulsive forces between particles are large compared to the weight of the particles themselves, and as a result, bonds and repulsion forces dominate the behavior of the soil skeleton under externally applied loads (Mitchell, 1993). At the other extreme, in soils with low plasticity or zero plasticity, such as sands and gravels, consisting of larger particles and less interparticle contacts, the gravitational forces and associated friction between grains exert a dominant role on the response to external loads. Therefore, it can be hypothesized that the microstructural bonds and repulsion forces in higher plasticity soils act like a system of relatively flexible linear springs, with the ability to take relatively large shear strains (as much as 10^{-3}) before they are *broken*, i.e. before

the particles are permanently displaced and nonlinear and stiffness degradation effects become apparent.

On the other hand, in low - plasticity soils, the elasticity of particles is practically the only source of linear behavior, resulting in significant nonlinear and stiffness degradation response starting at strains as low as 10^{-4}, at which particle sliding and permanent deformation (reorientation) occurs.

The combined effects of effective confining pressure and Plasticity Index on modulus reduction and damping behavior, were combined by Ishibashi and Zhang (1993), in the following form:

$$\frac{G}{G_{max}} = K(\gamma,PI)\cdot\left(\sigma_m'\right)^{m(\gamma,PI)-m_0}$$

$$\xi = 0.333\,\frac{1+\exp\left(-0.0145\cdot PI^{1.3}\right)}{2}\left[0.586\cdot\left(\frac{G}{G_{max}}\right)^2 - 1.547\left(\frac{G}{G_{max}}\right)+1\right]$$

where:

$$K(\gamma,PI) = 0.5\left\{1+\tanh\left[\ln\left(\frac{0.000102+n(PI)}{\gamma}\right)^{0.492}\right]\right\}$$

$$m(\gamma,PI)-m_0 = 0.272\left\{1-\tanh\left[\ln\left(\frac{0.000556}{\gamma}\right)^{0.4}\right]\right\}\cdot\exp\left(-0.0145\cdot PI^{1.3}\right)$$

$$n(PI) = \begin{cases} 0.0 & \text{for } PI=0 \\ 3.37\times10^{-6}\,PI^{1.404} & \text{for } 0<PI\le15 \\ 7.0\times10^{-7}\,PI^{1.976} & \text{for } 15<PI\le70 \\ 2.7\times10^{-5}\,PI^{1.115} & \text{for } PI>70 \end{cases}$$

The effect of Plasticity Index on the dynamic soil properties renders it one of the most significant properties for site-response evaluations, seismic microzonation, and other applications. This is also a very convenient conclusion from a practical point of view, as Plasticity Index is a common soil index property, determined practically in every project. The Atterberg limits needed to obtain the PI are among the simplest, most inexpensive and well-established geotechnical tests (e.g., Lambe & Whitman, 1969).

I.3.2 Number of Loading Cycles, N

Similarly to the behavior of cohesionless soils, the stiffness of a saturated cohesive soil decreases with number of cycles when subjected to undrained cyclic loading. The degradation of shear modulus G is accompanied by interparticle bond breakage and pore pressure built-up, with the rate of modulus degradation with number of cycles, for a given strain amplitude, decreasing with increasing Plasticity Index. Even for low plasticity cohesive soils, this rate is much smaller than for saturated sands, and for a small number of cycles, results from a single loading - unloading - reloading path can be used without modification.

For large amount of straining cycles ($N > 10^2 - 10^3$), the shear modulus after N cycles, G_N can be related to its value in the first cycle G_1 as follows:

$$G_N = \delta \cdot G_1 ,$$

where the degradation index, δ, is obtained as $\delta = N^{-t}$ and t is the degradation parameter (Idriss et al., 1978). The degradation parameter has been shown to decrease with increasing Plasticity Index and increasing OCR, and to increase with increasing cyclic strain amplitude (Idriss et al., 1978, Vucetic & Dobry, 1989, Tan & Vucetic, 1989).

I.3.3 Effect of Geologic Age, t_g

Another factor affecting the dynamic soil properties of cohesive soils is the time of loading. In particular, the small− strain shear modulus G_{max} increases with time of loading and material damping ratio ξ decreases. This is part of the explanation of why older geologic deposits tend to be stiffer (higher G_{max} and V_s values), and the effect must be considered when predicting G_{max} and V_s values from laboratory measurements. This effect is also present in the secant shear modulus G at larger cyclic strains.

Experimental data on the influence of time of loading on the shear modulus degradation curve is not conclusive, and two different procedures have been proposed to estimate the secant shear modulus of the field (G_{field}) from the corresponding measured in the lab using a short loading time (G_{lab}). Some laboratory data suggests that time of loading affects G_{max} but not the G/G_{max} versus γ_c curve, and Kokusho et al. (1982) have proposed to correct G measured in the lab, as follows:

$$G_{field} = (G_{max})_{field} \times (G / G_{max})_{lab}$$

where $(G_{max})_{field}$ is the corrected value of the small shear strain shear modulus.

For the material damping ratio, the following approach has been proposed by Kokusho et al. (1982):

$$(G \times \xi)_{lab} = (G \times \xi)_{field}$$

Anderson and Woods (1976) and Richard et al. (1977) have proposed a different approach for estimating G_{field}. Specifically, experimental data of shear modulus versus duration of confinement in a semi-log plot for different strain levels were plotting approximately parallel, therefore the value of shear modulus in the field could be approximated as $G_{field} \approx G_{lab} + A_r$, where $A_r = (G_{max})_{field} - (G_{max})_{lab}$. Therefore:

$$G_{field} = G_{lab} + [(G_{max})_{field} - (G_{max})_{lab}]$$

The two proposed methods for correcting laboratory results are schematically illustrated in Figure I.1.

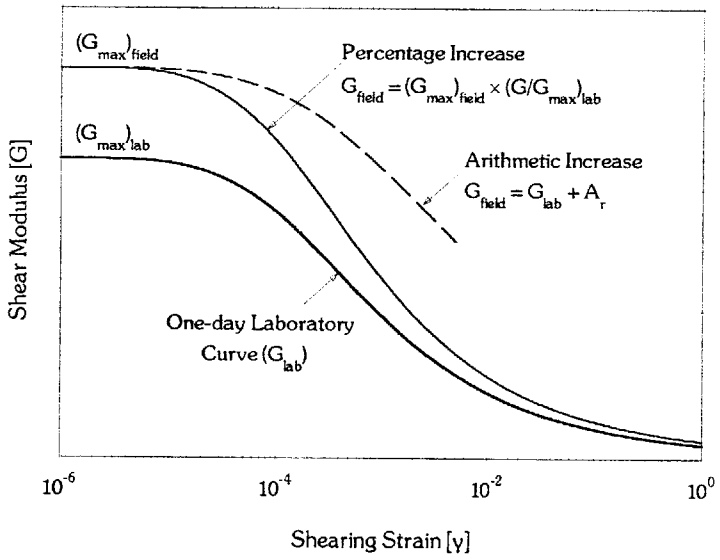

Figure I.1 Shear Modulus Reduction curve in the field, predicted assuming arithmetic and percentage increase in moduli.

I.3.4 Quick Clays

Shear modulus reduction and material damping curves, commonly used for cohesive soils are not applicable to soils with a very sensitive structure. An important example, are the quick clays which cover large extensions of Eastern Canada and the Scandinavian Peninsula in Europe. Quick clays are the result of a particular geological history and are very sensitive, behaving essentially as liquid if their structure is destroyed by remolding (Mitchell, 1993). Comparison of the degradation curves of quick clays with Plasticity Index of PI = 20, show

correspondence to a regular clay with PI = 50, while the values of material damping correspond to a regular clay with PI ≈ 200. This results from the unusual structure of this particular soil type, which can exhibit more linear behavior, including a much lower material damping, than would have been predicted from its Plasticity Index.

I.4 Other Soils

In the preceding sections, parameters affecting the shear modulus and material damping values for applications over a broad range of cohesive and cohesionless soils have been analyzed. However, some characteristics of the materials described above may not be applicable to so called *special* soils and other geotechnical materials of interest having a very different composition or structure as compared with the *normal* soils.

Laboratory measurements and analysis of earthquake records have provided valuable information on the shapes of modulus and damping curves for some of these *special* geotechnical materials of interest.

In some cases, like that of frozen soils, the cyclic stress - strain behavior is quite complicated and is strongly affected by parameters such as temperature and frequency. Experimental evidence for one marine calcareous soil near Western Australia indicates that the shear modulus degradation curves, G/G_{max}, characteristic for sands are applicable for this particular material as well, whilst the wide variety of calcareous soils, both onshore as well as offshore suggests that no generalization is possible.

Among other geotechnical materials of interest, soft rock and residual soils, peat and solid waste could be distinguished due to their irregular soil behavior. Comparison of experimental data obtained in two different projects in New York City and Washington State indicate that peats can exhibit both a very linear stress - strain response, accompanied by very low values of material damping, and significant non-linearity, associated with substantial amount of energy dissipation.

I.5 References

Anderson, D.G. & Woods, R.D. (1976)." Comparison of field and laboratory shear modulus" , *Proc. ASCE Conference on In-situ Measurement of Soil Properties*, Vol. 1, pp. 62-92.

Chen, A. T. F., Stokoe, K. H., II (1979). "Interpretation of Strain Dependent Modulus and Damping from Torsional Soil Tests", Report No. USGS - GD - 79 - 002, NTIS N0. PB - 298479, U.S. Geological Survey, 46 P.

Daniel, A. W. T., Harvey, R. C. and Burley, E. (1975). "Stress – Strain Characteristics of Sand", Technical Note, *Journal of the Geotechnical Division*, ASCE, Vol. 101, No. GT5, May, pp. 508-512

Das, B. M. (1993). "Principles of Soil Dynamics", PWS-KENT Publishing Company, Boston, MA

Dobry, R., Ladd, R.S., Yokel, F.Y., Chung, R.M. & Powell, D. (1982). "Prediction of pore water pressure buildup and liquefaction of sands during earthquakes using the cyclic strain method", *NBS Building Science Series 138*, National Bureau of Standards, Gaithersburg, Maryland

Dobry, R. & Vucetic, M. (1987). " Dynamic Properties and Seismic Response of soft clay deposits" , *Proc. International Symposium on Geotechnical Engineering of Soft Soils*, Mexico City, Vol. 2, pp. 51-87

Drnevich, V.P. & Richard, F.E. Jr. (1970)." Dynamic Prestraining of Dry Sand" , *Journal of the Soil Mechanics and Foundations Division*, ASCE, Vol. 98, No. SM8, pp. 807-825.

Finn, W. D. L., Lee, K. W. & Martin, G. R. (1975)." Stress-Strain Relations for Sand in Simple Shear" , *ASCE National Convention*, Denver, Colorado, November, Meeting Reprint 2517

Hall, J. R. Jr. & Richard, F. E. Jr. (1963)." Dissipation of Elastic Wave Energy in Granular Soils" ,*Journal of the Soil Mechanics and Foundation Division*, ASCE, Vol. 98, No. SM6, November, pp. 27-56

Hardin, B. O. (1965). "The nature of damping in sands", *Journal of Soil Mechanics and Foundation Engineering Division*, ASCE, Vol. 91, No. SM1, February, pp. 33-65.

Hardin, B. O. & Drnevich, V. P. (1970)." Shear modulus and damping in soils: I. Measurement and parameter effects, II. Design equations and curves" , *Technical Reports UKY 27-70-CE 2 and 3*, College of Engineering, University of Kentucky, Lexington, Kentucky.

Hardin, B. O. & Drnevich, V. P. (1972a)." Shear modulus and damping in soils: Measurement and parameter effects" , *Journal of Soil Mechanics and Foundation Engineering Division*, ASCE, Vol. 98, No. SM6, June, pp. 603-624.

Hardin, B. O. & Drnevich, V. P. (1972b)." Shear modulus and damping in soils: Design equations and curves" , *Journal of Soil Mechanics and Foundation Engineering Division*, ASCE, Vol. 98, No. SM7, pp. 667-692.

Ishibashi, I. & Zhang, X. (1993)." Unified Dynamic Shear Moduli and Damping Ratios of Sand and Clay" , *Soils and Foundations*, Vol. 33, No. 1, pp. 182-191.

Ishihara, K. (1996). "Soil Behavior in Earthquake Geotechnics", *Oxford Science Publications*, Oxford Science Press, Walton Street, Oxford OX2 6DP.

Iwasaki, T., Tatsuoka, F. & Takagi, Y. (1978). "Shear Moduli of Sands under Cyclic Torsional Shear Loading", *Soils and Foundations*, Vol. 18, No. 1, pp. 39-56.

Kramer, K. L. (1996)." Geotechnical Earthquake Engineering" , Prentice Hall Inc.

Kokushu, T., Yoshida, Y. & Esashi, Y. (1982)." Dynamic Properties of Soft Clay for wide strain range" , *Soils and Foundations*, Vol. 22, No.2, pp. 45-60.

Krizek, R. J. & Franklin, A. G. (1968)." Energy Dissipation in a Soft Clay" , *Proc. International Symposium on Wave Propagation and Dynamic Properties of Earth Materials*, University of New Mexico, pp. 797-807.

Laird, J. P. & Stokoe, K. H. (1993). " Dynamic properties of remolded and undisturbed soil samples tested at high confining pressures" , *Geotechnical Engineering Report GR93-6*, Electrical Power Research Institute.

Lambe, T.W. & Whitman, R.V. (1969). Soil Mechanics, Wiley, New York.

Mitchell, J.K. (1993)." Fundamentals of Soil Behavior" , John Wiley & Sons, Inc.

Ray, R. P. & Woods, R. D. (1988)," Modulus and Damping due to uniform and variable cyclic loading" , *Journal of Geotechnical Engineering*, ASCE, **114** (8), pp. 861-876.

Seed, H. B. & Idriss, I. M. (1970), " Soil moduli and damping factors for dynamic response analyses" , *Report EERC 70-10*, Earthquake Research Center, University of California, Berkeley.

Seed, H. B., Wong R. T., Idriss, I. M. & Tokimatsu T. (1984)," Moduli and damping factors for dynamic analyses of cohesionless soils" , *Report EERC 84-14*, Earthquake Engineering Research Center, University of California, Berkeley.

Seed, H. B., Wong R. T., Idriss, I. M. & Tokimatsu T. (1986)," Moduli and damping factors for dynamic analyses of cohesionless soils" , *Journal of Soil Mechanics and Foundation Division*, ASCE, Vol. 112, No. SM11, pp. 1016-1032.

Shibata, T. & Soelarno, D. S. (1975), " Stress strain characteristics of sands under cyclic loading" , *Proc.. Japanese Society of Civil Engineering*, **239**, pp. 57-65.

Shibuya, S., Mitachi, T. & Muira, S. (1994). "Pre-failure Deformation of Geomaterials", *Proc. International Symposium on Pre-Failure Deformation Characteistics of Geomaterials*, Sapporo, Japan, September.

Stokoe, K. H., Hwang, S. K., Lee, J. N. & Andrus, R. D. (1994)." Effects of various parameters on the stiffness and damping of soils at small to medium strains" , *Proc. Int. Symposium on Prefailure Deformation Characteristics of Geomaterials*, Japan.

Sun, J.I., Golesorkhi, R. & Seed, H.B. (1988). " Dynamic Moduli and Damping Ratios for Cohesive Soils" , *Report No. EERC-88/15*, Earthquake Engineering Research Center, University of California, Berkeley.

Tan, K. & Vucetic, M. (1989)." Behavior of medium and low plasticity clays under cyclic simple shear conditions" , *Proc. 4th International Conference on Soil Dynamics and Earthquake Engineering*, A.S. Cakmak & I. Hererra, eds., Mexico City, pp. 131-142.

Tatsuoka, F., Iwasaki, T., Fukushima, S. & Sudo, H. (1979). '' Stress Conditions and Stress Histories affecting Shear Modulus and Damping of Sand under Cyclic Loading'' , *Soils and Foundations*, Vol. 19, No. 2, pp. 29-43.

Vucetic, M. & Dobry, R. (1989)." Degradation of marine clays under cyclic loading" , *Journal of Geotechnical Engineering*, ASCE, Vol. 114, No.2, pp. 133-149.

Vucetic, M. & Dobry, R. (1989). " Effect of soil plasticity on cyclic response" , *Journal of Geotechnical Engineering*, ASCE, Vol. 117, No.1, pp. 89-107.

Whitman, R. V., Dobry, R. & Vucetic, M. (1997). *Soil Dynamics* (book manuscript in preparation).

Zen, K., Umehara, Y. & Hamada, K. (1978). " Laboratory tests and in-situ seismic survey on vibratory shear modulus of clayey soils with different plasticities" , *Proc. 5th Japan Earthquake Engineering Symposium*, Tokyo, pp. 721-728.

APPENDIX II

RCTS TEST EQUIPMENT AND MEASUREMENT TECHNIQUES

II.1 Introduction

Resonant column and torsional shear (RCTS) equipment has been employed in the laboratory program described in Section 2.4 of the present study, for measurement of the deformation characteristics (shear modulus and material damping) of intact soil specimens. This equipment has been developed at the University of Texas at Austin over the past two decades (Isenhower, 1979, Lodde, 1982, Ni, 1987, and Kim, 1991). The equipment is of the fixed - free type, with the bottom of the specimen fixed and torsional excitation applied at the top. Both resonant column (RC) and torsional shear (TS) tests were performed in a sequential series on the same specimen over a range of shearing strains from about 10^{-4} % to slightly more than 10^{-1} % by changing the frequency of the forcing function. The primary difference between the two types of tests is the excitation frequency. In the RC test, frequencies above 20 Hz are required and inertia of the specimen and drive system are needed to analyze these measurements. On the other hand, slow cyclic loading with frequencies generally below 5 Hz is prescribed in the TS tests and inertia does not enter the data analysis.

II.2 Resonant Column and Torsional Shear Equipment

The RCTS apparatus can be idealized as a fixed - free system, as shown in Fig. II.1. The bottom end of the specimen is fixed against rotation at the base pedestal, and top end of the specimen is connected to the driving system. The driving system, which consists of a top cap and drive plate, can rotate freely to excite the specimen in cyclic torsion.

The basic operational principle of a fixed - free resonant column (RC) test is to vibrate the cylindrical specimen in first - mode torsional motion. Harmonic torsional excitation is applied to the top of the specimen over a range of frequencies, and the variation of the acceleration amplitude of the specimen with frequency is obtained. Once first - mode resonance is established, measurements of the resonant frequency and amplitude of vibration are made. These measurements are then combined with equipment characteristics and specimen size to calculate shear wave velocity and shear modulus based on elastic wave propagation. Material damping is determined either from the width of the frequency response curve or from the free - vibration decay curve.

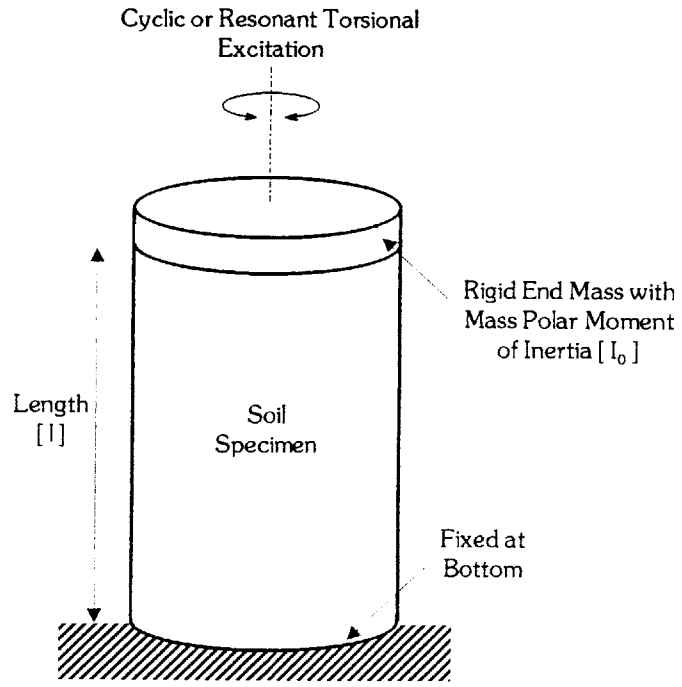

Figure II.1 Idealized Fixed - Free RCTS Equipment

The torsional shear (TS) test is another method of determining shear modulus and material damping, using the same RCTS equipment but operating it in a different manner. A cyclic torsional force at a given frequency, generally below 10 Hz, is applied at the top of the specimen. Instead of determining the resonant frequency, the stress - strain hysteresis loop is determined from measuring the torque - twist response of the specimen. Shear modulus is calculated from the slope of a line through the end points of the hysteresis loop, and material damping is obtained from the area of the hysteresis loop.

The RCTS apparatus consists of four basic subsystems, which are:

i. a confinement system, by which the specimen is isotropically confined using compressed air,
ii. a drive system,
iii. a height - change measurement system, and
iv. a motion monitoring system which, in the RC test, is designed to measure the resonant frequency, shearing strain and free - vibration decay curve, and in the TS test, to monitor the torque - twist hysteresis loops of the specimen.

II.3 Method of Analysis in the Resonant Column Test

The resonant column test is based on the one - dimensional wave equation derived from the theory of elasticity. The shear modulus is obtained by measuring the first - mode resonant frequency while material damping is evaluated from either the free - vibration decay curve or from the width of the frequency response curve assuming viscous damping.

Shear Modulus

The governing equation of motion for the fixed - free torsional resonant column test is:

$$\frac{\sum I}{I_0} = \frac{\omega_n \, l}{V_s} \cdot \tan\left(\frac{\omega_n \, l}{V_s}\right) \qquad \{1\}$$

where: $\sum I = I_s + I_m + \ldots$

I_s mass moment of inertia of soil specimen,

I_m mass moment of inertia of membrane,

I_0 mass moment of inertia of rigid end mass at the top of the specimen,

l length of the specimen,

V_s shear wave velocity of the specimen, and

ω_n undamped natural circular frequency of the system.

Once the first - mode resonant frequency is determined, the shear wave velocity can be calculated from eq. {1}, assuming that the resonant circular frequency and ω_n coincide.

As noted above, the resonant circular frequency, ω_r is measured instead of the undamped natural frequency, and ω_r is used to calculate shear wave velocity. If the damping in the system is zero, then ω_r and ω_n are the same. In particular:

$$\omega_r = \omega_n \sqrt{1 - 2\,\xi^2} \qquad \{2\}$$

A typical damping ratio encountered in the resonant column test is less that 20 percent, which corresponds to a difference of less that 5 percent between ω_r and ω_n .

Once the shear wave velocity is determined, shear modulus is calculated from the relationship:

$$G = \rho \cdot V_s^2 \qquad \{3\}$$

where ρ is the total mass density of the soil.

Shearing Strain

The shearing strain varies radically within the specimen and may be expressed as a function of the distance from the longitudinal axis. The equivalent shearing strain, γ_{eq} or γ, is represented by:

$$\gamma = \frac{r_{eq} \cdot \delta_{max}}{l} \qquad \{4\}$$

where: r_{eq} equivalent radius,

δ_{max} angle of twist at the top of the specimen, and

l length of the specimen.

Material Damping

In the resonant column test, the material damping ratio can be evaluated from either the free - vibration decay method or from the half - power bandwidth method. Each of these methods is briefly discussed below.

- Free - Vibration Decay Method

Material damping in soils can be quite complex to describe. However, the theory for a single - degree - of - freedom system with viscous damping is a useful framework for describing the effect of damping, which occurs in soil (Richard et al., 1970). The decay of free vibrations of a single - degree - of - freedom system with viscous damping is described by the logarithmic decrement, δ, which is the ratio of the natural logarithm of two successive amplitudes of motion as:

$$\delta = \ln\left(\frac{Z_1}{Z_2}\right) = \frac{2\pi\xi}{\sqrt{1-\xi^2}} \qquad \{5\}$$

where: Z_1, Z_2 two successive strain amplitudes of motion, and

ξ material damping ratio.

Once the free - vibration decay curve is recorded, Material damping ratio is calculated from logarithmic decrement according to:

$$\xi = \sqrt{\frac{\delta^2}{4\pi^2 + \delta^2}} \qquad \{6\}$$

In this method, it is not certain which strain amplitude is a representative strain for damping ratio calculated by eq. {6} because strain amplitude decreases during the free - vibration

decay. In the laboratory test program described in Chapter 2, a representative strain amplitude was used as the peak strain amplitude during steady - state vibration for shearing strains below 0.001%. However, at larger strains, the representative strain is smaller than the peak strain, and the average strain determined for the first three cycles of free vibration was used.

- Half - Power Bandwidth Method

Another method of measuring damping in the resonant column test is the half - power bandwidth method, which is based on the measurement of the width of the frequency response curve near resonance. From the frequency response curve, the logarithmic decrement can be calculated from:

$$\delta = \frac{\pi}{2} \frac{f_2^2 - f_1^2}{f_r^2} \sqrt{\frac{A^2}{A_{max}^2 - A^2}} \frac{\sqrt{1-2\xi^2}}{1-\xi^2} \qquad \{7\}$$

where: f_1 frequency below the resonance where the strain amplitude is A,

f_2 frequency above the resonance where the strain amplitude is A,

f_r resonant frequency, and

ξ material damping ratio.

If the damping ratio is small and A is chosen as 0.707 A_{max}, which is called the half - power point, eq. {7} can be simplified as:

$$\delta \cong \pi \cdot \frac{f_2 - f_1}{f_r} \qquad \{8\}$$

Therefore, the damping ratio can be expressed as:

$$\xi \cong \frac{f_2 - f_1}{2 f_r} \qquad \{9\}$$

Backround noise can lead to problems when measuring material damping using the free - vibration decay method at strains less than about 0.001%. On the other hand, backround noise generally has a smaller effect on the frequency response curve at strains below 0.001%. Therefore, the half - power bandwidth method is preferred to the free - vibration decay method for making small - strain damping measurements. However, at larger

strains, symmetry in the frequency response curve is no longer maintained, and serious errors can arise by using the half - power bandwidth method.

II.4 Method of Analysis in the Torsional Shear Test

The torsional shear test is another method f determining the deformational characteristics (modulus and damping) of soil using the same RCTS device. Rather than measuring the dynamic response of the specimen, the actual stress - strain hysteresis loop is determined by means of measuring the torque - twist curve. Shear modulus is calculated using the area of the hysteresis loop.

Shear Modulus

Because the shear modulus is calculated from the characteristics of the stress - strain hysteresis loop, shearing stress and shearing strain in the torsional shear test need to be defined. Once the stress - strain hysteresis loop is measured, the shear modulus, G, is calculated from the slope of a line through the end points of the hysteresis loop, as follows:

$$G = \tau / \gamma \qquad \{10\}$$

where: τ the peak shearing stress, and

γ the peak shearing strain.

Hysteretic Damping Ratio

Hysteretic damping ratio in the torsional shear test is measured using the amount of energy dissipated in one complete cycle of loading and the peak energy stored in the specimen during the cycle.

In the torsional shear test, the dissipated energy is measured from the area of the stress - strain hysteresis loop. The energy per cycle, E_d, due to a viscous damping force, F_d, is:

$$E_d = \int_0^T F_d \, \dot{x} \, dt \qquad \{11\}$$

where: $\dot{x}$ the velocity, and

T the period of motion.

For a simple harmonic motion with frequency ω, i.e. $x = A \cos(\omega t - \varphi)$, the energy dissipated per cycle of motion becomes:

$$E_d = \pi \, c \, \omega \, A^2 \qquad \{12\}$$

From eq. {12}, the viscous damping coefficient can be expressed as:

$$c = \frac{W_d}{\pi \omega A^2} \qquad \{13\}$$

The peak strain energy, W_s, stored by the spring is equal to the area under the secant modulus line and can be written as:

$$W_s = k A^2 / 2 \qquad \{14\}$$

The critical damping coefficient, C_c, is:

$$C_c = 2 \cdot \sqrt{k m} = 2 k / \omega_n \qquad \{15\}$$

where k is an elastic spring constant, m is a mass, and ω_n is a natural frequency of the system. Using eq. {14}, eq. {15} can be rewritten as:

$$C_c = \frac{4 W_s}{\omega_n A^2} \qquad \{16\}$$

and the damping ratio can be expressed as:

$$\xi = \frac{C}{C_c} = \frac{W_d}{4 \pi W_s} \frac{\omega_n}{\omega} \qquad \{17\}$$

For soils however, material damping is often assumed to be frequency indepednent. Therefore, the term ω_n / ω can be ignored, and hysteretic damping is written as:

$$\xi = \frac{1}{4 \pi} \frac{W_d}{W_s} \qquad \{18\}$$

where: W_d the area of the hysteresis loop, and

W_s the area under the secant modulus.

II.5 References

Chen, A. T. F., Stokoe, K. H., II (1979). "Interpretation of Strain Dependent Modulus and Damping from Torsional Soil Tests", Report No. USGS - GD - 79 - 002, NTIS N0. PB - 298479, U.S. Geological Survey, 46 P.

Isenhower, W. M. (1979). "Torsional Simple Shear/Resonant Column Properties of San Francisco Bay Mud", *M.S. Thesis*, GT 80-1, University of Texas at Austin, December, pp. 307.

Kim, D.S. (1991). "Deformational Characteristics of Soils at Small to Intermediate Strains from Cyclic Tests", *Ph.D. Dissertation*, Geotechnical Engineering, Department of Civil Engineering, University of Texas at Austin, August.

Ni, S. H. (1987). "Dynamic Properties of Sand under True Triaxial Stress States from Resonant Column/Torsional Shear Tests", *Ph.D. Dissertation*, Geotechnical Engineering, Department of Civil Engineering, University of Texas at Austin, August.

Richard, F. E., Jr., Hall, J. R., Jr. and Woods, R. D. (1970). "Vibrations of Soils and Foundations", *Prentice Hall Inc.*, Englewood Cliffs, New Jersey, 414 p.

APPENDIX III

FORTRAN COMPUTER CODES

III.1 Frequency Dependent Damping and Shear Modulus

Compares the true energy dissipated by a non-linear Masing soil (elastoplastic springs in parallel) with the energy dissipated by frequency - dependent linearly - hysteretic soil (represented by the MIT-S1 model). The excitation is a shearing strain time history, obtained by integration of an actual accelerogram (real earthquake).

Note. -The particle velocity is proportional to strain.

```
parameter (pi=3.14159265, two_over_pi=2./pi)
parameter (twopi=6.2831853)

parameter (x0=1.E-6)          !   Small strain limit
parameter (xmax=1)            !   Maximum strain for G/G0 curve
parameter (nn=1024)           !   Number of time intervals
parameter (nkmax=300)         !   Max. Number of elastoplastic springs
parameter (nf=nn/2)

character*80 eqfile
real st(0:nkmax)              !   Stiffness of springs
real xy(0:nkmax)              !   Yield deformation of springs
real fy(0:nkmax)              !   Yield force in each spring
real damp(0:nkmax)            !   Fraction of hysteretic damping
real energy(0:nn)             !   Dissipated energy
real stress(0:nn)             !   Stress time history
real strain(0:nn)             !   Strain time history
real v(0:nn)                  !   Rate of strain (initially = quake)
real gamma(0:nf)              !   Strain Fourier amplitude spectrum
real g(0:nf)                  !   Frequency Dependent Shear modulus
real d(0:nf)                  !   Frequency Dependent Damping
real tau(0:nn)                !   Hysteretic stresses
complex ctau(0:nf)            !   Fourier transform of hysteretic stresses
equivalence (tau(0), ctau(0))
integer plastic               !   Keeps track of springs in yield
integer unload                !   Indicator for unloading/reloading
```

```
**************************************************************************

!GAUSSIAN QUADRATURE COEFFICIENTS
dimension xi(5), wt(5)
data xi/-0.9061798459, -0.5384693101, 0.,
*         0.5384693101,  0.9061798459/          !       Gaussian points
data wt/ 0.2369268850, 0.4786286704, 0.5688888888,
*         0.4786286704, 0.2369268850/           !       Gaussian weights

**************************************************************************

call GET_PARAMETERS (eqfile, strmax, dt)
tt = nn*dt
df = 1./tt
dom = twopi*df
call MIT-S1 (x0)

open (1,file='damping')         !       Fraction of damping
open (2,file='modulus')         !       Secant & tangent shear modulus

fac = 10.**(0.05)               !       Factor for strain intervals
fac1 = fac - 1.
x1 = x0                         !       Small strain limit
g1 = 1.                         !       Small strain G/G0
nk = 0
st(0) = g1
xy(0) = x1
fy(0) = g1*x1
damp(0) = 0.                    !       Small strain damping
sum = x0**2                     !       sum = integral (2*x*G/G0*dx)
write (1,'(2e15.5)') x1, damp(0)
write (2,'(3e15.5)') x1, g1, g1
do while (x1.le.xmax .and. nk.lt.nkmax)
      nk = nk + 1
      x2 = fac*x1
      a = 0.5*(x2 + x1)         !       Center of integration interval
      b = 0.5*(x2 - x1)         !       Half-width integration interval
      s = 0.
      do j=1,5                  !       Gaussian integration
            x = a + xi(j)*b
            s = s + wt(j)*x/fun(x)
      end do
      sum = sum + 2.*b*s
      damp(nk) = (sum*fun(x2)/x2**2 - 1.)*two_over_pi
      g2 = 1./fun(x2)           !       Secant stiffness
      st(nk) = (fac*g2 - g1)/fac1   !       Tangent stiffness
```

```
      xy(nk) = x2                    !     Yield deformation
      write (1,'(2e15.5)') x2, damp(nk)
      write (2,'(3e15.5)') x2, (fac*g2 - g1)/fac1, g2
      x1 = x2
      g1 = g2
end do
do j=0,nk-1
      ts = st(j)                     !     Tangent stiffness
      st(j) = st(j) - st(j+1)        !     Spring stiffness
      fy(j) = st(j)*xy(j)            !     Yield force
end do
fy(nk) = st(nk)*xy(nk)
close (1)
close (2)

open (1,file='loop')
open (2,file='energy')
open (3,file='stress')
open (4,file='strain')
call INMOT (v, nt, nn, eqfile)
call INTEG (strain, v, nt, nn, strmax, dt)
call MODULI (xy, damp, gamma, tau, ctau, g, d, nk, nn, nf, df)

do i=0,nn
      energy(i) = 0.
      stress(i)  = 0.
end do
do k=0,nk
      n1 = 0
      u1 = 0.
      f1 = 0.
      plastic = 0
      uy = xy(k)
      do while (n1 .lt. nn)
            if (plastic .ne. 0) then
            call SPRING_IS_PLASTIC (strain, v, stress, energy, u1, n1,
     *           f1, fy(k), unload, plastic, nn)
            else
            call SPRING_IS_ELASTIC (strain, stress, u1, n1, f1,
     *           fy(k), uy, st(k), unload, plastic, nn)
            end if
      end do
end do
work = 0.
edis = 0.
do i=0,nn-1
```

```
      t = i*dt
      work = work + energy(i)
      write (1,'(2e15.5)') strain(i), stress(i)
      write (2,'(3e15.5)') t, work, edis
      write (3,'(3e15.5)') t, stress(i)
      write (4,'(2e15.5)') t, strain(i)
      edis = edis + tau(i)*(strain(i+1) - strain(i))
end do
close (1)
close (2)
close (3)
close (4)
end
```

****

SUBROUTINE MODULI (xy, damp, gamma, tau, ctau, g, d, nk, nn, nf, df)

Determines shear moduli and damping values as function of frequency as well as the hysteretic stress time history (tau)

```
parameter (twopi=6.28318)
real xy(0:nk), damp(0:nk)
real gamma(0:nf), tau(0:nn), g(0:nf), d(0:nf)
complex ctau(0:nf)

open (11,file='frd_damp')
open (12,file='frd_shmd')
do i=0,nf
      d(i) = damping (gamma(i), xy, damp, nk)
      g(i) = 1./fun(gamma(i))
      ctau(i) = df*g(i)*ctau(i)*cmplx(0.,2.*d(i))
      write (11,'(2e15.5)') i*df, d(i)
      write (12,'(2e15.5)') i*df, g(i)
end do
close (11)
close (12)
ctau(0) = 0.
call FFT[1] (tau, nn, 1, 1, -1)
```

---

[1] Note.-Subroutine FFT is a multi - dimensional Fast Fourier Transform routine. Computes the following:

$$F(J_1, J_2, \ldots) = \sum_{K_1=1}^{N_1} \sum_{K_2=1}^{N_2} \ldots G(K_1, K_2, \ldots)\ EXP_1 \cdot EXP_2 \cdot \ldots$$

where: $1 .LE. J_1 .LE. N_1$ (for each of the NDIM dimensions)

$EXP_1 = EXP\ (TWOPI\_I \cdot (K_1-1) \cdot (J_1-1)/N_1)$

in which: TWOPI_I = 6.28318*ISIGN*SQRT(-1)

```
return
end

*********************************************************************

SUBROUTINE SPECTRUM (strain, gamma, tau, nn, nf, strmax, rms, dt, df)
```

Computes the Fourier Amplitude Spectrum of Strains

```
real strain(0:nn), gamma(0:nf), tau(0:nn)

do i=0,nn
      tau(i) = strain(i)*dt
end do
tau(nn+1) = 0.
call fft (tau, nn, 1, -1, 0)
rms = 0.
peak = 0.
do i=0,nf
      j = 2*i
      sr = tau(j)          !  real part
      si = tau(j+1)        !  imaginary part
      a2 = sr**2 + si**2   !  amplitude squared
      rms = rms + a2
      gamma(i) = sqrt(a2)
      if (peak .lt. gamma(i)) peak = gamma(i)
end do
tt = nn*dt
rms = sqrt(2.*rms*df/tt)
factor = strmax/peak
do i=0,nf
      gamma(i) = gamma(i)*factor
end do[2]
write (*,'(a,e15.4)') ' Peak strain          = ', strmax
write (*,'(a,e15.4)') ' RMS  strain          = ', rms
rms = rms/strmax
write (*,'(a,f15.4)') ' RMS/peak  strain     = ', rms
return
end
```

---

[2] Note.-If frequency dependent damping linear hysteretic model was used with smoothed strain Fourier transform, the loop should be substituted with:

```
do i=0,nf
      gamma(i) = strmax*exp(-0.15*(df*i))/(df*i+1)**0.625
end do
```

```
**********************************************************************
```

SUBROUTINE INTEG (strain, v, nt, nn, ampl, dt)

Integrates the ground acceleration time - history, then scales the computed ground velocity to convert it into a strain time history (based on the assumption that the strain is proportional to the particle velocity)

```
real strain(0:nn), v(0:nn)
strain(0) = 0.
do i=1,nt
      strain(i) = strain(i-1) + v(i)
end do
du = strain(nt)/nt
amp = 0.
do i=1,nt
      strain(i) = strain(i) -i*du
      v(i) = v(i) - du
      if (abs(strain(i)) .gt. amp) amp = abs(strain(i))
end do
fac1 = ampl/amp
fac2 = fac1/dt
do i=0,nt
      strain(i) = strain(i)*fac1    !     Strain
      v(i) = v(i)*fac2              !     Rate of strain
end do
do i=nt+1,nn
      strain(i) = 0.
      v(i) = 0.
end do
return
end
```

```
**********************************************************************
```

FUNCTION DAMPING (strain, xy, damp, nk)

Returns the damping for the current level of strain

```
real xy(0:nk), damp(0:nk)
i = 0
do while (strain.gt.xy(i) .and. i.lt.nk)
      i = i + 1
end do
```

```
if (i .le. 1) then
      damping = damp(1)*strain/xy(1)
else if (strain .le. xy(nk)) then
      dd = log( xy(i)/xy(i-1)   )
      x1 = log( xy(i)/strain  )
      x2 = log( strain/xy(i-1))
      damping = (x1*damp(i-1) + x2*damp(i))/dd
else
      damping = damp(nk)          !     Must modify for strain > xy(nk)
end if
return
end

*********************************************************************

SUBROUTINE GET_PARAMETERS (inpfil, strmax, dt)
---------------------------------------------------------------------------------------------------
Returns the parameters on the command line
---------------------------------------------------------------------------------------------------

character*80 inpfil
character*5 type
real K0
integer*2 status
common /soil/ Cb, e0, K0, conf, xmin

! *** Default values
e0 = 0.5                  !     Void ratio
K0 = 0.5                  !     Coefficient of lateral earth pressure
conf = 1.                 !     Atmospheres
type = 'sand'

strmax = 1.e-3            !     Maximum strain
dt = 0.02                 !     Time step for earthquake

n = nargs ()
if (n .ge. 2) then
      call GETARG (1, inpfile, status)    ! Get name from command line
else
      write (*,'(a)') ' Input file?'
      read (*,'(a)') inpfile
end if
open (5,file=inpfil)
read (5,'(a)') type
read (5,*) e0
read (5,*) K0
```

```
read (5,*) conf
read (5,'(a)') inpfil
read (5,*) dt
read (5,*) strmax
close (5)
if (type.eq.'clay' .or. type.eq.'CLAY') then
      Cb = 450.
else
      Cb = 800
end if
return
end
```

****

SUBROUTINE MIT-S_1 (x0)

Computes the soil constants for the MIT - S1 model shear modulus degradation curves

---

```
real K0, K0NC
parameter (FTHRD=1.6666667, TWOTHRD=0.6666667)
parameter (SR15=1.224744871)          !     sqrt(1.5)
parameter (OCR1=6.67777)              !     OCR at K0 = 1
parameter (POIS0=0.25)                !     Small Strain Poisson's ratio
parameter (K0NC=0.5)
common /soil/ Cb, e0, K0, conf, xmin
common /constants/ C, C1, C2, C12, C3, C4, A1, A2, B1, B2, B3, G0

conf = (1.+2.*K0)*conf/3.
e = e0*exp(-0.00169*conf)             !     Void ratio
C1 = 2.4                              !     Exper. Data (Laird & Stokoe, 1993)
C = (1. - 2.*POIS0)/(1. + POIS0)
C2 = c*(1 + 2.*K0NC - 3./OCR1)
C2 = SR15*(K0NC - 1. + C2)*(1.+ 2*K0NC)/(1.- K0NC)**2
C = e*conf**TWOTHRD/( 1.5*C*Cb*(1. + e) )
C11 = C1**2
C12 = C1*C2
C22 = C2**2
A1 = 12.*C12**2
A2 = C*(C1 + C2)*(4.*C12 - C11 - C22)
B1 = 3.*A1
B2 = 6.*A2
B3 = (10.*C12 - 3.*(C11 + C22))*C**2
C12 = 2.*C12
C3 = (C1 - C2)**2
```

```
C4 = C1 + C2
G0 = 1.                    !     Set appropriate value before calling FUN ( )
G0 = 1./fun(x0)
xmin = x0
return
end

*************************************************************************
```

FUNCTION FUN(x0)

Shear modulus degradation curve

```
parameter (THIRD=0.3333333)
common /soil/ Cb, e0, K0, conf, xmin
common /constants/ C, C1, C2, C12, C3, C4, A1, A2, B1, B2, B3, G0

if (x .le. xmin) then
      FUN = 1.
else
      A = A1*x + A2
      B = C12*sqrt((B1*x + B2)*x + B3)
      A = ((A + B)/C)**THIRD
      T = conf*(A + C3/A - C4)/C12        !     Stress at strain = x
      G = T/x                             !     Shear modulus
      FUN = G0/G
end if
return
end

*************************************************************************
```

SUBROUTINE SPRING_IS_PLASTIC (u, v, stress, energy, u1, n1, f1,
*   fy, unload, plastic, nt)

Determines the point at which the spring will stop flowing as well as the energy dissipated by it in plastic flow

---

```
real u(0:nt), v(0:nt), stress(0:nt), energy(0:nt)
n2 = n1
if (plastic .eq. 1) then
      do while (v(n2).ge.0. .and. n2.lt.nt)     !     Flowing L->R
            n2 = n2 + 1
      end do
```

```
      unload = -1
      f2 = fy
else if (plastic .eq. -1) then
      do while (v(n2).le.0. .and. n2.lt.nt)     !       Flowing R->L
            n2 = n2 + 1
      end do
      unload = 1
      f2 = -fy
end if
plastic = 0
n2 = n2 - 1
u2 = u(n2)
work =  (u2 - u1)*f2
if (n2 .gt. n1) then
      work = work/(n2 - n1)
      energy(n1) = energy(n1) + 0.5*work
      energy(n2) = energy(n2) + 0.5*work
      do i=n1+1,n2-1
            energy(i) = energy(i) + work
      end do
else
      energy(n2) = energy(n2) + work
end if
do i=n1+1,n2
      stress(i) = stress(i) + f2
end do
f1 = f2
u1 = u2
n1 = n2
return
end

**************************************************************************

SUBROUTINE SPRING_IS_ELASTIC (u, stress, u1, n1, f1, fy, uy,
*                              st, unload, plastic, nt)
```

Determines the next point at which spring will flow (if at all)

```
real u(0:nt), stress(0:nt)
integer unload, plastic
n2 = n1 + 1
if (unload .lt. 0) then                 !       Spring unloading?
u2 = u1 - uy                            !       Yes. Set lower yield limit
do while (u(n2).lt.u1 .and. u(n2).gt.u2 .and. n2.lt.nt)
      n2 = n2 + 1
```

```
end do
if (u(n2) .ge. u1) then                !   Resumes flow L->R ?
      plastic = 1                      !   Yes, it does resume
      f2 = fy
      u2 = u1
else if (u(n2) .le. u2) then           !   Exceeds yield in unloading?
      plastic = -1                     !   Yes, begin flow R->L
      f2 = -fy
      u2 = u2
else
      f2 = f1 - st*(u1 - u(n2))
end if
else if (unload .gt. 0) then           !   Spring reloading?
      u2 = u1 + uy                     !   Yes. Set upper yield limit
      do while (u(n2).gt.u1 .and. u(n2).lt.u2 .and. n2.lt.nt)
            n2 = n2 + 1
      end do
if (u(n2) .le. u1) then                !   Resumes flow R->L ?
      plastic = -1                     !   Yes, it does resume
      f2 = -fy
      u2 = u1
else if (u(n2) .ge. u2) then           !   Exceeds yield in reloading?
      plastic =  1                     !   Yes, begin flow L->R
      f2 = fy
      u2 = u2
else
      f2 = f1 - st*(u1 - u(n2))
end if
else
      f1 = 0.                          !   Spring still virgin
      u2 = -uy
      do while (u(n2).lt.uy .and. u(n2).gt.u2 .and. n2.lt.nt)
            n2 = n2 + 1
      end do
if (u(n2) .ge. uy) then
      f2 = fy                          !   First flow L->R
      u2 = uy
      uy = 2.*uy
      plastic = 1
else if (u(n2) .le. u2) then
      f2 = -fy                         !   First flow R->L
      u2 = -uy
      uy = 2.*uy
      plastic = -1
else
      u2 = u(n2)
```

```
      f2 = st*u2
end if
end if
do i=n1+1,n2-1
      stress(i) = stress(i) + f1 - st*(u1 - u(i))
end do
stress(n2) = stress(n2) + f2
f1 = f2
u1 = u2
n1 = n2
return
end

*****************************************************************************
```

SUBROUTINE INMOT (th, nt, nn, eqfile)

Reads input earthquake

```
character*(*) eqfile
real th(0:nn)

open (5,file=eqfile)

! **** INITIALIZE TIME HISTORY VECTOR
do i=0,nn
      th(I) = 0.
end do

! **** READ THE TIME HISTORY
nt = nn-1
read (5,*,end=1) (th(i), i=0,nt)

! **** CHECK FOR END OF FILE
read (5,*,end=1) dummy

! **** END OF FILE NOT DETECTED, PRINT WARNING
write (*,'(A)') ' **** WARNING: Input time history too long!'
go to 2

! **** FIND NUMBER OF NON-ZERO POINTS IN TIME HISTORY
do while (th(nt).eq.0. .and. nt.ge.0)
      nt = nt - 1
end do
if (nt .lt. 0)
```

```
      *     stop  ' **** ERROR: Input time history is empty!'
close (5)
return
end

*************************************************************************
```

III.2 Non-linear Soil Amplification – Lumped Mass System

Computes the seismic response of a soil deposit modeled as a set of non-linear springs. The solution is obtained by modeling the non-linear elements as a set of elastoplastic springs in parallel (Masing's law). The properties of these springs are inferred from the shear modulus degradation curves of the MIT-S1 model.

The equations of motion are integrated in the time domain with the Central Differences Method.

```
implicit real*8 (a-h,o-z)
parameter (x0=1.D-6)                    !   Small strain limit
parameter (xmax=1.0)                    !   Maximum strain for G/G0 curve
parameter (nkmax=300)                   !   Max. Number of elastoplastic springs
parameter (ntmax=10000)                 !   Max. Number of time steps
real*8 acc(0:ntmax)                     !   Earthquake record (time history)

integer mat[allocatable](:)             !   Material index for each layer
real*8 G   [allocatable](:)             !   Shear modulus
real*8 h   [allocatable](:)             !   Layer thickness
real*8 am  [allocatable](:)             !   Lumped Soil mass
real*8 conf[allocatable](:)             !   Confining pressure (atmospheres)
real*8 e0  [allocatable](:)             !   Initial void ratio
real*8 K0  [allocatable](:)             !   Coefficient of lateral earth pressure
real*8 ak  [allocatable](:,:)           !   Spring stiffnesses
real*8 fy  [allocatable](:,:)           !   Spring yield forces
real*8 strain [allocatable](:)          !   Strain vector

call PROMPT_USER (acc, nt, ntmax, lay, nmat)
allocate (G(lay), h(lay), am(lay), conf(lay), mat(lay))
allocate (e0(0:nmat), K0(0:nmat), strain(nkmax))
call READ_INPUT (G, h, am, conf, e0, K0, mat, dt, dt1, ndt)
call MAKE_STRAIN (strain, nkmax, nk, x0, xmax, fac)
allocate (ak(nk,lay), fy(nk,lay))
call MAKE_SPRINGS (ak, fy, strain, conf, e0, K0, mat, fac, nk,
*                  lay, nmat)

call CENTRAL_DIFFERENCE (acc, G, h, am, ak, fy, dt, dt1, ndt,
*                        nt, nk, lay)
deallocate (ak, fy, strain, e0, K0, G, H, am, conf, mat)
end

*************************************************************************
```

```
SUBROUTINE CENTRAL_DIFFERENCE (acc, G, h, am, ak, fy, dt, dt1,
*                              ndt, nt, nk, lay)
```

Integrates the equations of motion by central differences

```
implicit real*8 (a-h,o-z)
real*8 acc(0:nt)
real*8 G(lay), h(lay), am(lay)
real*8 ak(nk,lay), fy(nk,lay)

real*8 u   [allocatable](:)      !  Relative displacements, next step
real*8 u1  [allocatable](:)      !  Relative displacements, current step
real*8 u2  [allocatable](:)      !  Relative displacements, previous step
real*8 aa  [allocatable](:)      !  Absolute accelerations, current step
real*8 f   [allocatable](:)      !  Forces in each layer
real*8 for [allocatable](:,:)    !  Forces in elastoplastic springs

parameter (ACCG=32.17)           !  Acceleration of gravity, ft/s**2

lay1 = lay + 1
allocate (aa(lay1), u(lay1), u1(lay1), u2(lay1))
allocate (f(0:lay), for(nk,lay1))
call INITIALIZE (u1, u2, u, f, for, lay1, nk)

open (3,file='response')
open (4,file='loop')
write (3,'(3e15.5)') 0., 0., 0.
write (4,'(3E15.5)') 0., 0.
dt2 = dt1**2
eps = dt1/dt
ac1 = acc(0)
k = 0
do ts=1,nt
      ac2 = acc(ts)
      do j=1,ndt
            xi = j*eps
            gacc = (1.d0-xi)*ac1 + xi*ac2
            do i=1,lay
                  du1 = u1(i) - u1(i+1)
                  du2 = u2(i) - u2(i+1)
                  dx = (du1 - du2)/h(i)
                  f(i) =force(ak(1,i), fy(1,i), for(1,i), g(i), dx, nk)
            end do
            do i=1,lay
                  aa(i) = (f(i) - f(i-1))/am(i)
```

```
                u(i) = 2.*u1(i) - u2(i) - dt2*(gacc + aa(i))
                u2(i) = u1(i)
                u1(i) = u(i)
            end do
            k = k + 1
            time = k*dt1
            write (3,'(3E15.5)') time, -aa(1)/ACCG, gacc/ACCG
            write (4,'(3E15.5)') u1(1), f(1)
      end do
      ac1 = ac2
end do
deallocate (aa, u, u1, u2, f, for)
close (3)
close (4)
return
end

*************************************************************************
```

REAL*8 FUNCTION FORCE (ak, fy, for, G, dx, nk)

Computes the non-linear force in current layer

```
implicit real*8 (a-h,o-z)
dimension ak(*), fy(*), for(*)
force = 0.
do i=1,nk
      for(i) = for(i) + ak(i)*dx
      if (for(i) .gt. fy(i)) then
            for(i) = fy(i)
      else if (for(i) .lt. -fy(I)) then
            for(i) = -fy(i)
      end if
      force = force + for(i)
end do
force = g*force
return
end

*************************************************************************
```

REAL*8 FUNCTION FUN (x)

Shear modulus degradation curve

```
implicit real*8 (a-h,o-z)
parameter (THIRD=0.33333333333333D0)
common /soil/ Cb, conf
common /constants/ C, C1, C2, C12, C3, C4, A1, A2, B1, B2, B3, G0

A = A1*x + A2
B = C12*sqrt((B1*x + B2)*x + B3)
A = ((A + B)/C)**THIRD
T = conf*(A + C3/A - C4)/C12          !     Stress at strain = x
G = T/x                               !     Shear modulus
FUN = G0/G
return
end
```

****

SUBROUTINE INITIALIZE (u1, u2, u, f, for, lay1, nk)

Initializes the arrays

```
implicit real*8 (a-h,o-z)
real*8 u1(*), u2(*), u(*), f(*)
real*8 for(nk,lay1)
do i=1,lay1
      do j=1,nk
            for(j,i) = 0.
      end do
      u1(I) = 0.
      u2(I) = 0.
      u(I)  = 0.
      f(I)  = 0.
end do
return
end
```

****

```
SUBROUTINE MAKE_STRAIN (strain, nkmax, nk, x0, xmax, fac)
```

Generates the strain vector

```
implicit real*8 (a-h,o-z)
real*8 strain(nkmax)

fac = 10.**(0.05)                    !  Factor for strain intervals
strain(1) = x0                       !  Small strain limit
nk = 1
x1 = x0
do while (x1.le.xmax .and. nk.lt.nkmax)
      nk = nk + 1
      x1 = fac*x1
      strain(nk) = x1
end do
return
end

************************************************************************

SUBROUTINE MAKE_SPRINGS (ak, fy, strain, conf, e0, K0, mat,
*                        fac, nk, lay, nmat)
```

Computes the elasto-plastic springs for current soil

```
implicit real*8 (a-h,o-z)
real*8 ak(nk,lay), fy(nk,lay), strain(nk)
real*8 conf(lay), e0(0:nmat), K0(0:nmat)
integer mat(nmat)

fac1 = fac - 1.
nk1 = nk - 1
do i=1,lay
      m = mat(i)
      call MIT_S1 (strain(1), conf(i), e0(m), K0(m))
      g1 = 1.                                  !     Small strain G/G0
      fy(1,i) = g1*strain(1)
      ak(1,i) = g1
      do j=2,nk
            x2 = strain(j)
            g2 = 1./fun(x2)                    !     Secant stiffness
            ak(j,i) = (fac*g2 - g1)/fac1       !     Tangent stiffness
            g1 = g2
```

```
      end do
      do j=1,nk1
            ak(j,i) = ak(j,i) - ak(j+1,i) !       Spring stiffness
            fy(j,i) = ak(j,i)*strain(j)   !       Yield force
      end do
      fy(nk,i) = ak(nk,i)*strain(nk)
end do
return
end
```

****

SUBROUTINE MIT-S_1 (x0, sconf, e0, K0)

Computes the soil constants for the MIT - S1 model shear modulus degradation curves

---

```
real K0, K0NC
parameter (FTHRD=1.6666667, TWOTHRD=0.6666667)
parameter (SR15=1.224744871)          !       sqrt(1.5)
parameter (OCR1=6.67777)              !       OCR at K0 = 1
parameter (POIS0=0.25)                !       Small Strain Poisson's ratio
parameter (K0NC=0.5)
common /soil/ Cb, e0, K0, conf, xmin
common /constants/ C, C1, C2, C12, C3, C4, A1, A2, B1, B2, B3, G0

! DEFAULT VALUES
Cb = 800.                             !       Sand (for Clay, use Cb = 450.)

! DEFINE CONSTANTS
conf = (1.+2.*K0)*sconf/3.
e = e0*exp(-0.00169*conf)             !       Void ratio
C1 = 2.4                              !       Exper. Data (Laird & Stokoe, 1993)
C = (1. - 2.*POIS0)/(1. + POIS0)
C2 = c*(1 + 2.*K0NC - 3./OCR1)
C2 = SR15*(K0NC - 1. + C2)*(1.+ 2*K0NC)/(1.- K0NC)**2
C = e*conf**TWOTHRD/( 1.5*C*Cb*(1. + e) )
C11 = C1**2
C12 = C1*C2
C22 = C2**2
A1 = 12.*C12**2
A2 = C*(C1 + C2)*(4.*C12 - C11 - C22)
B1 = 3.*A1
B2 = 6.*A2
B3 = (10.*C12 - 3.*(C11 + C22))*C**2
```

```
C12 = 2.*C12
C3 = (C1 - C2)**2
C4 = C1 + C2
G0 = 1.                    !     Set appropriate value before calling FUN ( )
G0 = 1./fun(x0)
return
end

*************************************************************************

SUBROUTINE PROMPT_USER (acc, nt, ntmax, lay, nmat)
-------------------------------------------------------------------------
Returns the parameters on the command line, or prompts the user
-------------------------------------------------------------------------

implicit real*8 (a-h,o-z)
integer*2 status
real*8 acc(*)
character*80 input, quake, output

n = nargs ()
if (n .ge. 4) then

! *** GET FILE NAMES FROM COMMAND LINE
      call GETARG (1, input, status)
      call GETARG (2, quake, status)
      call GETARG (3, output, status)
else
      write (*,'(a)') ' Input data file?   '
      read  (*,'(a)') input
      write (*,'(a)') ' Earthquake file?'
      read  (*,'(a)') quake
      write (*,'(a)') ' Output file?    '
      read  (*,'(a)') output
end if
open (1,file=input, status='old')
open (2,file=quake, status='old')
call SCAN_INPUT (lay, nmat, scale)
call READ_QUAKE (acc, scale, nt, ntmax, 2)
close (2)
open (2,file=output)
return
end

*************************************************************************
```

```
SUBROUTINE READ_QUAKE (th, scale, nt, nn, unit)
```

Reads – Scales input earthquake

```
implicit real*8 (a-h,o-z)
integer unit
real*8 th(0:nn)
character*1 marker
character*80 row
parameter (ACCG=32.17)          !       Acceleration of gravity, ft/s**2

marker = ' '
do while (marker.ne.';' .and. marker.ne.'/')     ! Find marker
      read (unit,'(a1)', end=1) marker
enddo
if (marker .eq. '/') then
      do while (marker .eq. '/')                 ! Skip over remaining /'s
            read (unit,'(a1)') marker
      enddo
      backspace (unit)
endif
go to 2
1     write (*,'(a)')
     * ' Could not find marker in earthquake. Will try without...'
rewind (unit)
2     read (unit,'(a)') row     !       Read first line of quake...
backspace (unit)                !       ... and return to previous line
nl = 0
i = 80
do while (i .gt. 0)             !       Find number of items in line
      do while (row(i:i).eq.' ' .and. i.gt.0)          ! Jump over white
            i = i - 1
      enddo
      if (i .gt. 0) then
            nl = nl + 1
            do while (row(i:i).ne.' ' .and. i.gt.0)    ! Jump over number
                  i = i - 1
            enddo
      endif
enddo

! *** INITIALIZE TIME HISTORY FILE
do i=0,nn
      th(i) = 0.
enddo
```

```
if (nl .gt. 4) then

! *** READ NORMAL EARTHQUAKE FILE
      nl1 = nl - 1
      do nt=0,nn-nl1,nl
            read (unit,*,err=3,end=3) (th(i), i=nt,nt+nl1)
      enddo
else if (nl .eq. 1) then

! *** READ A SINGLE COLUMN OF ACCELERATION VALUES
      do nt=0,nn
            read (unit,*,err=3,end=3) th(nt)
      enddo
else

! *** READ A "Time history" FILE (TIME, ACC, VEL, DISP)
      do nt=0,nn
            read (unit,*,err=3,end=3) t, th(nt)
      enddo
endif

3     nt = nn
do while (nt.ge.0 .and. th(nt).eq.0.)
      nt = nt - 1
enddo
if (nt .lt. 0)
*    stop  ' **** ERROR: Input time history is empty!'

!  ** SCALE THE "Time history" FILE
call GETMAX(nt, NMAX, dt, TMAX, ATHMAX, THMAX, th)
if (scale .EQ. 0.) scale = ATHMAX
FACTOR = scale/ATHMAX
do i=0,nt
      th(i) = th(i)*FACTOR*ACCG
end do
return
end

*************************************************************************
```

SUBROUTINE GETMAX (NEQ, NMAX, DT, TMAX, ATHMAX, THMAX, TH)

Finds the signed and absolute maxima of the array TH, ie. THMAX = TH (NMAX), and ATHMAX =ABS (THMAX) where NMAX is the corresponding index, and TMAX the time of max.

```
integer neq, nmax
real*8 dt, tmax, athmax, thmax, th
DIMENSION TH(0:NEQ)
ATHMAX = 0.
NMAX = 0
DO I=0,NEQ
      A = ABS( TH(I) )
      IF (ATHMAX .LT. A) THEN
            ATHMAX = A
            NMAX = I
      END IF
END DO
TMAX = NMAX*DT
THMAX = TH(NMAX)
RETURN
END
```

****

SUBROUTINE READ_INPUT (G, h, am, conf, e0, K0, mat, dt, dt1, ndt)

Reads the input data for the current problem:

TITLE (any title)	
DT, DT1, SCALE	Parameters for earthquake, in which
DT	Time step for earthquake
DT1	Time step for analysis (should be less/equal to DT)
SCALE	Scaling factor for earthquake
NMAT	Number of different materials (=0 if using defaults)
Enter NMAT lines with:	
e0, K0	Void ratio and coeff. of lateral earth pressure
NLAY	Number of physical soil layers
Enter NLAY lines, each of which contains:	
N, H, W, Cs, M	Material properties, in which
N	Number of sub-layers for dividing current layer
W	Specific weight (in lb/cf)
Cs	Shear wave velocity (ft/s)
M	Material index to choose e0 etc (if = 0, use default)

```
implicit real*8 (a-h,o-z)

! *** ASSUMED UNITS: LB (FORCE), FT, SEC
parameter (ACCG=32.17)          !     Acceleration of gravity, ft/s**2
parameter (ATMU=2116.22)        !     Atm. pressure, lb/ft**2
parameter (PCF=ACCG/ATMU)       !     Pressure conversion factor
parameter (PMIN=0.5)            !     Minimum confining pressure used
integer mat(*)
real*8 G(*), h(*), am(*), conf(*)
real*8 e0(0:*), K0(0:*)
character*80 title
common /titles/ title

101   format (/, ' Time step for earthquake       = ', f10.4, /,
*               '  "    "    "  analysis         = ', f10.4, /,
*               '  Scaling factor for earthquake = ', f10.4)

102   format (//, 'Material Properties:', /,
*                '  Material     e0          K0 ', /, I5, 2f12.3)

103   format (//, 'Soil Profile:', /,
*                '  Layer  Mater   Thickn    Sp. Weight',
*               6x, 'Cs', 10x, 'G', 8x, 'Conf. P.')

read  (1,'(a)') title
write (2,'(a)') title
read  (1,*) dt, dt1, scale
if (dt1.eq.0 .or. dt1.gt.dt) dt1 = dt
ndt = (dt + 0.5*dt1)/dt1        !     Number of intervals in dt
dt1 = dt/ndt
write (2,101) dt, dt1, scale

e0(0) = 0.5                     !     Default value for void ratio
K0(0) = 0.5                     !     Default value for coefficient of lat. earth pressure
write (2,102) 0, e0(0), K0(0)
read (1,*) nmat
do i=1,nmat
      read (1,*) e0(i), K0(i)
      write (2,'(i5, 2f12.3)') i, e0(i), K0(i)
end do
pr = 0.
bm = 0.
lay = 0
read (1,*) nlay
write (2,103)
do i=1,nlay
      read (1,*) nn, hh, ww, cs, mtype
```

```
      if (mtype .gt. nmat) then
      write (*,'(a,i5,a)') ' *** Warning: Material ', mtype,
*                          ' does not exist!'
      mtype = 0
      end if
      dh = hh/nn
      ro = ww/ACCG
      gg = ro*cs*cs
      dp = ro*dh*PCF
      dm = ro*dh/2.
      do j=1,nn
            lay = lay + 1
            pr  = pr + dp
            G(lay) = gg
            h(lay) = dh
            am(lay) = bm + dm
            mat(lay)  = mtype
            conf(lay) = pr - 0.5*dp  !      Overburden pressure, atm. units
            if (conf(lay) .lt. PMIN) conf(lay) = PMIN
                  bm = dm
                  write (2,'(i5,2x,i5,5e12.3)') lay, mtype, dh, ww, cs
*                                                gg, conf(lay)
        end do
end do
close (1)
return
end

**********************************************************************

SUBROUTINE SCAN_INPUT (lay, nmat, scale)
----------------------------------------------------------------------------------------------------

Scans the input files to determine max. dimensions
----------------------------------------------------------------------------------------------------

implicit real*8 (a-h,o-z)
character*4 title

read (1,'(a)') title                    !       Ignore title
read (1,*) dt, dt1, scale
read (1,*) nmat
do i=1,nmat
      read (1,*) e0
end do
lay = 0
read (1,*) nlay
do i=1,nlay
```

```
      read (1,*) nn
      lay = lay + nn
end do
rewind 1
return
end

*************************************************************************
```